ARL 67-0276

ANALYSIS AND DESIGN OF A HIGH PRESSURE A.C. ARC HEATER

D. E. GEISTER

GAS DYNAMICS LABORATORIES
DEPARTMENT OF AEROSPACE ENGINEERING
THE UNIVERSITY OF MICHIGAN
ANN ARBOR, MICHIGAN

DECEMBER, 1967

Contract No. AF 33(615)-1326
Project No. 7065

AEROSPACE RESEARCH LABORATORIES
OFFICE OF AEROSPACE RESEARCH
UNITED STATES AIR FORCE
WRIGHT-PATTERSON AIR FORCE BASE, OHIO

FOREWORD

This is one of two reports constituting the final technical report of research performed by personnel of the Gas Dynamics Laboratories, Department of Aerospace Engineering, the University of Michigan, Ann Arbor, Michigan for the Aerospace Research Laboratories, Office of Aerospace Research, Wright-Patterson AFB, Ohio. The research was supervised by Professor J. A. Nicholls, Head of the Gas Dynamics Laboratories. The work reported herein was accomplished under contract AF33(615)-1326, on Project 7065, "Aerospace Simulation Techniques Research," under the technical cognizance of Major Ralph Prete of the Fluid Dynamics Facilities Research Laboratory. This work was performed January 1964 to July 1966 as a continuation of work performed on Contract AF33(657)-8630 and reported in ARL 64-29.

This report describes the design background for a high pressure A. C. arc heater.

ABSTRACT

This work reports on the analysis and design of an A. C. arc heater capable of steady state operation at 2500 psia.

A generalization based on the arc column gas flow interaction is postulated whereby all arc heaters are divided into two types. In the parallel flow arc heater the gas flow is parallel to the arc column whereas in the normal flow case the gas flow is perpendicular to the column. In the latter case an applied D. C. magnetic field is essential for successful operation. The problem of scaling each type to a different operational level is discussed. In the parallel flow case a simple analytical model of the gas-arc column interaction is available thus providing a good basis for any scaling process. The lack of such a model for the normal flow arc heater, which must include the effects of the applied D. C. field, makes the scaling process very complicated. It was found that the normal flow arc heater is best suited for application to a 3-phase A. C. power source. The problem of scaling each type is discussed. Scaling trends were found for each type and are presented herein.

Using the results of the scaling studies and previous experimental data, detailed studies concerning the material selection, expected heat transfer rates, stress levels, and the required cooling system are presented. These studies indicated that the structural material needed to withstand the high pressure and thermal stresses would have to be an alloy of copper, the final choice being copper-zirconium. The heat transfer studies indicated that the dominant heat

loss mechanism in the arc chamber would be radiation, while for the nozzle convective heat losses predominated. The stress analysis showed that the wall thickness determinations could not be based on the assumption of only pressure stresses acting, but had to include the thermal stress terms. Finally, the high thermal loads imposed on these components coupled with the limited laboratory pump equipment indicated the need for an efficient cooling system. A cooling system which incorporated fins on the surfaces next to the coolant was used. Analysis would indicate this system to be two to three times more effective tnan the conventional water jacket.

TABLE OF CONTENTS

LIST OF ILLUSTRATIONS

NOMENCLATURE

A	surface area
B	magnetic field strength
B_{th}	thermal stress coefficient
B_ν	Planck function
C_p	specific heat at constant pressure
D	diameter
d	dimension defined in Eq. (92)
E	modulus of elasticity
$E_n(t)$	exponential integral as defined in Eq. (22)
F	force
f	friction factor
H	enthalpy
h	heat transfer coefficient
I	current
I_1	modified Bessel function
I_o	modified Bessel function
I_ν	monochromatic intensity of radiation
k	thermal conductivity-gas
k_w	thermal conductivity-water
k_{cu}	thermal conductivity-copper
L	length
ℓ	dimension defined in Eq. (92)
$\dot{m}$	mass flow
P	pressure
Q	power
q_r	radiative heat flux
$R(\tau)$	surface radiant flux
r	radius

S	fin height
T	temperature
$\overline{T}$	mean temperature as defined in Eq. (26)
T_o	bulk temperature
u	velocity
x	coordinate along length of the arc chamber
y	coordinate perpendicular to the arc chamber
α	linear coefficient of thermal expansion
β	constant as defined in Eq. (64)
γ	ratio of specific heats
δ	fin thickness
ϵ	emissivity
κ	absorption coefficient
$\overline{\kappa}$	Planck mean absorption coefficient
μ	Poisson's ratio
μ	cos Θ as defined in Eq. (22)
ν	frequency
ν	kinematic viscosity as used in Eq. (116)
ρ	density
σ	stress as used in Section V
σ	Stefan-Boltzman constant as used in Section III
τ_o	optical depth
ω	solid angle

subscript

c	chamber
e	material 0. 2% offset yield strength
o	flow stagnation conditions
m	mean value
t	tube in Section VI

w	wall
1	inside dimension
2	outer dimension
*	conditions at M = 1.0

I. INTRODUCTION

All of the experimental facilities that are capable of true temperature and pressure simulation at the very high Mach numbers (hot shot tunnels, shock tunnels, or shock tubes) are limited by short run times. Pebble bed and resistance heaters have been used for much longer run times but these devices cannot produce the stagnation temperatures characteristic of hypersonic flight at Mach numbers above 7 or 8. For example, at Mach 10 and an altitude of 155,000 ft, the required stagnation conditions are 2500 psia and 4150^{o}K. These conditions (and even higher temperatures) can, potentially, be effectively produced on a steady state basis by an arc heater. Thus the arc heater has a definite complementary place in the arsenal of high temperature gas dynamic facilities.

The task of developing arc heaters for these purposes has been vigorously undertaken by numerous industrial and research organizations (1, 2, 3, 4). The result of these endeavors has been the development of numerous low pressure D.C. arc heaters. This developmental work has encountered two major difficulties; the extrapolation of the design of low pressure arc heaters to the high pressure regime and the realization that arc technology is still in the research stage.

For a number of years personnel of the Department of Aerospace Engineering, Gas Dynamics Laboratories, have been engaged in the development of a high pressure 3-phase A.C. arc heater for the Fluid Dynamic Facilities Research Laboratory, Aerospace Research Laboratories. Due to the pucity of work on A.C. arc heaters, the lack of understanding of arcs under the conditions of interest, and the new problems associated with A.C. as compared to D.C., it was necessary to conduct substantial

---

Manuscript released by the authors October 1967
for publication as an ARL technical report.

research along with the development. It was found necessary to consider the entire arc heater system rather than the arc heater alone.

In effecting this research and development program, the arc heater system was divided into the following general areas, each found to strongly affect the performance of the arc heater as pressure levels increased; 1) the A. C. power supply and stabilizing elements, 2) the gas flow-arc interaction scheme, 3) the electrode system, 4) the D. C. magnetic field, and 5) the basic arc heater structural components. Studies were conducted in each of these areas with the aim of developing an arc heater operable over a given pressure range. It was found that optimization in each of the above individual subsystems would not produce an optimized arc heater. Consequently, considerable trade off studies and sub-system developmental work had to be done before and/or concurrent with the actual arc heater design and development.

The program to date has resulted in the design, development and operation of two A. C. arc heaters; a low pressure unit and a high pressure unit. The former arc heater, capable of operating in the 500 psi pressure range, provided some operational and experimental data for an extrapolation to the higher pressure unit. These data served to show the effects of pressure level on power requirements, the component thermal loads, and the new requirements that must be met in a subsequent heater. A detailed report on this low pressure unit is given in Ref. (5) and (6).

The aim of the follow-on studies was to develop an arc heater capable of operating in the 2500 psi range with a power input of 1 Megawatt. There were two distinct phases to its development; 1) a detailed design investigation of those arc heater

structural components most effected by the higher pressure levels, 2) the development and testing of the arc heater and its numerous auxillary components at their new design conditions. To adequately summarize this effort, it was felt that two reports need be presented, each covering the salient features of the above phases. This report summarizes the investigations into the problems of designing an arc heater capable of operating at the pressure and power levels stated. The trends observed in operating the low pressure arc heater and how this information affected the design considerations on the high pressure unit are discussed. A generalization of all heaters, classifying them either as parallel or "normal" flow, is presented. This distinction is of consequence in scaling an arc heater. Detailed studies are presented on the design of the arc chamber and nozzle.

Part two of this final report, which appears as a separate report (7), gives the final design and experimental performance of the high pressure A. C. unit.

II. GENERAL DESIGN CONSIDERATIONS

With the design, development and successful operation of a low pressure arc heater (up to 550 psi) completed, it was tempting to merely scale the existing configuration for the structural loads that would be imposed by a chamber designed for operation up to 2500 psia. However, the scaling of an arc heater is extremely complicated in that it is a complete system involving a number of distinct scientific disciplines (gas dynamics, arc physics, electrical engineering, heat transfer and structural mechanics). Therefore the scaling process requires either an intimate knowledge of each of these fields as they relate to arc heaters or the development and testing of a number of model arc heaters with appropriate scaling similarities. An extensive literature search was conducted in hopes of determining the influence of power level, arc voltage, arc rotational speed, radiative heat transfer, electrode characteristics, and other variables on arc chamber performance. It was determined that the fundamental information was simply not available nor was sufficient information available on experimental tests of various scale models. This was especially true in the case of A. C. arc heaters. It was further determined that a five fold increase in pressure, from 500 psi to 2500 psi, would not be accomplished by a small perturbation of the existing low pressure arc heater system.

Of the many sizes and shapes of arc heaters built and tested there appears to be one "type" most generally developed. This is the "parallel flow" or tube arc (an outgrowth of the Gerdien arc) which takes the form of a water cooled tube in which the arc is contained and the gas to be heated passed through and parallel to

the arc column. This unit usually runs on D. C. power with the tube or arc chamber serving as one electrode as shown in Fig. 1. Some success has been achieved in determining scaling laws for this type. The "type" we have been investigating has the arc attached to two or more electrodes; so oriented in the arc chamber that the gas flow to be heated is passed perpendicularly through the arc column as shown in Fig. 2. In the following the characteristics and scaling of these two types of arc heaters are discussed.

A. PARALLEL FLOW ARC HEATERS

The "parallel flow" or tube type arc heater has a number of characteristics which can make scaling much simpler. Commonly, one electrode is the arc chamber wall and hence the arc column scales with the arc chamber dimensions (thus eliminating one degree of freedom). A most important feature is that the gas flow-arc interaction can be solved analytically by using an asymptotic column solution (8). In general, the theory of the cylindrically symmetric arc is firmly established and compares well with experiment; the most accurate investigation being made by Stine and Watson (9). Therefore, an important set of design guide lines is already available.

Even though vast amounts of experimental data exist on the "parallel flow" arc heater there was only one study found that was directed toward establishing the arc heater scaling parameters. This was done by the Speedway Research Laboratories of the Linde Company and was directed toward the development of a 50 Megawatt D. C. arc heater (10). For the sake of completeness, this study is summarized here.

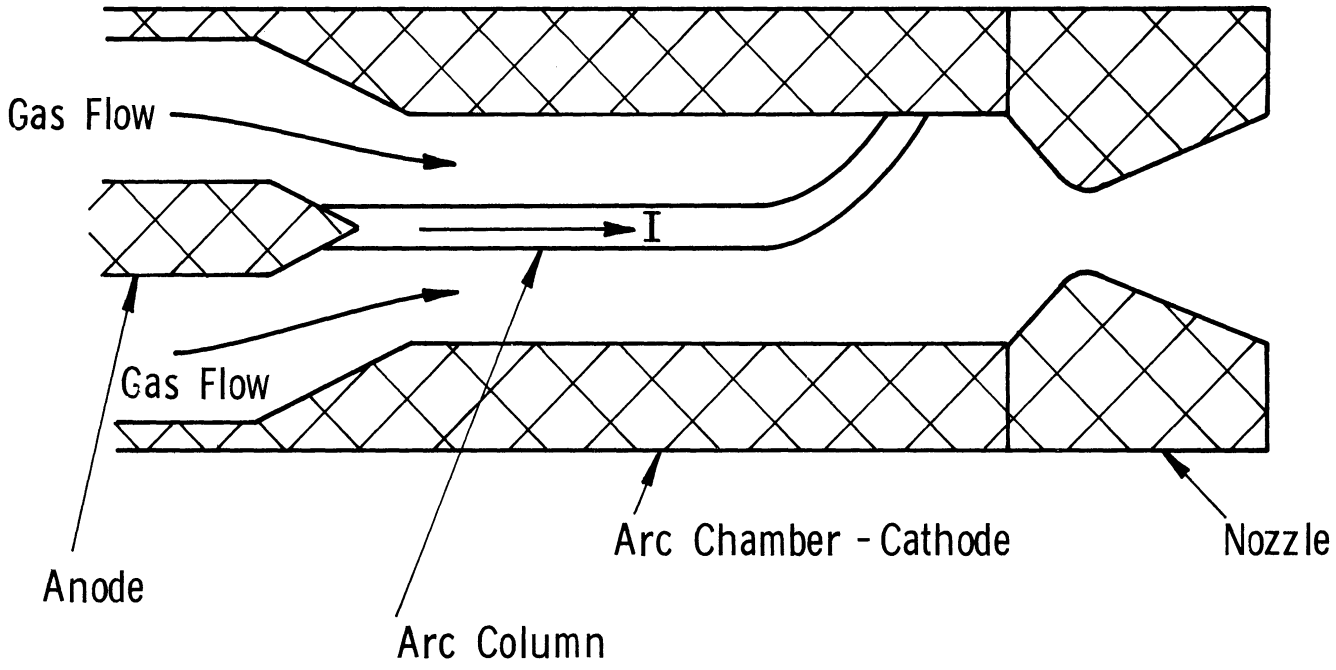

FIG. 1. PARALLEL FLOW ARC HEATER.

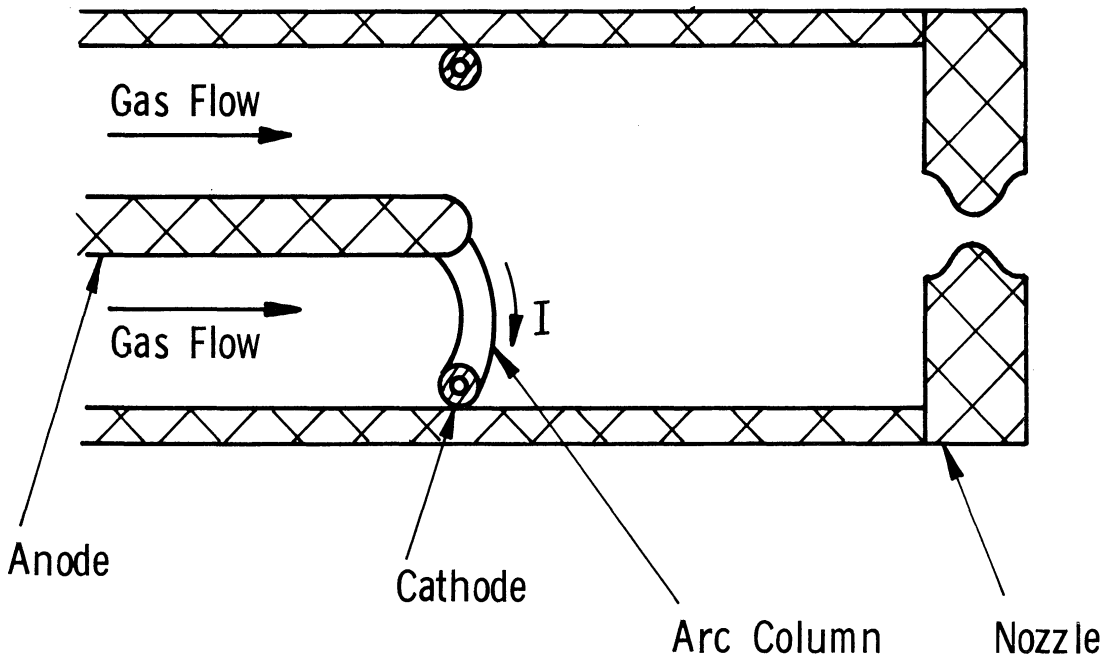

FIG. 2. NORMAL FLOW ARC HEATER.

If a reference or standard arc heater is designated by subscript (1) and S is the ratio of linear dimension of the new unit to the standard, the following scaling is indicated.

If

$$I = SI_1 \tag{1}$$

$$\dot{m}/A = (\dot{m}/A)_1 \tag{2}$$

Then,

$$V = SV_1 \tag{3}$$

$$Q = S^2 Q_1 \tag{4}$$

$$P = P_1 \tag{5}$$

$$H = H_1 \tag{6}$$

This scaling produces an arc heater operating at the same pressure level and effluent enthalpy as the standard unit but with higher mass flow.

Equation (2) can be written,

$$\dot{m} = S^2 (\dot{m})_1 \tag{7}$$

Defining the effluent enthalpy as $Q/\dot{m}$ and holding it constant:

$$Q/\dot{m} = (Q/\dot{m})_1 \tag{8}$$

or

$$Q = S^2 (Q)_1 \tag{9}$$

Therefore a proportionate increase in power with mass flow is needed.

The above scaling gives no information relative to different pressure and/or enthalpy levels. These effects can be estimated by following an analysis first proposed by Suits (11); the arc column being treated as if it were a hot cylindrical body. This analysis, however, neglected the effect of radiation losses and forced convection on the arc column. These effects are important and have been included in Ref. (12) which then leads to a fairly accurate representation of the "parallel" flow arc heater.

Using the latter analysis, the following general trends can be expected. An increase in arc chamber pressure level increases the arc column voltage gradient, power loss due to radiation, and gross power input, and decreases the arc column diameter. An increase in chamber mass flow increases the arc column voltage gradient, arc column length, and the gross power input, and decreases the gas enthalpy. An increase in arc current increases the arc column diameter and power loss due to radiation, and decreases the arc column length, arc column voltage gradient and generally the gas enthalpy level.

If one now considers the coupling that exists for the parallel flow arc heater between the arc chamber and the arc column, a fairly general set of scaling trends can be established. Assuming one has an arc heater operating at a given pressure, enthalpy and mass flow level and a new unit is to be developed to operate with an increase in one of these variables; the direction the arc heater scaling parameters must go can be obtained from the above trends. Considering the following cases; I) increased pressure while holding mass flow and enthalpy constant, II) increased

mass flow while holding pressure and enthalpy constant, III) increased enthalpy while holding pressure and mass flow constant, the following table summarizes the necessary change in scaling parameter.

TABLE I*

Scaling Parameter	Case I	Case II	Case III
Arc voltage	increase	increase	decrease
Power	increase	increase	increase
Thermal losses	increase	increase	increase
Arc heater length	increase	increase	decrease
Arc heater diameter	decrease	increase	increase

*Thermal losses are shown here in lieu of a scaling parameter that would reflect the arc heater thermal "efficiency."

These relatively simple observations stem from the fact that the arc chamber is one of the arc heater electrodes and hence the arc column assumes its dimensions. Therefore the arc heater scales to meet the requirements of the arc column.

B. NORMAL FLOW ARC HEATER

As previously described, the arc column in the "normal" flow arc heater will be oriented 90^{o} with respect to that of the parallel flow arc heater. A stationary arc column so oriented will fill only a small fraction of the arc chamber cross sectional

area and thus lead to inefficient heating of the working fluid. Further, the thermal loads imposed by the concentration of the arc roots on a small area of the electrodes would cause frequent burn throughs. To overcome these problems a D. C. magnetic field, in the form of a solenoid wrapped around the arc heater, is applied to the arc column with its field vector so arranged (along the axis of the chamber) that the resulting Lorentz force causes the arc column to rotate in the annular region between the electrodes. Thus an applied D. C. magnetic field becomes an important feature of the "normal" flow arc heater and is of consequence to the scaling procedures.

Since a high arc column rotational rate is desirable, the driving Lorentz forces should be a maximum for a given field strength. The Lorentz force is given by:

$$\vec{F} = \vec{B} \times \vec{I} \tag{10}$$

and the magnitude by

$$F = BI \sin \theta \tag{11}$$

Applying this to the geometry of the arc heater, Fig. 2, the force will be a maximum when the magnetic field is oriented parallel to, and the arc column normal to, the arc chamber axis. This indicates the wisdom of locating the second active electrode at the same axial position as the first. Further it indicates the disadvantage of using the arc chamber wall as an electrode for then the higher mass flow rates would tend to blow the arc root at the wall downstream; thereby reducing θ and F. Finally, when electrodes fail (as they eventually will), it is far easier to replace a simple electrode than the chamber wall. A possible disadvantage is that the separate electrode essentially divorces the arc column from the arc chamber and thus complicates scaling procedures.

It should be pointed out that the application of a D. C. magnetic field to the arc column is not unique to the "normal" flow type arc heater. The "parallel" flow arc heater previously discussed must also have some means of spreading the imposed heat load of the arc root over the electrode surface area. Here too, the arc root is rotated with two methods available to accomplish this; magnetic or aerodynamic.

If we consider the region of the arc column in the vicinity of its root, Fig. 1, we see it must turn 90^{o} in order to attach to the cathode (arc chamber wall). In so doing the current vector is locally so oriented that a D. C. magnetic field, applied as previously mentioned, will create a Lorentz force which tends to rotate the arc root over the surface of the arc chamber wall. The same effect can be also obtained by introducing the gas flow tangentially thereby creating a strong vortex in the arc chamber which in turn will drive the arc root. The latter method, however, is limited to low pressure operation and is found primarily in the parallel flow arc heater.

Nevertheless, being concerned with the effects of a D. C. magnetic field on the "parallel" flow arc heater we find; 1) any applied field is done so locally at the arc roots, 2) looking at the orientation of the field vector with the major portion of the arc column, the resultant Lorentz force will be small. Therefore, the effects of a magnetic field on the arc heater scaling are considered negligible. Just the opposite effects are felt and indeed, required in the "normal" flow arc heater.

1. Normal Flow Scaling Characteristics

A plausible assumption might be that the same scaling that existed between the length of the "parallel" flow arc heater and the arc column would still exist here but

applied now to the diameter of the "normal" flow arc heater, i. e., if a longer arc column is required the electrode spacing has to increase, and consequently, the arc chamber diameter has to increase. Therefore, just as the parallel flow arc heaters can be described as being small in diameter and rather lengthy, the normal flow arc heater would manifest itself as being short and rather large in diameter (a distinct disadvantage for high pressure operation). This general description, however, is accurate only to the extent that the normal flow arc heater will be larger in diameter than the parallel flow type and that its diameter will be governed by the largest electrode.

The normal flow arc heater has available two mechanisms which will allow a change in arc column length without physically changing the electrode spacing; a necessity if stable operation is required over a range of arc heater power, mass flow, and pressure levels. The "effective" electrode spacing can be changed by either blowing (magnitude of gas velocity vector through the electrode region) on the arc column or by applying a D. C. magnetic field to the arc column. Each mechanism will cause the column to lengthen in one of two different planes, the resultant arc column becoming a rather complicated three-dimensional shape. Figure 3 illustrates these effects. These features were used to advantage in designing the 2500 psi arc heater to be smaller than the low pressure unit.

As shown in Fig. 3(a), the effect of increasing the velocity vector into the arc column causes the column to bow thereby lengthening the arc column in the axial plane and moving the arc root forward, axially, around the electrode. The effect of

the D. C. magnetic field, Fig. 3(b) is to rotate the arc column at constant angular velocity. Therefore, that part of the arc column farthest from the axis of rotation will tend to have the highest velocity.

Defining for the moment, the head of the arc column as that part moving at the highest velocity and the base the slowest part, our investigations with the low pressure arc heater showed that the head of the arc column could lead its base by as much as 90^{o}, this lead being a function of D. C. field strength and arc chamber pressure. The angular lead was limited by the maximum field strength available (3000 gauss). The investigations of Jedlicka (13) also show the same trend. It was shown theoretically and verified experimentally that the shape of the arc column in the radial plane would be that of a cycloid of a circle. Therefore, the length of the arc, so driven, can be significantly greater than the physical electrode spacing, approaching what may be considered a mean circumference of the electrode spacing.

An interesting limit is evident for by creating a large enough Lorentz force, the head of the arc column can lead its base by 360^{o}. The resultant discharge would no longer take the form of a column, but rather that of a current sheet completely filling the annular electrode gap. This phenomenon, referred to as a diffuse arc, would spread the concentrated heat load of the arc column roots over the entire electrode surfaces, significantly reducing their rate of erosion. This type of arc discharge would be very desirable from the standpoint of arc heater operation, particularly the normal flow type which requires an applied

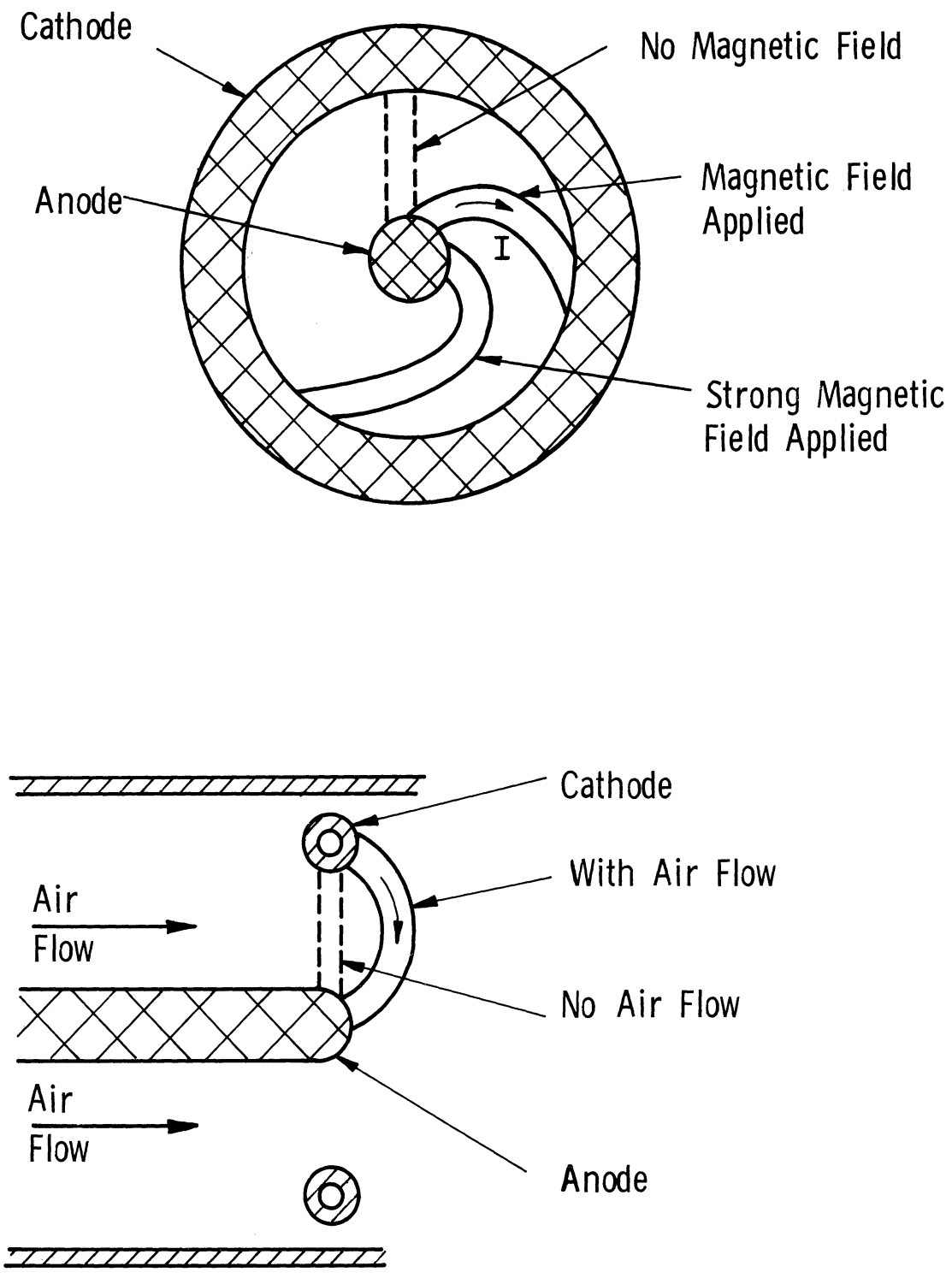

FIG. 3. EFFECTS—MAGNETIC FIELD AND BLOWING ON ARC COLUMN.

D. C. magnetic field. Although frequently mentioned in the literature (14), no one as yet has developed an arc heater system that can produce a diffuse arc at even moderate pressure levels. The primary difficulty in high pressure arc heater operation ($>$ 1 atm) is the large field strengths required ($>$ 20,000 gauss) due to the large aerodynamic drag forces experienced at high pressure levels.

We find, then, for the normal flow arc heater, that the length of the arc column can be significantly larger than the physical spacing of the electrodes and that its shape will be more than a simple cylinder normal to the electrode surface. Both now become a strong function of arc chamber mass flux and D. C. magnetic field strength. These features not only serve to complicate any scaling between the arc column and some characteristic length (e. g. electrode spacing) but also require that any meaningful theoretical model of the arc column must assume it to be three dimensional. As yet, no theoretical model for an arc under the influence of blowing (normal to its axis) is available. It is felt that this lack of a theoretical model is the major difficulty found in either initially designing the normal flow arc heater for a given operational regime or scaling a given design to a new operational condition. For this reason most of the theoretical and empirical data found is for the "parallel" flow arc heaters.

The following scaling trends were arrived at by using the conclusions derived from Ref. (12) and qualitatively allowing for the previously discussed arc-column interactions found in the "normal" flow arc heater. Due to the lack of experimental as well as theoretical information on these arc interactions most of the trends or

conclusions were establisned by the information obtained in developing and operating our low pressure arc heater. An increase in arc chamber pressure level increases the arc column voltage gradient, power loss due to radiation, and gross power input, and decreases the arc column diameter and arc column rotational rate (the latter decreasing arc column length). An increase in chamber mass flow increases the arc column voltage gradient, arc column length, and the gross power input and decreases the gas enthalpy and arc column rotational rate. An increase in arc current increases the arc column diameter, power loss due to radiation, and arc column rotational rate, and decreases the arc column voltage gradient and the gas enthalpy level. It can either increase or decrease the arc column length.

Assuming one has a "normal" flow arc heater operating at a given pressure, enthalpy, and mass flow level and a new unit is to be developed to operate with an increase in one of these variables, the direction of change for the scaling parameters can be obtained from the above trends. Table II summarizes this for three particular cases; I) increased pressure while holding mass flow and enthalpy constant, II) increased mass flow while holding pressure and enthalpy constant; III) increased enthalpy while holding pressure and mass flow constant.

In keeping with the generalization on arc heater scaling, changes in scaling parameters, length and diameter, were included in Table II. The indicated changes were based on the assumption that if one were scaling to a new performance regime, the resulting unit would be slanted toward improving and/or at best maintaining

TABLE II*

Scaling Parameter	Case I	Case II	Case III
Arc voltage	increase	increase	decrease
Power	increase	increase	increase
Applied D. C. magnetic field	increase	increase	increase
Thermal losses	increase	increase	increase
Arc heater length	(decrease)	(decrease)	(decrease)
Arc heater diameter	decrease	increase	increase

*Thermal losses are shown here in lieu of a scaling parameter that would reflect the arc heater thermal "efficiency."

thermal and structural efficiency. However, due to the weak coupling between the arc chamber and the arc column, the scaling of the arc heater dimensions can become quite arbitrary. This is particularly true with respect to the arc heater length (so designated by bracketing the suggested changes). In fact, quite often these dimensions can be completely dictated by other arc heater components, e. g., optimum size of the solenoid needed to produce the required D. C. magnetic field strength. This type of interaction turned out to have a significant effect on the eventually scaling of our 2500 psi arc chamber. This point will be elaborated upon in the following section.

2. Power Considerations

Considering now the question of using A. C. applied directly to the arc heater electrodes instead of D. C., it is felt that the "normal" flow arc heater is best suited for A. C. operation. This statement is based on the assumption that if one uses A. C. it would take the form of multiphase A. C. The minimum number of electrodes needed would then be three which, looking at possible electrode configurations, will lend itself best to the normal flow arc heater. These statements are not meant to exclude single phase A. C. for it can readily be used in either type of arc heater. However, it is concluded, as a result of our research and others (Ref. 15 and 16), that there are few, if any, advantages of using single phase A. C. instead of D. C. power. Some reservations must be made, however, as this conclusion is based on single phase A. C. operation of an arc heater designed for D. C.

In keeping with the generalization on two types of arc heaters, we have purposely neglected the possibility of electrically paralleling a number of parallel flow units and exhausting them into a common plenum chamber. Such arc heaters usually take the form of a multi-arc chambered unit and have been proposed and developed (Ref. 17) for both A. C. and D. C. operation. In view of the limitations of the understanding of arc heater fundamentals, it was felt that this sophistication was not warranted.

The low pressure arc heater previously developed was of the "normal" flow type using a three phase A. C. power source. One of the considerations that had to be made before designing another unit for higher pressure operation was what

type of arc heater was best suited for our particular application. Investigations into both types of arc heaters indicates the "parallel" flow arc heater will result in the smallest diameter unit, hence structurally lends itself better to high pressure operation. The use of multi-phase A. C. power (a major point of research interest in this program) requires a multi-electrode configuration which can, in general, only be obtained in the "normal" flow arc heater. Therefore only a design of the latter type was considered feasible in the allotted research period.

3. Application to 2500 psi A. C. Arc Heater

The objective of the extension of the A. C. arc heater program was to develop a heater for higher pressures (up to 2500 psia). Therefore, the scaling trends indicated in Table II, along with structural and thermal analyses, indicated the changes necessary for a new unit. These considerations showed that the high pressure arc heater must be capable of handling higher arc voltages, power levels, and thermal heat loads; the applied D. C. magnetic field strength would have to be increased and the arc chamber volume decreased. These trends were supported by the experimental data from our low pressure unit. These data showed that for a given open circuit voltage, power input, and D. C. magnetic field strength, an increase in arc chamber pressure produced a decrease in arc heater stability (arc column extinction), increased electrode erosion (decrease in arc column rotational rate), and an increase in thermal losses to the arc chamber walls (increased radiative heat losses). It was felt that these three trends would best establish the guide lines leading to the development of the 2500 psi arc heater.

The above guides were used in concentrating on the design of the arc chamber and nozzle, those components being considered the most sensitive to scaling. The design was further restricted by magnetic field considerations. Experimental data from the low pressure arc heater indicated that a D. C. magnetic field strength increase on the order of six would be optimum for high pressure operation, the low pressure unit having a field strength of 3000 Gauss with a power input of 120 KW. With our power supply limited to 120 KW, it was found impossible to achieve the desired six fold increase in magnetic field strength and still have a chamber capable of withstanding the new performance levels. Accordingly, a compromise was required and the final solenoid design resulted in a field strength of 11,000 Gauss.

III. HEAT TRANSFER ANALYSIS

The results of the scaling studies and the experimental data from the low pressure arc heater indicated that the new arc heater would be subjected to higher thermal losses as the operational pressure level was increased. Therefore an analytic heat transfer model was sought that could predict the heat loads impressed on the major arc heater components in the new operational regime. The major difficulty expected was the prediction of radiation losses at increased pressure levels.

A model was chosen that included all three modes of heat transfer (convection, conduction, and radiation). It was anticipated that experimental data obtained from the new arc heater could be used to better establish radiative heat losses as a function of pressure level. Since the radiative heat losses will limit the ultimate pressure levels an arc heat can produce, this type of information would prove useful for any future arc heater development. This type of data is also required since the assumptions made which allow for solutions of the energy equation with the radiative term (i. e. gray gas, optically thin or thick, etc.) do not hold as the pressure level is increased.

A. ARC HEATER OPERATING CONDITION

Preliminary to the heat transfer estimates, it is necessary to establish the state of the gas in the arc chamber. It is assumed that the new arc heater will produce a gaseous effluent with stagnation conditions of; temperature $1000^{o}K$ to $5000^{o}K$ and pressure to 170 atmospheres. These conditions would be produced with

a nominal power input greater than 1 megawatt with a maximum mass flow capability of 0. 5 lb/sec at any given pressure level.

Assuming the arc heated gas to obey the perfect gas law and that slug flow prevails in the arc chamber, conservation of mass indicates that the flow velocity will be very low (less than 3 ft/sec for a 6 in. diameter chamber). This is conducive to good arc column stability.

A calculation of the Reynolds number, based on the arc chamber diameter indicates that the chamber flow could be either laminar or turbulent, dependent on the operating conditions. For either case, data from Schlicting (18) indicates that the flow will be far from fully developed as the L/D of the chamber is less than 5. Therefore, it is concluded that the flow through the arc chamber can be treated as slug flow. Also, with a heat source (arc column) located approximately in the middle of the arc chamber, the temperature profile should develop very quickly in the axial flow direction so that $\partial^2 T/\partial x^2$ is small.

Postulating that the above conditions represent the gaseous flow in the arc chamber, the following analytic model is assumed to describe the heat transfer process.

B. ARC CHAMBER HEAT TRANSFER

The heat transfer characteristics of the flow through the arc heater is estimated by assuming it to be analogous to slug flow of a radiating gas in a constant height duct formed by two parallel plates. This simplification is used to avoid the complexities of the dependence of the radiant heat flow on the flow configuration.

The configuration considered is shown schematically in Fig. 4. A hot, nonscattering, absorbing and emitting gas with uniform velocity across the channel flows in the x direction between two infinite parallel plates separated by a distance L. The two plates (chamber walls) extend to infinity normal to the y axis and parallel to the x axis. The walls (y = 0, y = L) are at constant temperature T_w and both have the same emissivities. Steady state conditions are also assumed.

Since the velocity is assumed constant in the x and y directions, the conservation equations of mass and momentum are both satisfied. Therefore only the conservation of energy equation need be considered. The two-dimensional steady-state energy equation including conduction, convection and radiation terms but neglecting work, heat generation and viscous heat dissipation, is expressed as

$$\rho C_p u \frac{\partial T}{\partial x} = k\left(\frac{\partial^2 T}{\partial x^2} + \frac{\partial^2 T}{\partial y^2}\right) + \int_0^\infty \frac{\partial q_{r\nu}(x)}{\partial x} d\nu + \int_0^\infty \frac{\partial q_{r\nu}(y)}{\partial y} d\nu \qquad (12)$$

where $q_{r\nu}(x)$ and $q_{r\nu}(y)$ are the monochromatic radiant flux, in the x and y directions.

Applying the previous assumption of small axially gradients, we neglect the axial (x) gradient of temperature and radiant heat flux with respect to the y direction, therefore

$$\frac{\partial^2 T}{\partial^2 y} \gg \frac{\partial^2 T}{\partial^2 x} \quad , \quad \frac{\partial q_{r\nu}(y)}{\partial y} \gg \frac{\partial q_{r\nu}(x)}{\partial x} \qquad (13)$$

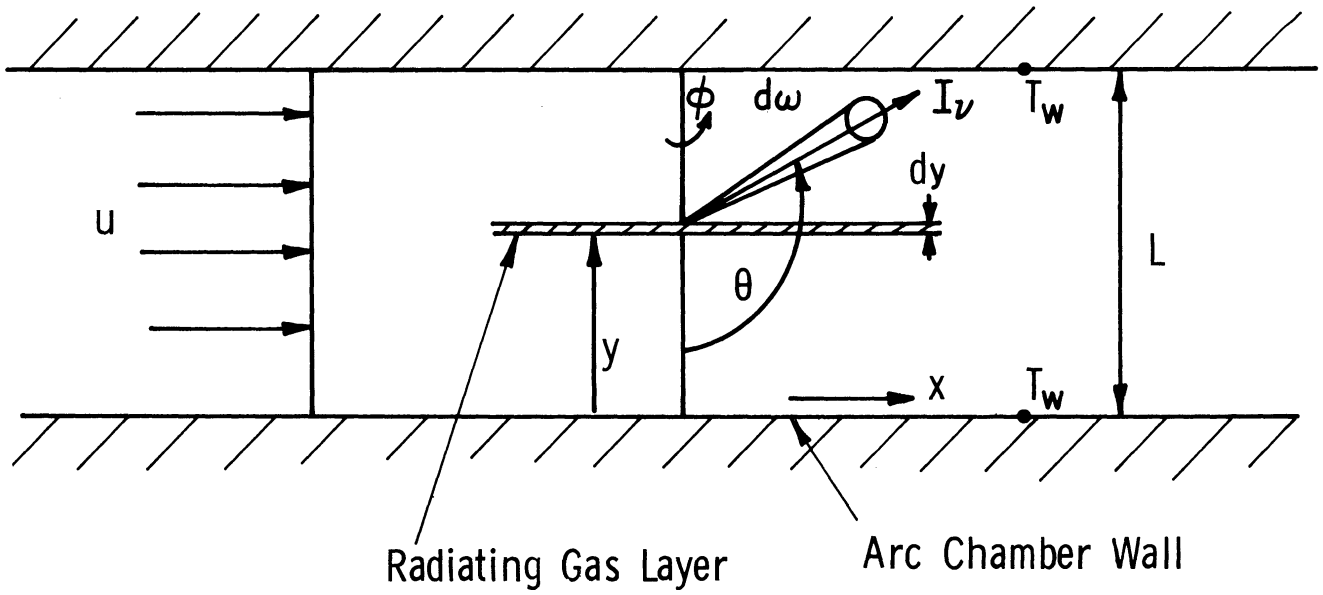

FIG. 4. HEAT TRANSFER MODEL

The energy equation (Eq. 12) simplifies to:

$$\rho C_p u \frac{\partial T}{\partial x} = k\left(\frac{\partial^2 T}{\partial y^2}\right) + \int_0^\infty \frac{\partial q_{r\nu}(y)}{\partial y} d\nu \tag{14}$$

The radiant energy flux $q_{r\nu}(y)$ across any plane in the fluid is found by integrating the intensity of radiation, $I_\nu(\theta, y)$ over all solid angles, ω.

$$q_{r\nu}(y) = \int_{4\pi}^{0} I_\nu(\theta, y) \cos\theta \, d\omega \tag{15}$$

$I_\nu(\theta, y)$ is obtained from the radiative heat transfer equation

$$-\cos\theta \frac{d I_\nu(\theta, y)}{\kappa_\nu \, dy} = I_\nu(\theta, y) - S_\nu(\theta, y) \tag{16}$$

where $S_\nu(\theta, y)$ is a source function.

Assuming the gas to be gray, isotropic, in local thermodynamic equilibrium with an index of refraction of 1, the intensity of radiation and absorption coefficient will be independent of wavelength. The source function will also be expressed as $(\sigma/\pi)T^4(y)$. Equations (15) and (16) can now be written as

$$q_r(y) = \int_{\omega=4\pi} I(\theta, y) \cos\theta \, d\omega \tag{17}$$

with

$$-\cos\theta \frac{d I(\theta, y)}{\kappa \, dy} = I(\theta, y) - \frac{\sigma T^4}{\pi}(y) \tag{18}$$

The formal solution of the radiative transfer equation has been given by Chandrasekhar (19), for a plane parallel gray gas and can be shown to be

$$q_r(\tau) = q_r + (\tau) - q_r - (\tau)$$

$$= 2R(\tau_o)\, E_3(\tau_o - \tau) + \sigma \int_{\tau}^{\tau_o} T^4(t)\, E_2(t - \tau)\, dt \qquad (19)$$

$$- R(o)\, E_3(\tau) - \sigma \int_{0}^{\tau} T^4(t)\, E_2(\tau - t)\, dt$$

where τ, the optical depth, defined as

$$\tau = \int_{0}^{y} \kappa\, dy \qquad (20)$$

is the new independent variable. The optical thickness τ_o is defined as

$$\tau_o = \int_{0}^{L} \kappa\, dy \qquad (21)$$

and the functions $E_n(t)$ are the exponential integrals defined as

$$E_n(t) = \int_{0}^{1} \mu^{n-2} \exp(-\tau/\mu)\, d\mu \qquad (22)$$

where $\mu = \cos \theta$. The radiant flux leaving the surfaces of the duct wall is due to both radiation emitted from the wall and the fraction of incident radiation which is diffusely reflected from the surface.

$$R(o) = \int_{\omega=2\pi} I(o) \cos \theta \, d\omega \qquad \text{for} \quad \begin{cases} \tau = 0 \\ \mu > 0 \end{cases}$$

$$= \epsilon T^4(o) + 2(1 - \epsilon) \left[R(\tau_o) \, E_3(\tau_o) + \sigma \int_0^{\tau_o} T^4(\tau) \, E_2(\tau) \, d\tau \right] \tag{23}$$

and

$$R(\tau_o) = \int_0^{2\pi} I(\tau_o) \cos \theta \, d\omega \qquad \text{for} \quad \begin{cases} \tau = \tau_o \\ \mu < 0 \end{cases}$$

$$= \epsilon T^4(\tau_o) + 2(1 - \epsilon) \left[R(o) \, E_3(\tau_o) + \sigma \int_0^{\tau_o} T^4(\tau) \, E_2(\tau_o - \tau) \, d\tau \right] \tag{24}$$

Using the previous assumption of a fully developed temperature profile, the axial-temperature gradient can be expressed as (Ref. 20)

$$\frac{\partial T}{\partial x} = \left(\frac{T_w - T}{T_w - \overline{T}} \right) \frac{d\overline{T}}{dx} \tag{25}$$

where the mean temperature, $\overline{T}$, for slug flow is defined as:

$$\overline{T} = \int_0^L T\, dy \Big/ L \tag{26}$$

Taking an energy balance for an element dx of the duct

$$\rho\, C_p\, u L\, d\overline{T} = 2q_w dx \tag{27}$$

where the total heat flux at the wall, q_w, is represented by

$$q_w(\tau) = -\, k \frac{\partial T}{\partial \tau}\bigg|_{\tau=0} - q_r(\tau)\bigg|_{\tau=0} = k \frac{\partial T}{\partial \tau}\bigg|_{\tau=\tau_o} + q_r(\tau)\bigg|_{\tau=\tau_o} \tag{28}$$

Introducing the dimensionless quantities $\theta = T/T_o$, $\underline{R} = R/\sigma T_o^4$ and $Q_w = q_w/\sigma T_o^4$ and combining Eq. (19) through (28) with the gradient of $q_r(\tau)$ gives the following form of the energy equation.

$$N \frac{d^2\theta}{d\tau^2} = \frac{2Q_w}{\tau_o} \frac{(\theta_w - \theta)}{(\theta_w - \theta_m)} + \theta^4 - \frac{1}{2}\left[\underline{R}(o)\, E_2(\tau) + \underline{R}(\tau_o)\, E_2(\tau_o - \tau) + \int_0^{\tau} \theta^4(t)\, E_1(\tau - t)\, dt + \int_{\tau}^{\tau_o} \theta^4(t)\, E_1(t - \tau)\, dt\right] \tag{29}$$

where the dimensionless parameter N is defined as

$$N = \frac{k\kappa}{4\sigma T_o^3} \tag{30}$$

which expresses the relative role of energy transport by conduction to that by radiation.

The boundary conditions for Eq. (29) are:

$$\tau = 0 \quad , \quad \theta = \theta_w$$

$$\tau = \tau_o \quad , \quad \theta = \theta_w$$

Since the temperature profiles will be symmetrical, i. e. $T(o) = T(\tau_o) = T_w$, the fluxes $R(o)$ and $R(\tau_o)$ will also be equal. Therefore

$$\underline{R}(o) = \underline{R}(\tau_o) = \frac{\left[\epsilon\theta_w^4 + 2(1-\epsilon)\int_0^{\tau_o} \theta^4(\tau)\, E_2(\tau)\, d\tau\right]}{1 - 2(1-\epsilon)\, E_3(\tau_o)} \tag{31}$$

The energy equation in its final form is:

$$N\frac{d^2\theta}{d\tau^2} = \frac{2Q_w}{\tau_o}\frac{(\theta_w - \theta)}{(\theta_w - \theta_m)} + \theta^4 - \frac{1}{2}\left[\underline{R}(o)[E_2(\tau) + E_2(\tau_o - \tau)]\right.$$

$$\left. + \int_0^{\tau} \theta^4(t)\, E_1(\tau - t)\, dt + \int_{\tau}^{\tau_o} \theta^4(t)\, E_1(t - \tau)\, dt\right] \tag{32}$$

which is a non-linear integro-differential equation satisfied by a temperature distribution T(y)* yet to be determined.

Unfortunately, there is no closed solution to the above equation, and one must use numerical means and a computer to obtain solutions. However, this equation or a similar form, has been solved numerically by Goulard (21),

*Once the distribution $\theta_{(\tau)} = T_{(\tau)}/T_o$ is established, T(y) is obtained through the relation $dT = kdy$.

Viskanta and Grosh (22), and Usiskin and Sparrow (23), using an iteration procedure. Viskanta (24) and Yoshikawa and Chapman (25) also solved a similar equation based on a truncated series expansion of $T^4(y)$. The former's results must be relied upon for this analysis.

1. Wall Heat Transfer

The solution of Eq. (32) gives the temperature distribution between the two walls. Its solution is by no means trivial but all heat transfer results can be calculated once the temperature distribution has been established. Dismissing this for now, the local radiant energy flux can be written as:

$$Q_r(\tau) = \frac{q_r(\tau)}{4\sigma T_o^4}$$

$$= \frac{1}{2}\left[\underline{R}(\tau_o)\, E_3(\tau_o - \tau) + \int_{\tau}^{\tau_o} \theta^4(t)\, E_2(t - \tau)\, dt - \underline{R}(o)\, E_3(\tau) \right. \tag{33}$$

$$\left. - \int_0^{\tau} \theta^4(t)\, E_2(\tau - t)\, dt \right]$$

Again using the property of a temperature profile symmetric about the duct centerline

$$Q_r(o) = - Q_r(\tau_o) \tag{34}$$

which allows Eq. (33) to be rewritten as:

$$Q_r(o) = \frac{1}{2}\left[\underline{R}(\tau_o)\, E_3(\tau_o) + \int_0^{\tau_o} \theta^4(\tau)\, E_2(\tau)\, d\tau - \underline{R}(o)/2\right] \tag{35}$$

The total heat flux at the wall will be

$$Q_w = \frac{q_w}{\sigma T_o^4} = -\, N \left.\frac{d\theta}{d\tau}\right|_{\tau=0} - Q_r(o) \tag{36}$$

Viewing Eq. (35) and (36) in light of the equations for $\underline{R}(o)$ and $\underline{R}(\tau_o)$, we find a solution is possible if the functional form of $\theta^4(\tau)$ is known. This single dependence on $\theta^4(\tau)$ suggests the following simple approximation to the radiative heat flux equation. It is assumed that the gas confined by the walls radiates at a mean temperature. This mean, as previously defined in Eq. (26) is

$$\theta_m{}^4 = \frac{1}{\tau_o} \int_0^{\tau_o} \theta^4(\tau)\, d\tau \tag{37}$$

The integrals in Eq. (33) for the local radiative flux $Q_r(\tau)$ can now be evaluated, giving

$$Q_r(\tau) = \frac{1}{2}\left[\underline{R}(o)\, E_3(\tau_o - \tau) - E_3(\tau)\right] + \theta_m{}^4 \left[E_3(\tau_o - \tau) + E_3(\tau)\right] \tag{38}$$

The radiate flux at the wall ($\tau = 0$) with $\underline{R}(o)$ evaluated at the mean temperature will be

$$Q_r(o) = \frac{\epsilon(\theta_w^4 - \theta_m^4)\left[E_3(\tau_o) - (1/2)\right]}{1 - 2(1 - \epsilon)E_3(\tau_o)} \tag{39}$$

One assumes the flow between the walls to be isothermal. Its absolute value is $\overline{T}$ which, for application in the arc chamber, would be the stagnation temperature of the arc heater effluent. This assumption should be fairly accurate, if the temperature distribution across the duct were flat and/or the contribution to the radiant energy flux from the gas small (optically thin approximation). As will be shown this approximation will not be valid for estimating the radiative wall flux to the arc chamber walls, but does find application for the arc heater nozzle.

2. Application to Arc Heater Operational Regime

To effect a solution of the energy equation, values for the independent parameters, θ_o, θ_w, ϵ, τ_o, and N, must be established. These parameters are functions of the arc heater structural material, gas properties, and arc heater power input. The effects of pressure level are reflected in the conductive heat transfer parameter, N, and the optical thickness, τ_o. Once established, there still exists the mathematical difficulties of finding the temperature distribution that satisfies the energy equation.

Considering the effect of increasing temperatures on the yield strength of copper alloys leads to the conclusion that the wall temperature, T_w, should be kept below 600^oF ($\approx 590^oK$) if reasonable safety factors are to be maintained. Therefore, we find

$$\theta_w < 0.3$$

for the stagnation temperature range considered. The stagnation temperature is assumed to be the average temperature of a given temperature distribution. This relationship then determines the values of θ_o, for a given stagnation temperature and temperature distribution.

The value for the wall emissivity, ϵ, is somewhat arbitrary, being dependent on both the material and surface condition (the assumption is made that emissivity as used in this gray gas approximation is also independent of wavelength). The material used in the arc heater is a copper alloy which, if highly polished, has an emissivity of the order

$$\epsilon \approx .15$$

It would be highly optimistic to expect this surface condition, if obtained, to last for any period of time. It was found from the experimental data on the low pressure arc heater that after a relatively short period of time the interior surfaces of the arc heater became covered with a dark layer of material. Analysis indicated that it had to be a combination of a number of the oxides of copper. These oxides are either formed due to erosion of the copper electrodes or by chemical reaction of the surfaces with the high temperature air. Now the emissivity of copper oxide ranges from

$$\epsilon = .60 \rightarrow .80$$

for a smooth surface. The formation of the compound on the arc heater surface was in the form of a rough powder, which would yield higher values for the emissivity. Hence, it is felt that a surface emissivity of the order of one would be more accurate for the heat transfer analyses.

Using the values for the thermal conductivity of air given in Ref. 26 and 27, and shown here in Fig. 5, and the mean linear absorption coefficient as shown in Fig. 6, we find that

$$N \ll 1$$

for the stagnation pressure and temperature range of the arc heater flow. Again these properties were evaluated assuming the stagnation temperature to be a mean temperature. The highest value for N occurs at the maximum in temperature and pressure ($T_m = 5000^{\circ}K$, P = 2500 psia). As such these values are very low and indicate that the role of conduction as a heat loss mechanism, either in establishing the wall heat load or the temperature distribution across the flow, would be small compared to that of radiation. This statement must be qualified, however, if large temperature gradients are present or if the temperature distribution across the flow is fairly flat and a cold wall exists. The latter case is approached as the absorptivity of the gas is increased, i. e. optical thickness is large.

The effects of thermal radiation on the temperature distribution and heat transfer to the wall can be characterized by the role that the optical thickness, τ_o, plays in the energy transport mechanisms. To couple this parameter to some physical dimension of the arc heater, we will define τ_o as the ratio of the diameter of the arc chamber, D, to the mean free path of radiation, $1/\kappa$,

$$\tau_o = \kappa D$$

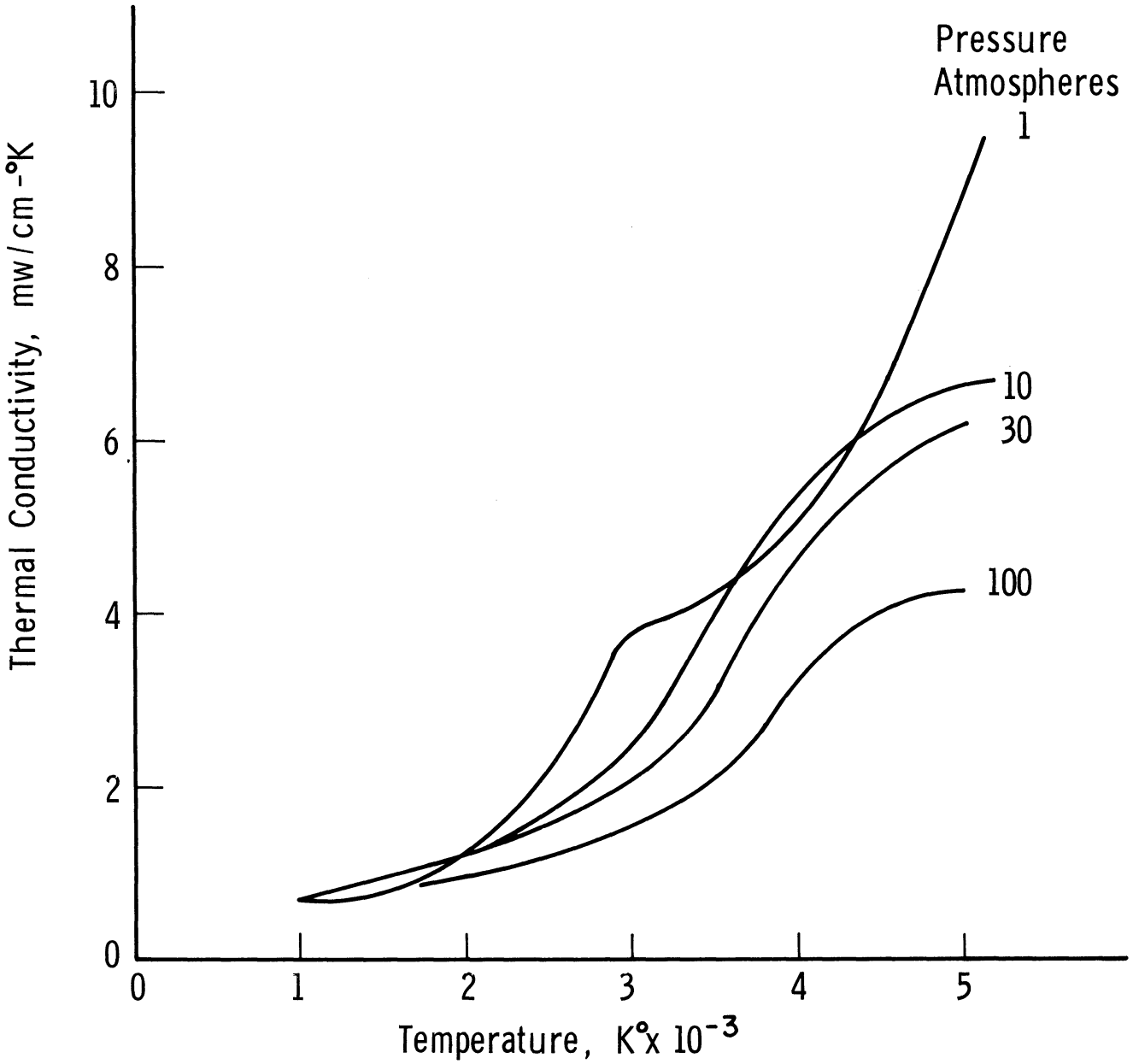

FIG. 5. THERMAL CONDUCTIVITY OF EQUILIBRIUM AIR

This is a measure of the diameter of the arc chamber in radiation mean free paths which can serve to show the effect of a change in either physical size or arc heater operational level on the heat transfer mechanism.

It should be noted here that for a gray gas approximation, the linear absorption coefficient κ is constant, but κ for air varies considerably as indicated in Ref. 28 and 29. Hence a mean value snould be used. The mean value, which was presented in Fig. 6 as a function of temperature and pressure, will be the Planck mean absorption coefficient

$$\bar{\kappa} = \frac{\int_0^\infty \kappa_\nu B_\nu \, d_\nu}{\int_0^\infty B_\nu \, d_\nu} \tag{41}$$

The values for $\bar{\kappa}$ are computed from the above references.

The optical thickness is then defined as

$$\tau_o = \bar{\kappa} D \tag{42}$$

Evaluating the optical thickness for the arc heater stagnation temperature and pressure levels for an arc chamber diameter of 6 in., we find

$$10^{-4} \leq \tau_o < .6$$

indicating that the radiative heat transfer cannot be accurately assessed by an optically thin approximation. Equation (39), which gives a simple approximation for the radiative heat transfer to the arc chamber wall, is valid only over part of

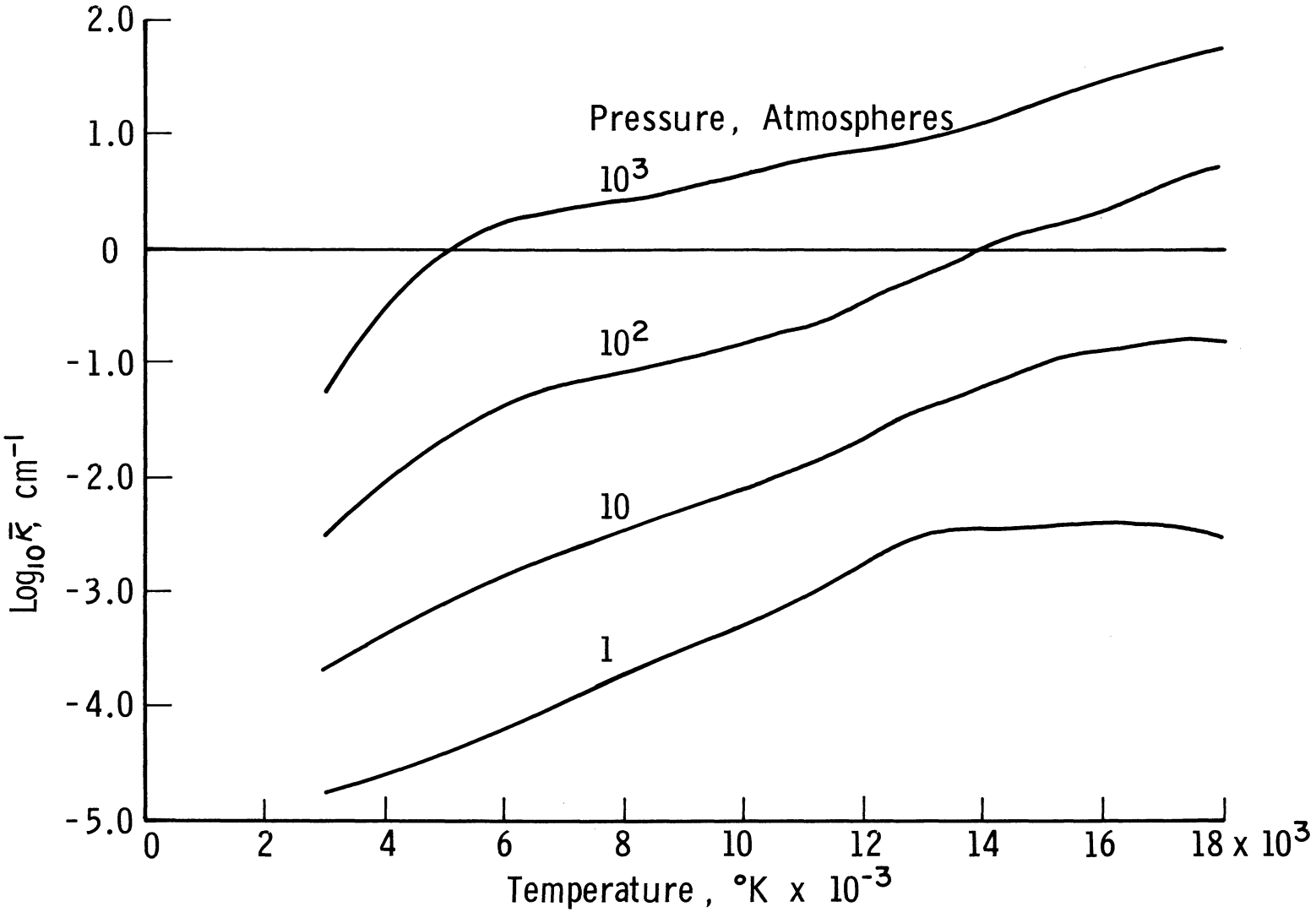

FIG. 6. PLANCK MEAN ABSORPTION COEFFICIENT OF AIR.

the arc heater operational regime. Therefore the estimate for the maximum wall heat flux must be made. This is particularly true considering the role that the heat flux plays in any structural analyses coupled with high pressures.

Since the design of the arc heater system is directed toward a unit capable of encompassing its operational range with as much latitude as its materials and design schemes allow, the main interest lies in the maximum heat loads that will be encountered. To ascertain these levels, the magnitude of these independent parameters will be chosen such that the maximum heat transfer is indicated for the given operating conditions. Hence, it is assumed that these operational levels are characterized by a conductivity parameter, $N = 0.001$, optical thickness, $\tau_o \leq 1.0$, wall temperature T_w of 500^oK, and wall emissivity, $\epsilon = 1.0$.

The temperature distributions used, which are solutions of the energy equation, are those resulting from the analysis of Viskanta and Grosh (24). These distributions are presented in Fig. 7, for two values of Θ_w. As shown, the effects on the temperature distribution for Θ_w varying from 0.1 to 0.5 are very small. Therefore over the range of Θ_w previously indicated, it will be assumed that the heat transfer estimates will not vary strongly with the wall temperature and can be adequately established by assuming T_w to be constant.

It must be noted here that for the temperature distribution shown a value of $N = 0.01$ was used instead of the required value of 0.001. The information of Ref. 30 and 31 indicates a small affect of N on the flow temperature distribution. The chamber wall transfer estimates, however, are made assuming $N = 0.001$.

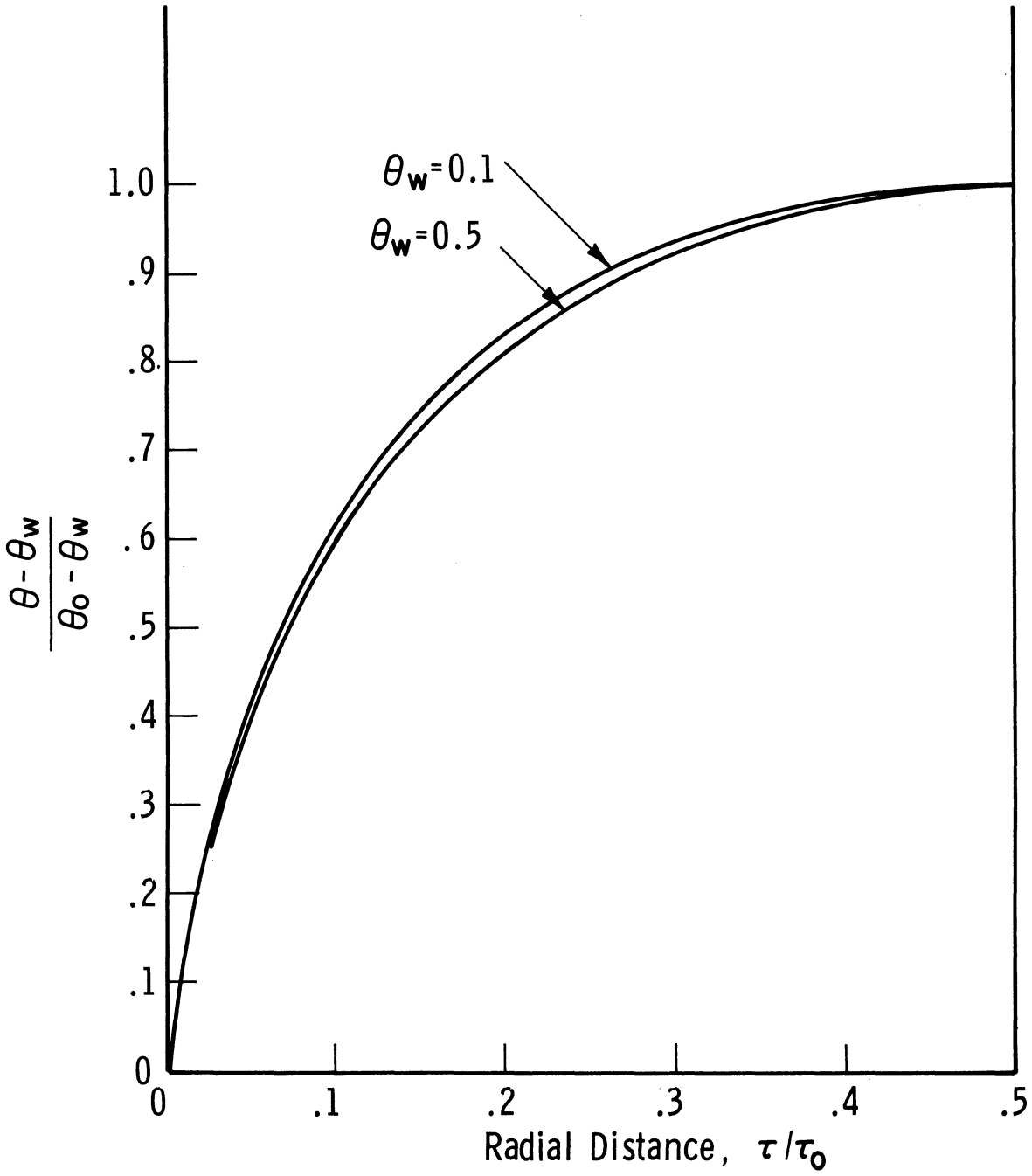

FIG. 7. EFFECT OF WALL TEMPERATURE ON ARC CHAMBER TEMPERATURE DISTRIBUTIONS.

Values for θ_o were obtained by integrating the various temperature distributions, $\theta - \theta_w / \theta_o - \theta_w$, and finding a mean value, $\overline{T}$. The stagnation temperatures investigated were equated to this mean value and the corresponding values for T_o established. These values were used in non-dimensionalizing the various heat transfer parameters.

The resulting arc chamber temperature distributions for various values of optical thickness are presented in Fig. 8. These curves show the effect that changes in either stagnation temperature or stagnation pressure have on the temperature profile. An increase in either quantity is reflected by an increase in $\overline{\kappa}$ and hence τ_o. This tends to drive the gas layer between the arc chamber walls toward blackbody radiation, i. e. $q_w \rightarrow \sigma T_o^4$.

A simple illustration of this is to look at the radiation from a constant temperature slab of gas between two black walls. Equations (33) through (36) for this case reduce to

$$q_w = 2 \int_0^{\tau_o} \sigma T^4 E_2(\tau) \, d\tau \tag{43}$$

where q_w is the radiative heat flux at the wall

$$q_w = \sigma T^4 \left[1 - 2E_3(\tau_o)\right] \tag{44}$$

and since

$$\begin{aligned} E_3(\tau_o) &\rightarrow 0 \\ \tau_o &\rightarrow \infty \end{aligned} \tag{45}$$

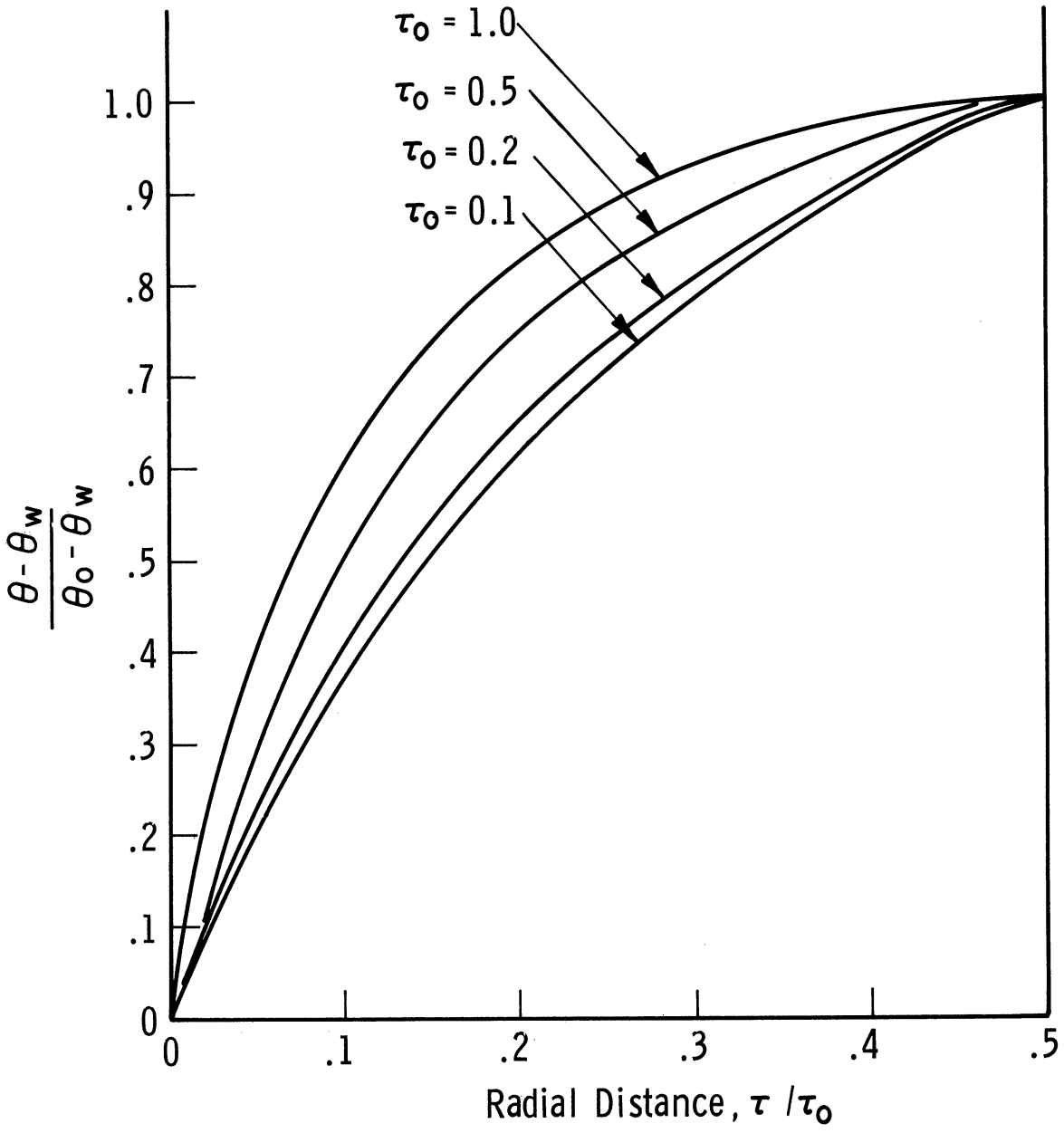

FIG. 8. EFFECT OF OPTICAL THICKNESS ON ARC CHAMBER TEMPERATURE DISTRIBUTIONS.

as

$$q_w \rightarrow \sigma T^4 \tag{46}$$

These observations, coupled with the low values of the conductivity parameter, N, point to radiation as the dominant source of wall heat flux.

The resultant heat flux to the arc chamber wall as a function of stagnation temperature and pressure is presented in Fig. 9. These values are obtained by using the temperature distribution of Fig. 8.

This range of wall heat flux is used in the analyses on the arc chamber structural and cooling requirements. These studies in turn, help map the arc heater's operational levels of stagnation temperature and pressure.

C. NOZZLE HEAT FLUX

The arc chamber is considered to be terminated by a sonic nozzle. Thus, the highest velocity, and probably highest heat transfer, in the nozzle will occur at the throat. Assuming an isentropic compression from the arc chamber stagnation conditions the local temperature and pressure in the nozzle throat can be expressed as

$$T_* = T_o \left(1 + \frac{\gamma - 1}{2}\right)^{-1} \tag{47}$$

$$P_* = P_o \left[\left(1 - \frac{\gamma - 1}{2}\right)^{-\frac{\gamma}{\gamma - 1}}\right] \tag{48}$$

where the subscript * indicates conditions at M = 1.0. Values of γ will be functions of both temperature and pressure, with a nominal value of 1.2 felt to be

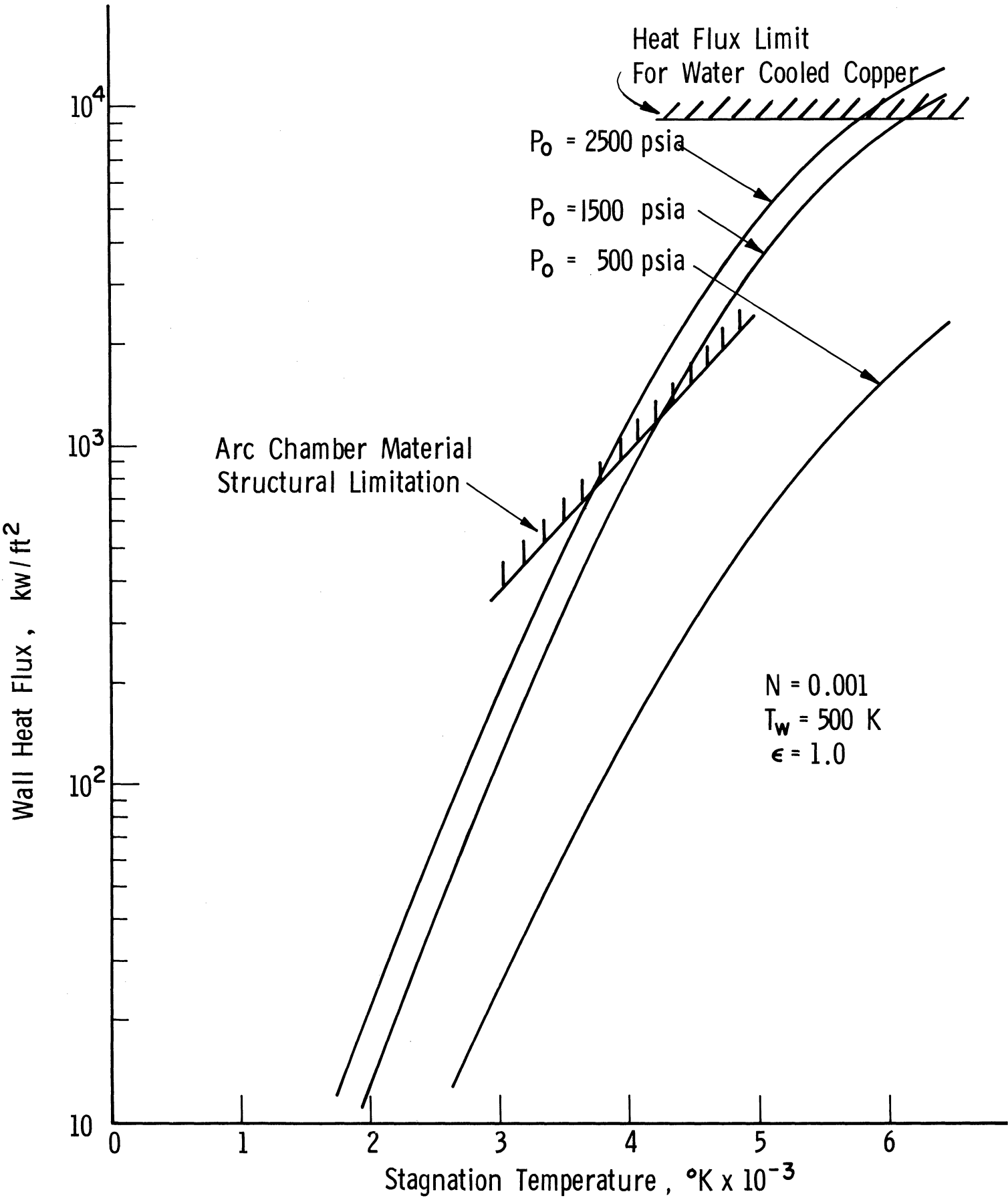

FIG. 9. ARC CHAMBER WALL HEAT FLUX.

representative of the arc heater flow conditions. The decrease in temperature and pressure from stagnation conditions causes a decrease in the ability of the gas flow to absorb thermal radiation. This effect becomes more pronounced if we consider its optical thinness. Defining the optical thickness in terms of the nozzle throat diameter,

$$\tau_o = \bar{\kappa} D_t \tag{49}$$

The maximum value of τ_o occurs at the highest values of stagnation temperature and pressure with the throat diameter sized to the arc heater mass flow.

For the range of operating conditions previously discussed we find

$$\tau_o \leq 2 \times 10^{-4}$$

which is considered to be indicative of an optically thin gas. The radiative heat flux at the wall is small compared to the convective heat flux and therefore the approximation previously discussed for the thermal radiation from an optically thin gas should be valid at the nozzle throat. This also uncouples the radiative terms from the energy equation allowing the contribution of each mode of heat transfer to be calculated separately and summed. The wall heat flux is then:

$$q_w = q_{conv}\Big|_{wall} + q_{rad}\Big|_{wall} \tag{50}$$

1. Radiative Heat Flux

Rewriting Eq. (33) for the local radiative heat flux after letting

$$Q_r(\tau) = \frac{q_r}{4\sigma T_m^4} \tag{51}$$

$$Q_r(\tau) = \frac{1}{2}\left[\underline{R}(\tau_o)\, E_3(\tau_o - \tau) + \int_{\tau}^{\tau_o} \theta^4(t)\, E_2(t - \tau)\, dt - R(o)\, E_3(\tau) \right.$$

$$\left. - \int_{0}^{\tau} \theta^4(t)\, E_2(\tau - t)\, dt \right] \tag{52}$$

Assuming a symmetric temperature profile the radiative heat flux at the wall becomes

$$Q_r\Big|_{wall} = \frac{1}{2}\left[\underline{R}(\tau_o)\, E_3(\tau_o) + \int_{0}^{\tau_o} \theta^4(\tau)\, E_2(\tau)\, d\tau - \underline{R}(o)\, \frac{1}{2}\right] \tag{53}$$

Applying the assumption of an optically thin gas, radiating at the mean temperature defined in Eq. (26),

$$\theta_m{}^4 = \frac{1}{\tau_o} \int_{0}^{\tau_o} \theta^4(\tau)\, d\tau \tag{54}$$

Re-evaluating $Q_r(\tau)$ at the wall ($\tau = 0$) and assuming a wall emissivity of 1.0.

$$Q_r\Big|_{wall} = (\theta_m{}^4 - \theta_w{}^4)\,[1 - 2\, E_3(\tau_o)] \tag{55}$$

For $\tau_o \ll 1$, $E_3(\tau_o)$ can be approximated by

$$E_3(\tau_o) \simeq \frac{1}{2} - \tau \tag{56}$$

Hence

$$Q_r\Big|_{wall} = (\theta_m^4 - \theta_w^4)\left[1 - 2\,\frac{1}{2} - \tau_o\right]$$

$$= 2\,(\theta_m^4 - \theta_w^4)\,(\tau_o) \tag{57}$$

Substituting in Eq. (57) and assuming $T_w = 500^{\circ}K$ and $T_m = T_*$, we find

$$q_r\Big|_{wall} \leq 5 \text{ kw/ft}^2$$

2. Convective Heat Flux

The convective heat flux, q_c, is estimated using the empirical equation of Lobb (32). The heat flux at the throat is expressed as

$$q_c\Big|_{wall} = 1.19 \times 10^{-3}\,\frac{(P_o)^{.75}\,(T_o)^{.23}}{(D_t)^{.08}}\,(T_o - T_w) \tag{58}$$

The resulting convective heat load is shown in Fig. 10 as a function of stagnation pressure and temperature. A material limitation will again be felt and maximum allowable stagnation temperatures of the order of $3500^{\circ}K$ to $4500^{\circ}K$ at the higher pressure levels are indicated.

Comparison of the range of convective heat flux values to the maximum value for the radiative heat flux indicates the small role radiation plays in the nozzle. The values used in the analysis on structural and cooling requirements are those of Fig. 10.

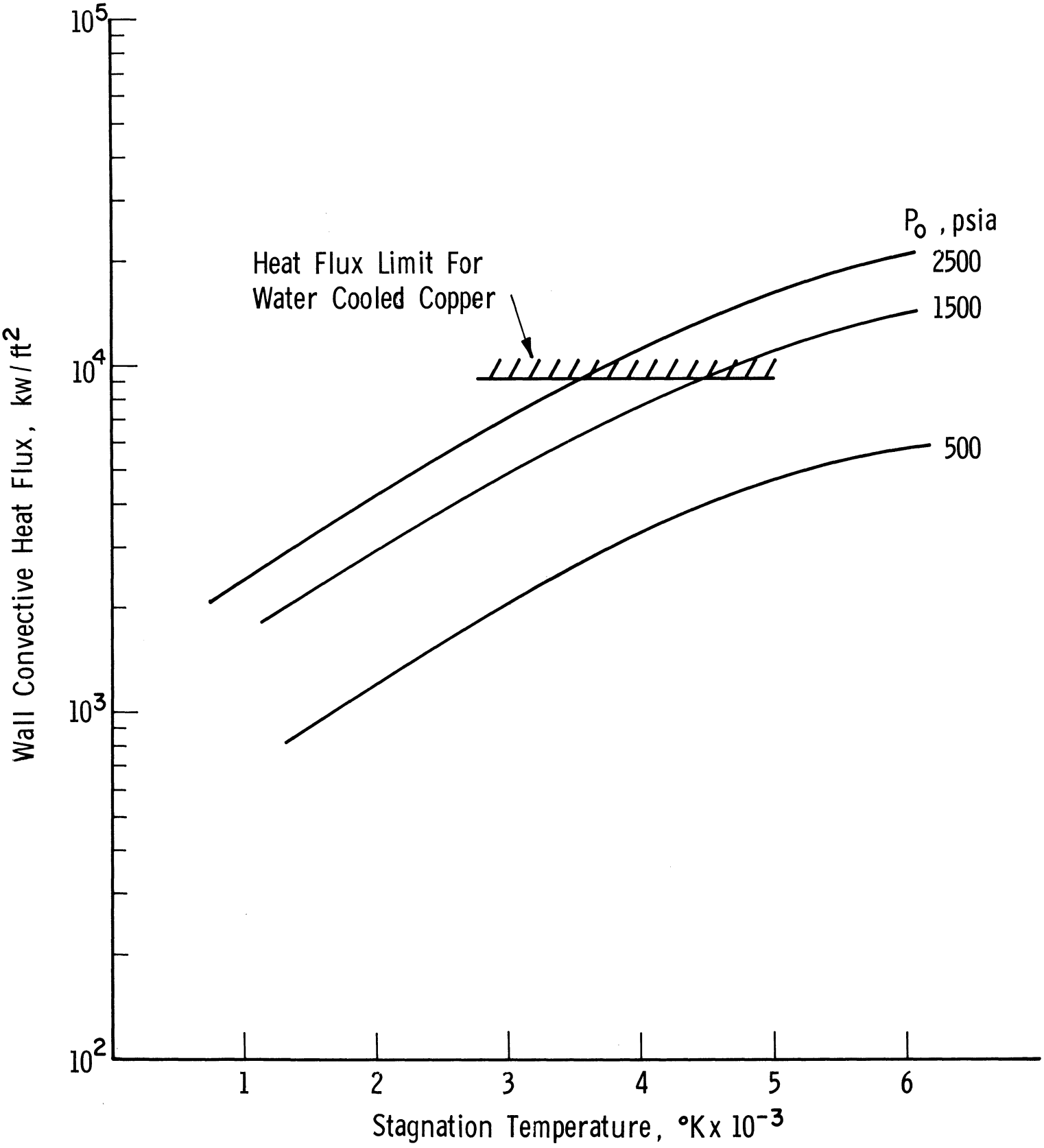

FIG. 10. NOZZLE WALL HEAT FLUX.

IV. MATERIAL SELECTION

Since the temperature of the gas confined by the arc heater is above the melting point of available metals and refractory materials, a conductive material in conjunction with a cooling scheme is required. This scheme, however, introduces temperature gradients in the material which can cause high thermal stress. Coupled with this are the stresses due to the high pressure levels so that the requirement of high strength at elevated temperatures is also necessary.

If one is to survey available materials for the purposes of arc heater construction a meaningful guide to material selection must be made. One such comparison will be made by looking at a simple analytic study of the stress in the arc chamber wall. The total stress is assumed to be the sum of the stress due to chamber pressure differential and the thermal stress from the temperature difference across the wall.

If we idealize the chamber as a thin walled, semi-infinite cylinder the stress can be expressed as follows:

$$\begin{aligned} \sigma_{total} &= \sigma_{thermal} + \sigma_{pressure} \\ &= \frac{E\alpha\Delta T}{2(1-\mu)} + \frac{\Delta PD}{2t} \end{aligned} \tag{59}$$

We can get Eq. (59) in terms of material properties by using the Fourier heat conduction equation. Substituting for the wall thickness, t, its equivalent $k\Delta T/q$:

$$\sigma_{total} = \frac{E\alpha\Delta T}{2(1-\mu)} + \frac{\Delta PqD}{2k\Delta T} \tag{60}$$

so

$$\frac{d\sigma_{total}}{d(\Delta T)} = \frac{E\alpha}{2(1 - \mu)} - \frac{\Delta PqD}{2k\Delta T^2} \tag{61}$$

Minimizing σ_{total} allows a solution for the minimum stress at a given ΔT

$$\Delta T = \left[\frac{qD\Delta P(1 - \mu)}{\alpha kE}\right]^{1/2} \tag{62}$$

Substituting into Eq. (60) gives

$$\sigma_{min} = \left[\frac{E\alpha qD\Delta P}{k(1 - \mu)}\right]^{1/2} \tag{63}$$

Therefore any material used must have an allowable stress equal to or greater than σ_{min}

If for the moment we let the allowable stress be equal to σ_{min} and assume μ to be constant (Poisson's ratio is generally 0.25 to 0.33 and does not vary appreciably for most materials), a figure of merit can be established for any material.

$$\sigma^2_{allowable} = \frac{E\alpha qD\Delta P}{k(1 - \mu)}$$

or, (64)

$$\frac{\sigma^2_{allowable}\, k}{E\alpha} = \frac{qD\Delta P}{(1 - \mu)}$$

We now have a relationship between the physical properties of a material and the parameters pertinent to the design of the arc heater. Therefore, allowable stress and thermal conductivity of the material should be high while the modulus of

elasticity and thermal expansion coefficient should be small. The higher this ratio the more effectively the material can withstand high pressures and high heat loads.

Letting $(\sigma^2_{\text{allowable}}\ k/E\alpha) = \beta$, we can now survey available materials. Since the material is subjected to high heat load, the properties will be taken at a temperature on the order of 600°F. The following table shows the pertinent properties of a number of commercially available metals.

TABLE III

Material	σ_{allow}	k	α	E	β
	psi $\times 10^{-3}$	$\frac{\text{BTU-ft}}{\text{hr ft}^2\ ^{\circ}\text{F}}\ \frac{1}{F^{\circ}} \times 10^{6}$		psi $\times 10^{-6}$	$\times 10^{-8}$
Cu-Be (alloy 25) C. W. and H. T.	140	80	10	19	82.7
Cu-Be (alloy 50) C. W. and H. T.	90	135	10	17	64.3
Cu-Zr (.15% Zr) C. W. and H. T.	58	200	10	17	39.5
Tungsten	47	72	2.5	40	15.9
Molybdenum	35	75	2.5	40	9.2
Rene 41 (Nickel alloy)	140	6.3	7	30	5.9
Aluminum	20	116	13	10	3.58
Stainless Steel	100	9.3	10	29	3.2
Silver	8	240	11	8	1.75
V-36 (cobalt base alloy)	50	11	9	30	1.05
OFHC copper	8	225	10	17	.85
Columbium	10	31	3.5	14	.63
Monel	22	17	10	24	.343

Table III indicates that the materials having the highest β are the copper alloys. However, this can only serve as a guide to material selection. It is yet to be determined if these materials can withstand the stress levels imposed by the arc heater.

If ΔP and D are held constant and q made a parameter, curves of σ_{min} can be shown versus $(E\alpha/(1 - \mu)$, Fig. 11. Typical values for the arc heater will be ΔP = 2500 psia, D = 6 in., and with q's of 100 to 500 KW/ft^2. Superimposed on Fig. 11 are the properties of the materials given in Table III. Here again the copper base alloys are the only materials with the proper physical characteristics which allow them to withstand the design temperatures and pressure loads. It remains, then, to determine which one of the two alloys is best suited to our particular design; copper-beryllium or copper-zirconium.

In view of the data presented in Table III and Fig. 11, it is interesting to note how poorly the standard OFHC-Copper compares to the other material. It appears to be of little use as an arc heater structural material. However, the effect of one very important variable is not shown in these data. Since the comparison is based on minimizing the stress levels in the material, for a given ΔT, it does not reflect the magnitude of the temperature differential necessary to transfer a given heat flux. A more complete comparison is made if the results of Eq. (62) are included. Using the same range of parameters as in Fig. 11, curves of ΔT versus αkE are shown in Fig. 12. Here the reason for using copper or copper alloys is evident. For a number of the materials showing favorable characteristics, by the previous comparison, we find here an increasing operating

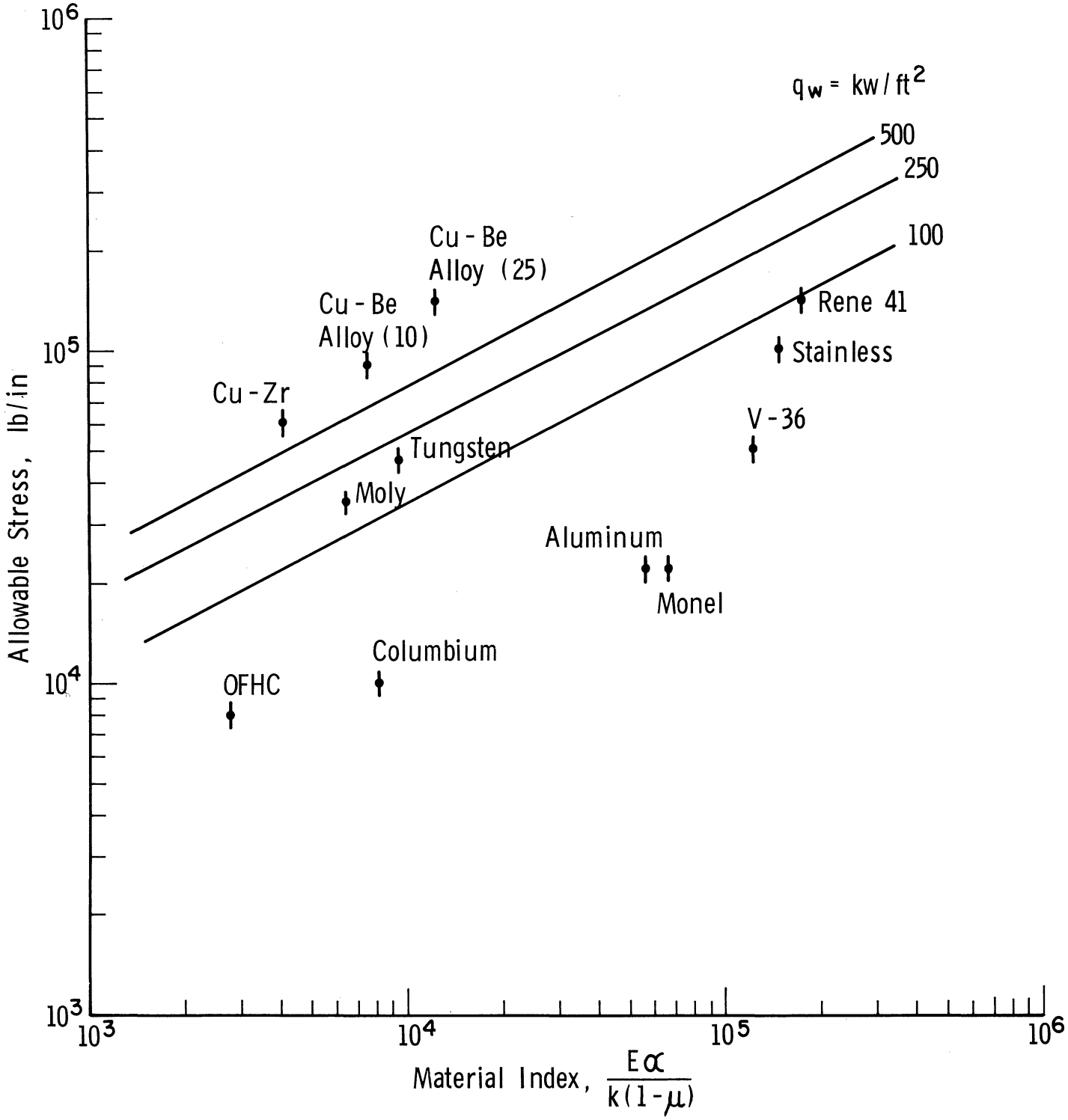

FIG. 11. ARC HEATER MATERIAL GUIDE vs STRESS

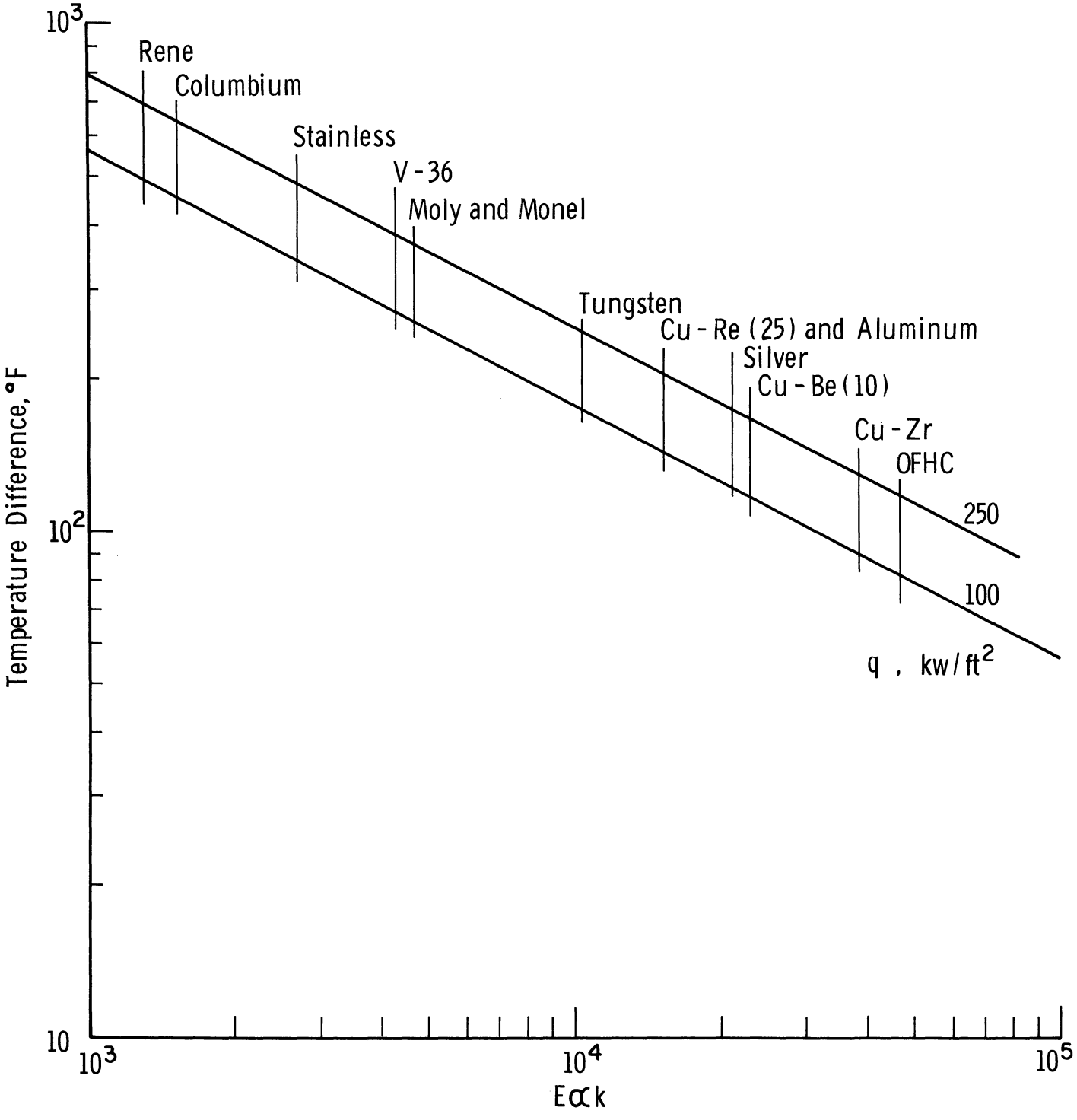

FIG. 12. ARC HEATER MATERIAL GUIDE vs TEMPERATURE DIFFERENCE.

temperature level. By this comparison OFHC-copper, and copper-zirconium would produce the lowest wall temperatures and hence have a simple cooling scheme. Regardless, while the standard copper was adequate for the low pressure arc heater, the two copper alloys still appear to be best suited for high pressure application.

If we look at the strength of both alloys at elevated temperatures, Fig. 13, we find that copper-zirconium has a slow falloff of strength with temperature, while copper-beryllium exhibits a rather sharp falloff. Although copper-beryllium has a 3 to 1 strength advantage over copper-zirconium, the falloff in strength with temperature is considered to be characteristic of a brittle material. Further evidence of the hot brittleness of copper-beryllium is indicated by the data shown in Table IV, (33).

TABLE IV

Test Temperature	Reduction of Area %	
	Cu-Be-Alloy 50	Cu-Z_R R_b 57
Room	28	67
200	30	70
300	33	--
400	25	70
500	10	--
600	6	70
800	--	67.5
1000	--	78.0

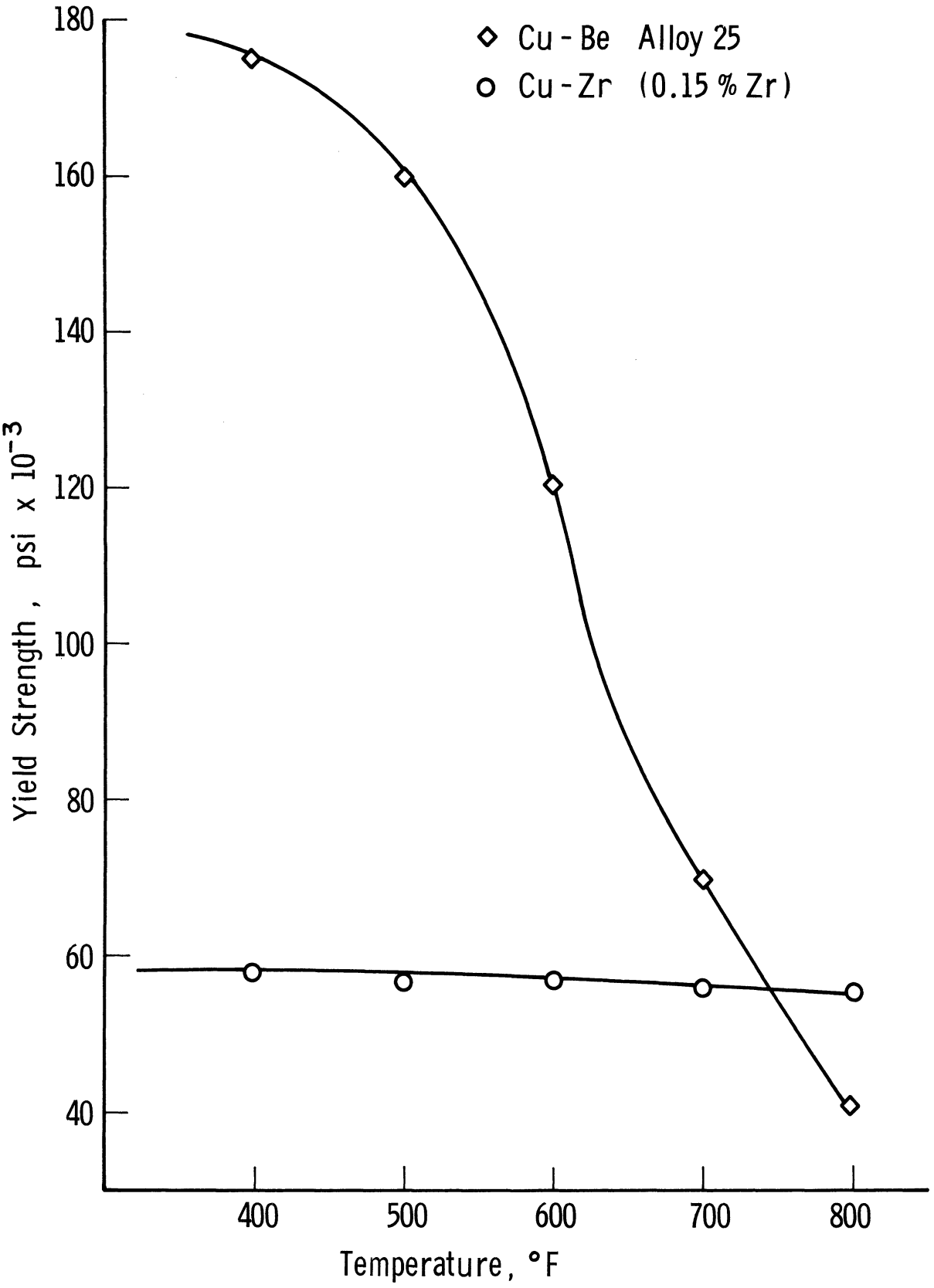

FIG. 13. EFFECT OF TEMPERATURE ON YIELD STRENGTH OF Cu-Zr AND Cu-Be.

Also, copper-beryllium alloys are notch sensitive beginning at $500^{o}F$. The reduction of area data in Table IV indicates that Cu-Zr is more ductile throughout the temperature range and that increasing the temperature of Cu-Be above $400^{o}F$ causes increasing brittleness in the material.

Although Cu-Be has a room temperature yield strength advantage over Cu-Zr, it is the notch sensitivity and brittle character of Cu-Be which makes it undesirable for the arc heater material. The arc chamber design will incorporate threads as a means of mounting both the end closures and electrode glands so that a material with notch sensitivity is not desirable. It is concluded that a copper-zirconium alloy is the best material for this particular application.

V. STRESS ANALYSIS

The physical model of the arc heater's chamber, nozzle, and cooling system upon which the stress calculations are based is shown in Fig. 14. The principal features are that the wall is unrestrained axially with no external loads imposed on either the arc chamber or nozzle. Therefore all wall loading arises from pressure and thermal differentials. The effective wall thickness is also assumed to end just below the spiral groove in the chamber or nozzle outside surface. All material properties used are those derived from tests subjecting material samples to "short term" heating. Properties of interest for copper-zirconium are shown in Fig. 15 and Table V, (34).

TABLE V

Property	Cu-Zr
κ-Thermal Conductivity $\frac{\text{BTU-in.}}{\text{ft}^2\text{-sec} - {}^{o}\text{F}}$	.66
α linear coefficients of thermal expansion $1/F^{o}$	10×10^{-6}
E modulus of elasticity-lb/in.^{2}	1.6×10^{7}
μ Poisson's Ratio	0.33

The octahedral shearing stress theory is the basis for determining the loads required to cause material failure by yielding. The maximum octahedral stress

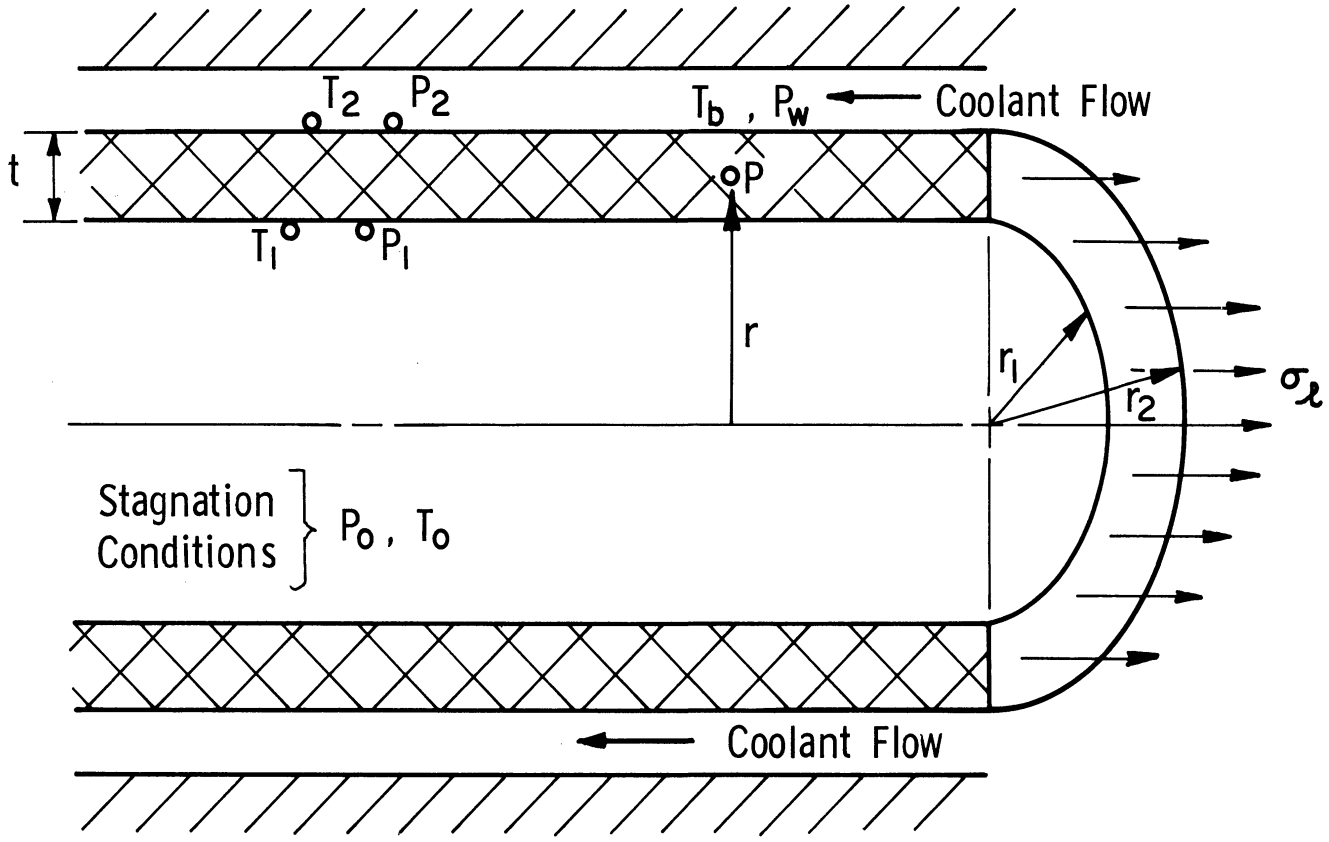

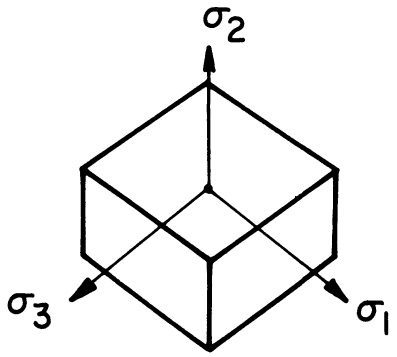

FIG. 14. MODEL FOR ARC CHAMBER AND NOZZLE—THROAT STRESS ANALYSIS.

at a point in the material must not exceed the allowable stress. Values of heat flux, wall thickness, and gas side wall temperature are chosen as the independent variables and varied over limited ranges. Optimum wall thickness and wall temperature are determined by plotting various combinations of the independent parameters.

Consider the free body in Fig. 14, which shows a section of the particular wall subjected to pressure and temperature differentials. For a thick walled cylinder, the various normal stresses are expressed as:

Longitudinal Stress:

$$\sigma_\ell = \frac{P_1 r_1^2}{r_2^2 - r_1^2} \tag{65}$$

Circumferential Stress:

$$\sigma_t = \frac{P_1 r_1^2 - P_2 r_2^2 + \frac{r_1^2 r_2^2}{r^2}(P_1 - P_2)}{r_2^2 - r_1^2} \tag{66}$$

Radial Stress:

$$\sigma_r = \frac{P_2 r_2^2 - P_1 r_1^2 + \frac{r_1^2 r_2^2}{r^2}(P_1 - P_2)}{r_1^2 - r_2^2} \tag{67}$$

Thermal Stress for thin wall cylinder:

$$\sigma_{th} = B_r (T_1 - T_2) \tag{68}$$

For steady state heat transfer the thermal stress coefficient is expressed as:

$$B_r = \frac{E\alpha}{2(1 - \bar{\mu})}\left[\frac{2r - (r_2 + r_1)}{(r_2 - r_1)}\right] \tag{69}$$

The three principal stresses at a point, P, in the material for any wall location in the cylinder are as follows:

$$\left.\begin{aligned} \sigma_1 &= \sigma_\ell + \sigma_{th} \\ \sigma_2 &= \sigma_R \\ \sigma_3 &= \sigma_t + \sigma_{th} \end{aligned}\right\} \tag{70}$$

The preceding may be substituted into the octahedral shearing stress relation which is written

$$\tau_c = \frac{1}{3}\left[(\sigma_1 - \sigma_2)^2 + (\sigma_2 - \sigma_3)^2 + (\sigma_3 - \sigma_1)^2\right]^{1/2} \tag{71}$$

Allowable octahedral shear stress:

$$\tau_A = \frac{\sqrt{2}}{3}\sigma_e \tag{72}$$

Resulting in a safety factor,

$$N = \frac{\tau_A}{\tau_c} \tag{73}$$

Taking a heat balance on an element $\Delta\ell$ of the arc chamber wall

$$Q = \frac{\bar{k}}{t_w} 2\pi\, r_m\, \Delta\ell\, (T_1 - T_2)$$

or,

$$T_1 - T_2 = \frac{Q\, t_w}{2\pi\, r_m\, \Delta\ell\, \bar{k}} = \frac{q\, t_w}{\bar{k}} \tag{74}$$

There are two criteria that can be used to establish an optimum wall thickness for the chamber or nozzle. One criterion is to assume that the material is most efficiently loaded when the total combined stress is equally divided between the inside and outside wall elements, i. e.

$$(\sigma_1 - \sigma_2)^2 + (\sigma_2 - \sigma_3)^2 + (\sigma_3 - \sigma_1)^2 \Big|_{r_1} = (\sigma_1 - \sigma_2)^2 + (\sigma_2 - \sigma_3)^2 + (\sigma_3 - \sigma_1)^2 \Big|_{r_2} \tag{75}$$

The other criterion is to find the point in the wall where the stress is the maximum and independent of wall thickness. The latter criterion is used in the ensuing stress analyses on the arc chamber and nozzle.

A. ARC CHAMBER

From this general analysis it is apparent that numerous solutions are possible, each dependent on the particular assumptions made at various stages of the calculations. These assumptions are quite arbitrary, provided they tend toward the functional purpose of the design and meet the requirements of practicability in manufacturing and assembly. In the following sections, a number of assumptions will be made and values used without argument or presentation of studies establishing a standard of "best possible" value. In these instances, it will be the basic

design ground rules and/or arc heater support equipment which will dictate that particular assumption.

Listed below are the design parameters for the arc chamber:

Chamber pressure, psia	2500
Chamber inside radius - in.	3
Cooling water pressure, psia	250

Mechanical and physical properties of the chamber materials are snown in Fig. 15 and Table V. It should be noted that the values used result from "short-term" tests at elevated temperatures on small specimens, with optimum cold working and heat treatment. These data show high tensile properties but represent the only information that could be obtained on the alloy. Final values of tensile properties will depend, of course, on the material fabricator's heat treating and cold working facilities.

In applying the stress equations to the arc chamber wall, it is assumed that the pressure stress is created by the difference between the cooling water pressure and the arc heater stagnation pressure. Since the radial stress contributes very little to the total combined stress, the stress system is also assumed to be biaxial. This allows, σ_2, to be dropped from Eq. (71). A significant reduction in the number of calculations can also be realized if the dependence on the variable, r, can be eliminated.

1. Point of Maximum Stress

Equations (65) through (69) indicate that the point of maximum pressure or thermal stress occurs on the inside of the wall surface. However, considering

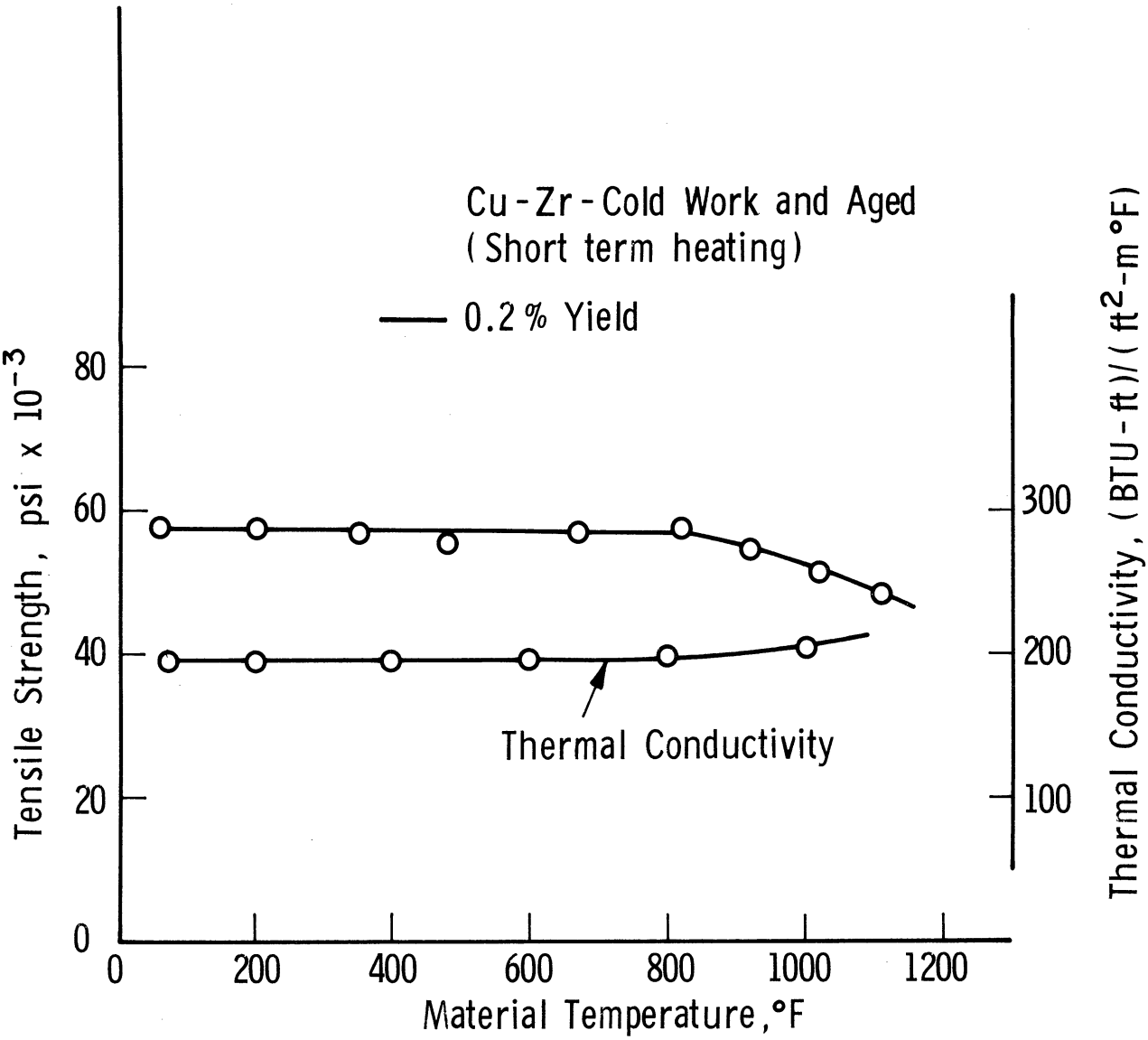

FIG. 15. EFFECT OF TEMPERATURE ON THE PROPERTIES OF Cu-Zr

the total stress at a point, the thermal stress is subtractive on the inside and additive on the outside of the wall. The difference between the stress at the inner and outer surface is

$$\sigma_1\Big|_{r_2} - \sigma_1\Big|_{r_1} = (B_{r_2} - B_{r_1})(T_2 - T_1) \tag{76}$$

$$\sigma_1\Big|_{r_2} > \sigma_1\Big|_{r_1} \tag{77}$$

and

$$\sigma_3\Big|_{r_2} - \sigma_3\Big|_{r_1} = -(P_o - P_w) + (B_{r_2} - B_{r_1})(T_2 - T_1) \tag{78}$$

or

$$\sigma_3\Big|_{r_2} > \sigma_3\Big|_{r_1} \tag{79}$$

if

$$(B_{r_2} - B_{r_1})(T_2 - T_1) > (P_o - P_w) \tag{80}$$

Therefore the effect of thermal stress is to shift the maximum stress point to the outer surface of the wall. Thus the maximum stress point will be at the outer surface and invariant if Eq. (80) is satisfied.

For the purposes of the analysis on the arc chamber and nozzle it is necessary to establish whether the magnitude of the thermal stresses anticipated will shift the point of maximum stress. To estimate these levels the following analysis is

made assuming, for the moment, that the various stresses can be found using the "thin wall" stress equations. Rewriting Eq. (80), we have the requirement.

$$2B\Big|_{r_2}(T_2 - T_2) > (P_o - P_w) \tag{81}$$

or

$$\sigma_{th} > \frac{(P_o - P_w)}{2} \tag{82}$$

Letting

$$\sigma_{th} = \frac{E\alpha\Delta T}{2(1 - \mu)} \tag{83}$$

and including the Fourier heat conduction equation gives,

$$\sigma_{th} = \frac{E\alpha qt}{2(1 - \mu)\, k} \tag{84}$$

The minimum wall thickness, t, is established by pressure stress requirements:

$$t = \frac{\Delta P D_m}{2\sigma_e} \tag{85}$$

Therefore

$$\sigma_{th} = \frac{E\alpha q\Delta P D_m}{4(1 - \mu)\, k\sigma_e} \tag{86}$$

This must be greater than $\Delta P/2$ or

$$\frac{E\alpha q D_m}{4(1 - \mu)\, k\sigma_e} > \frac{1}{2} \tag{87}$$

For a given material and size, a minimum heat flux can now be established.

For our particular material this would correspond to heat fluxes into the arc chamber wall greater than 35 KW/ft^2, and greater than 200 KW/ft^2 into the nozzle wall. Therefore, for the heat loads considered (Fig. 9 and 10), the point of maximum stress will be on the outer surface and invariant with wall thickness.

2. Optimization of Wall Thickness

The arc chamber is the component most affected by the increase in heat flux at increasing pressure level. However, the main emphasis is placed on operation at the high pressures and, therefore, its design is slanted toward a structure capable of withstanding the design pressure at the highest possible thermal load.

To help establish the pertinent arc chamber dimensions, a computer program using Eq. (65) through (74) was utilized. The chamber stress was calculated for various combinations of wall thickness, heat load, and stagnation pressures. Figures 16 through 19 show the results of this analysis.

Examination of the generated data revealed that a heat flux of 500 KW/ft^2 at a stagnation pressure of 2500 psia could be handled using copper-zirconium as the arc chamber material. Safety factors at various heat fluxes and two stagnation pressures are shown in Fig. 16 and 17. The safety factor is as defined in Eq. (73). Superimposed on these figures are lines of constant gas side wall temperature, T_w. These values are obtained assuming a cooling system which allows no localized boiling. As shown, the wall temperature would not exceed 500^{o}F. Therefore the previous assumption, used in the section on material selection, of an average material temperature below 600^{o}F will be realized.

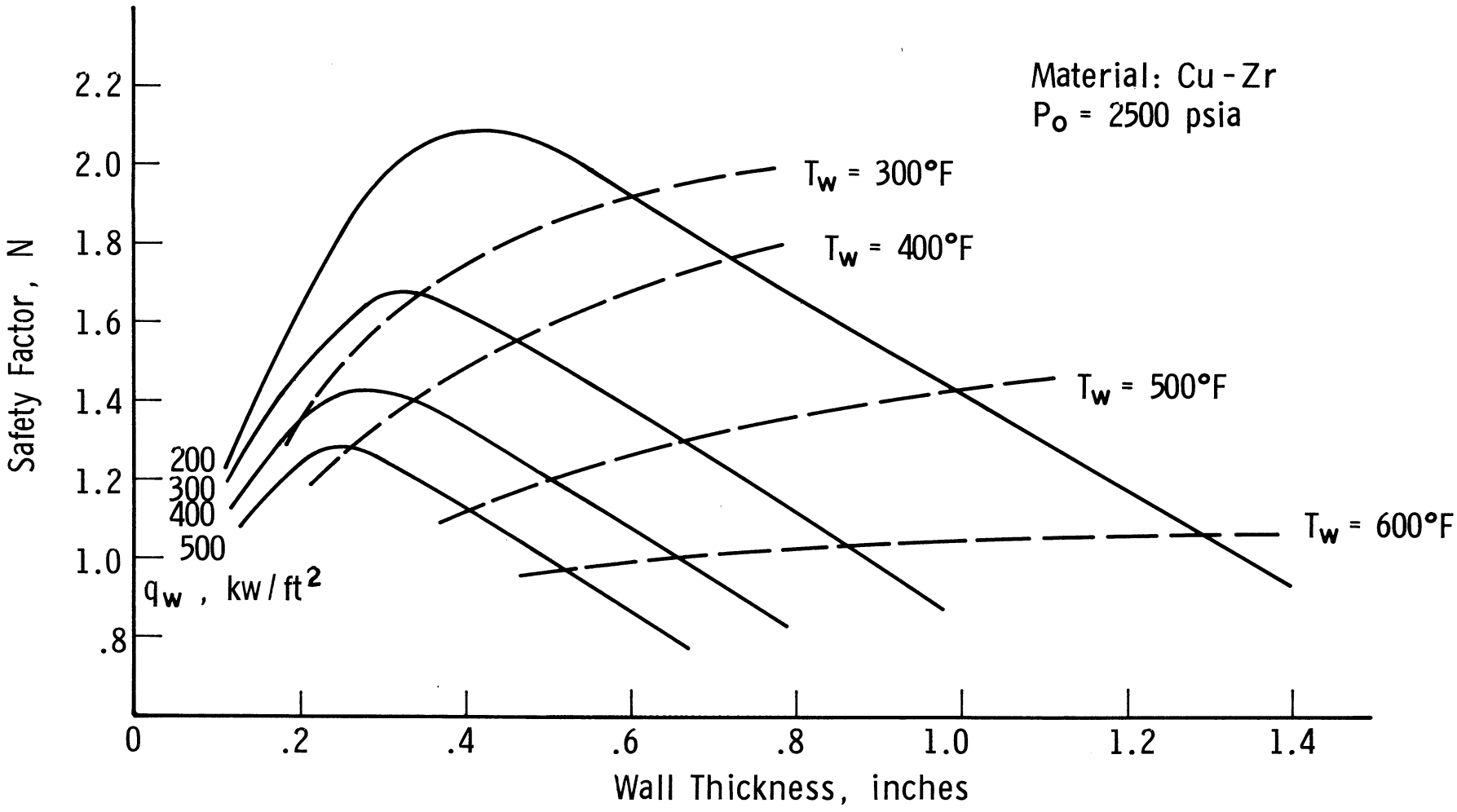

FIG. 16. SAFETY FACTOR vs ARC CHAMBER WALL THICKNESS

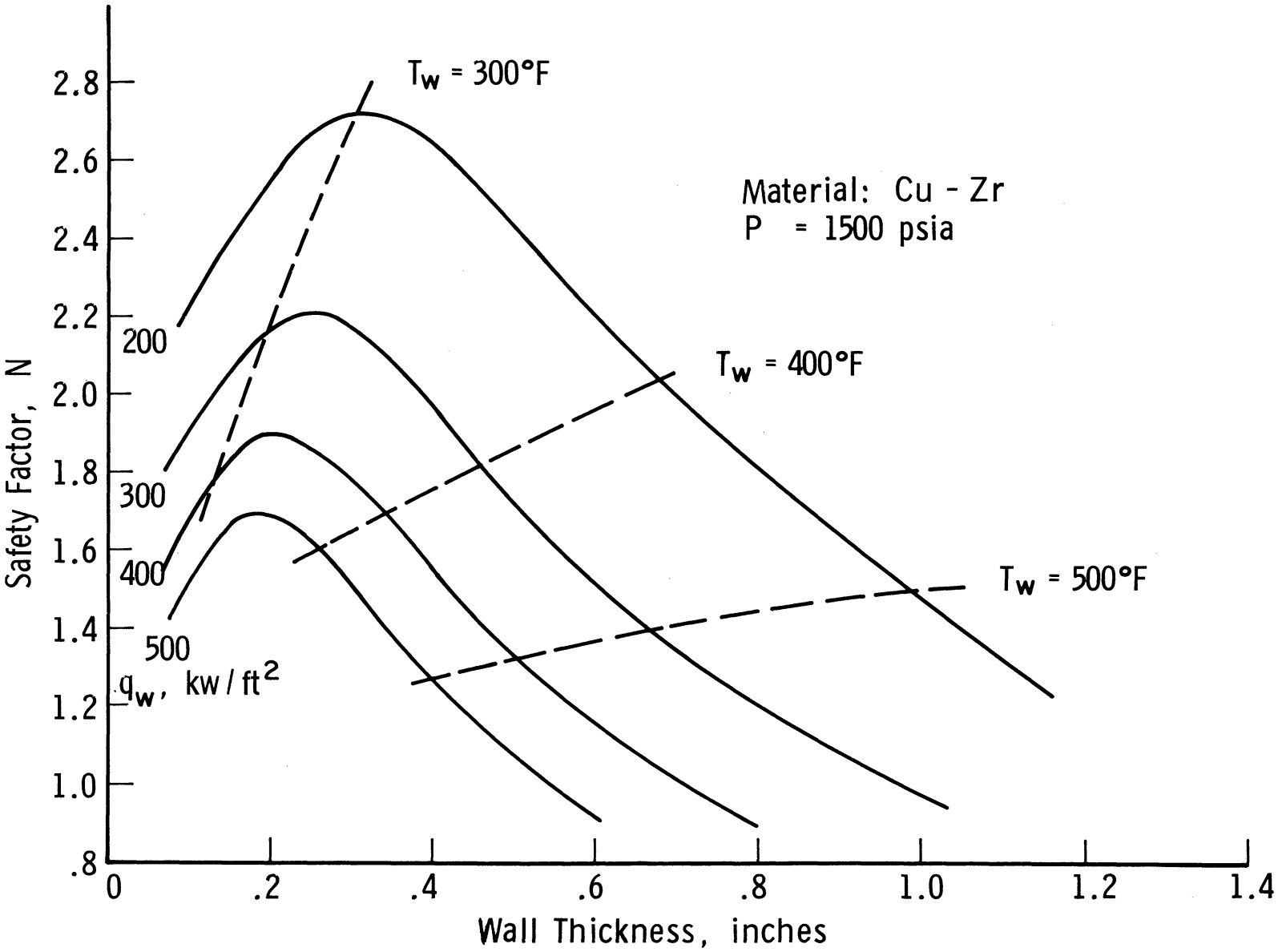

FIG. 17. SAFETY FACTOR vs ARC CHAMBER WALL THICKNESS.

These plots would indicate an optimum wall thickness of 0. 25 in. for the case of highest pressures and heat fluxes. This wall thickness is impractical, however, when one considers the overall design of the arc chamber. Since the arc heater end closures are attached by threads in the chamber wall, the effective wall thickness would be reduced to a value smaller than required to counteract pressure stresses alone. This design feature coupled with the emphasis on high pressure levels, led to a final wall thickness of 0. 6 in. In doing so, the resulting heat flux that can be carried by the chamber wall at the 2500 psia level will be 400 KW/ft^2. A plot of safety factor versus wall heat flux for this wall thickness at two stagnation pressure levels is shown in Fig. 18. The relatively small effect that the pressure stress, in comparison to the thermal stress, has on the safety factor is apparent.

The calculated stresses used to determine the safety factor are those at the outer surface of the arc chamber wall since maximum stress occurs at this point. Figure 19 presents the variation of safety factor through the arc chamber wall. Further, the results of the stress calculation, if reflected back to the chamber heat transfer analyses, would tend to lower the allowable stagnation temperature levels at 2500 psia. This effect is shown on Fig. 9.

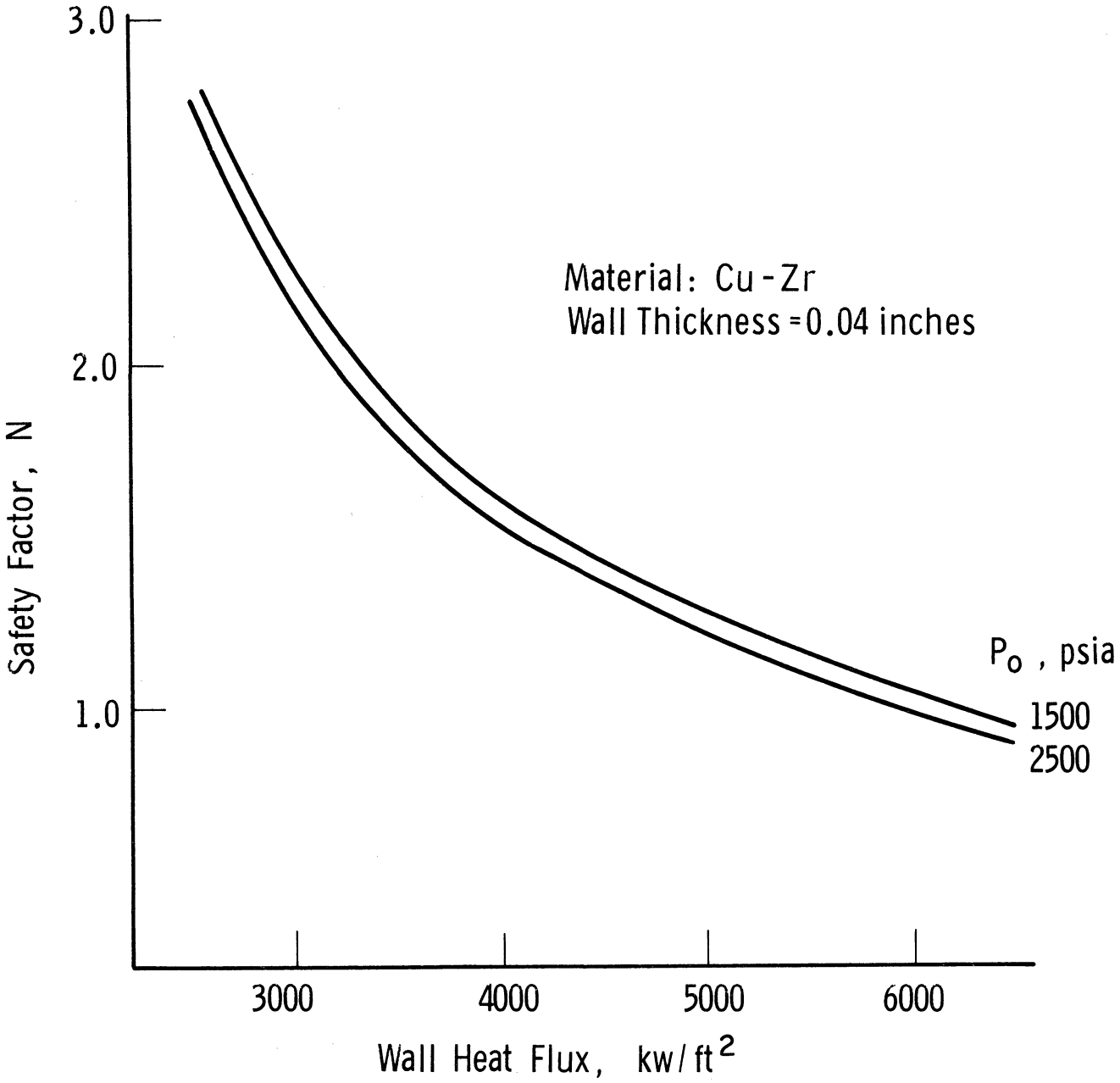

FIG. 18. VARIATION OF SAFETY FACTOR WITH ARC CHAMBER HEAT FLUX.

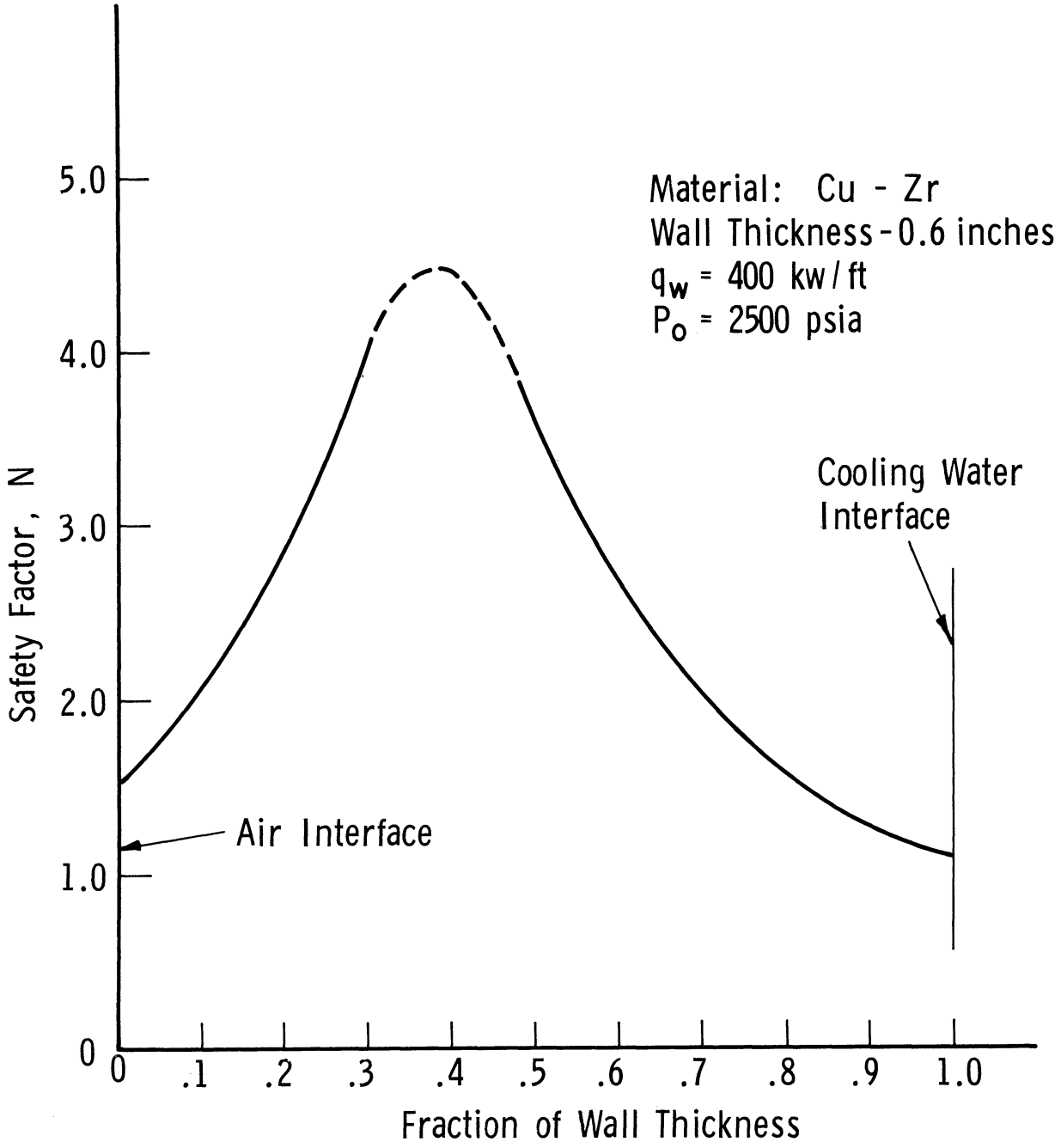

FIG. 19. VARIATION OF SAFETY FACTOR THROUGH THE ARC CHAMBER WALL.

B. NOZZLE

As in the heat transfer study, the nozzle throat was selected as the point for the stresses calculations. It is assumed that the throat structure can also be modeled by the free body shown in Fig. 14. Again it is assumed that all wall stress is a result of pressure and temperature differentials. Copper-Zirconium will also be used for the nozzle, therefore the material properties will be those of Fig. 15 and Table V. Since the nozzle is used only to constrict the arc chamber flow it takes the form of an orifice.

The axial pressure stress at the throat is now due to the difference between the gas flow pressure distribution on the converging portion of the nozzle and the cooling water pressure acting on the cooling system geometry. The cooling water pressure for this analysis is assumed to be 250 psig. The radial pressure stress term P_1, is assumed to be functionally determined from the well known isentropic relationship given in Eq. (48). As in the case of the arc chamber, the isentropic exponent, γ, is assumed to be constant through the nozzle and a value of 1.2 to be representative for our enthalpy range. The resultant equation for radial pressure being

$$P_1 = .563\ P_o$$

For the range of throat wall heat flux shown in Fig. 9 and the nozzle geometry given in Fig. 20, the equations and computer program used to calculate the arc chamber stress levels was modified to give the stress levels at the nozzle throat. The throat wall stress was calculated for various combinations of wall

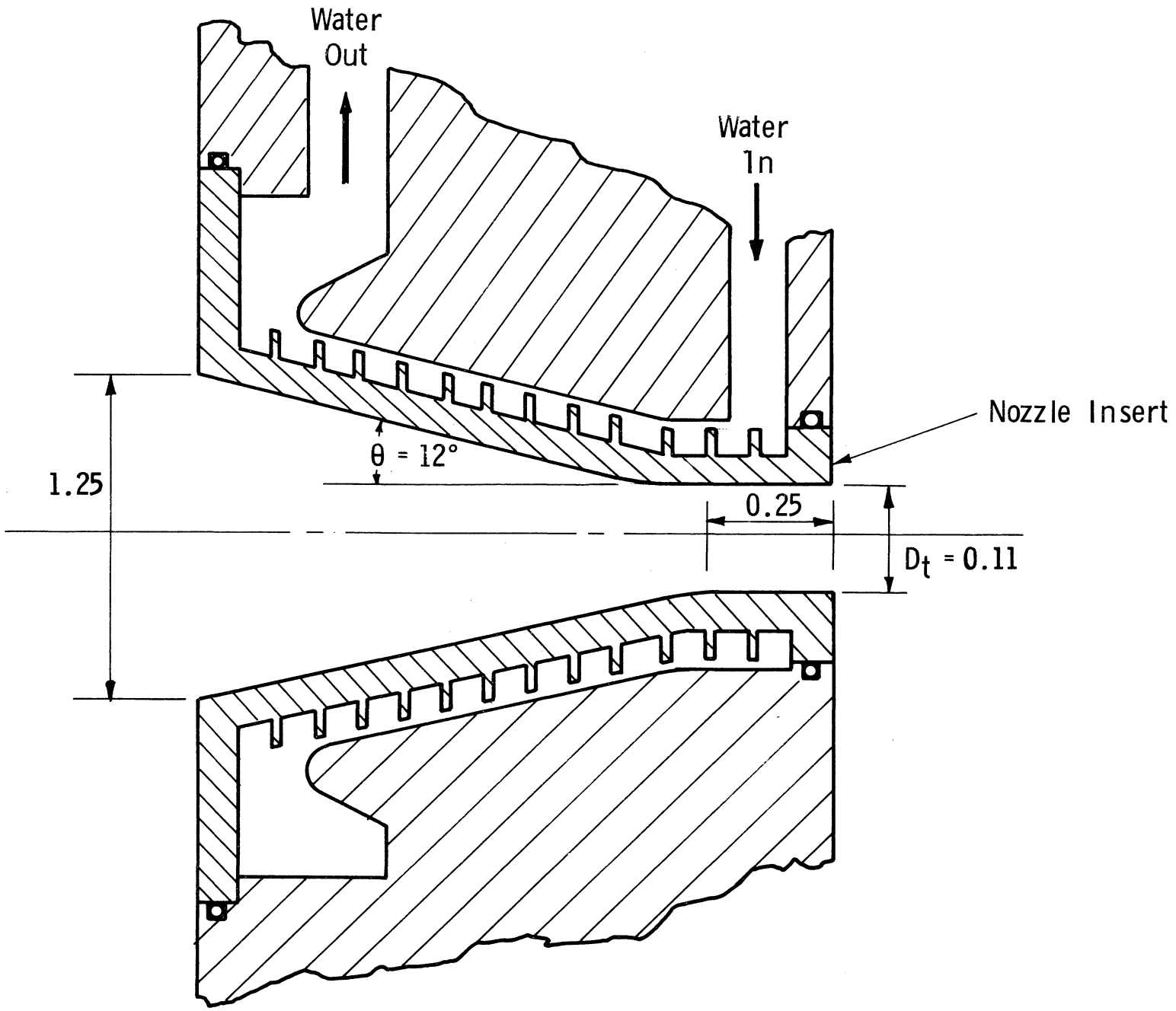

FIG. 20. SCHEMATIC OF ARC HEATER NOZZLE.

thickness, heat flux, and stagnation pressure. Figures 21 and 22 reflect the primary results of these calculations. The calculated stresses used to determine the safety factor are those at the outer surface of the nozzle throat wall.

These data would indicate an optimum wall thickness on the order of 0.01 in. for the nozzle throat. However, the machining of the nozzle throat to this dimension is quite impractical. The fabrication of the nozzle being the prime consideration, a wall thickness of 0.04 in. was the final choice. In doing so, the resulting heat flux that can be carried by the chamber wall at the 2500 psia level will be 5000 KW/ft^2. A plot of safety factor versus wall heat flux for this wall thickness at two stagnation pressure levels is shown in Fig. 22. The relatively small effect that the pressure stress has on the safety factor is again apparent.

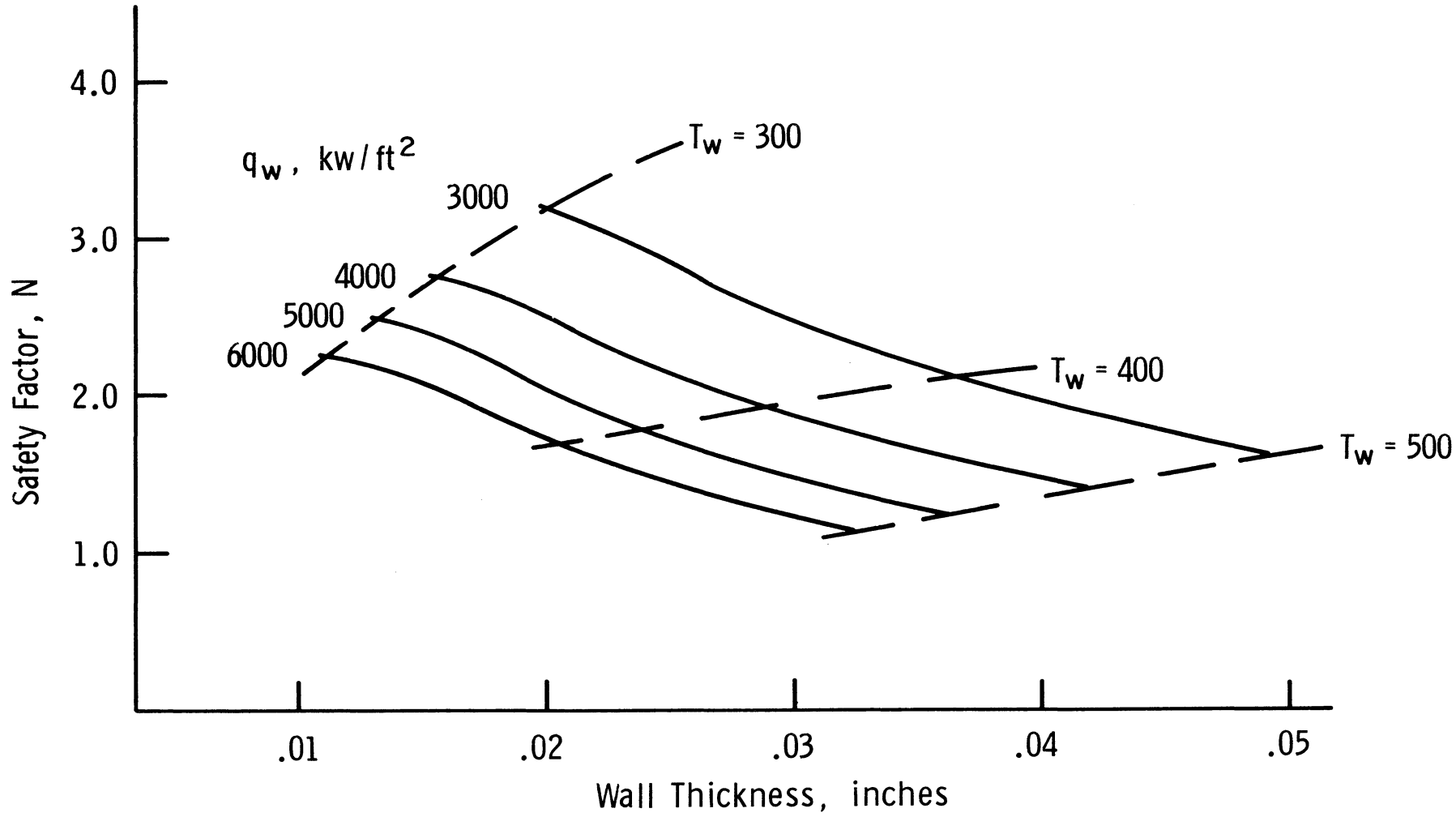

FIG. 21. SAFETY FACTOR vs NOZZLE THROAT WALL THICKNESS.

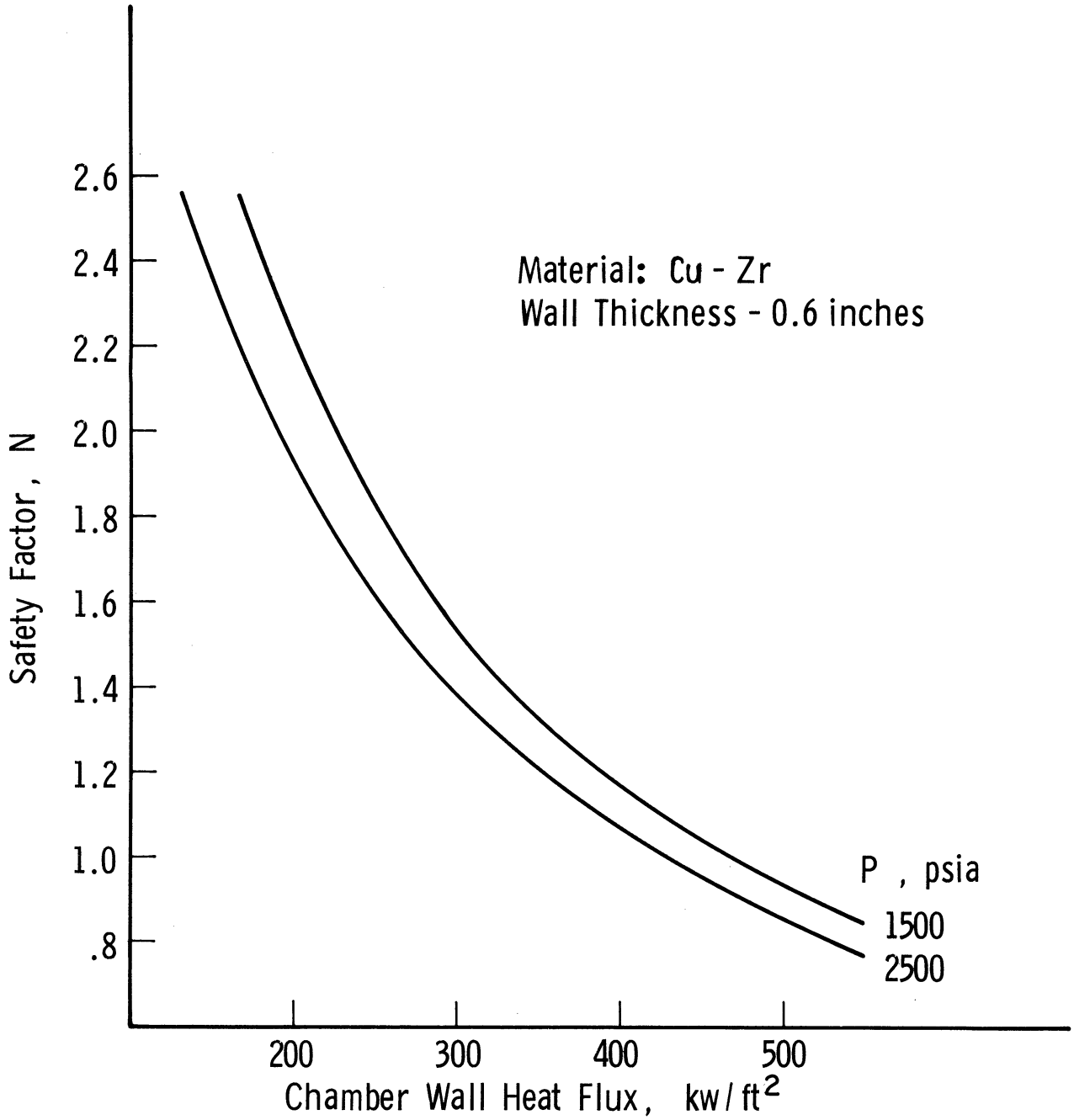

FIG. 22. VARIATION OF SAFETY FACTOR WITH NOZZLE THROAT HEAT FLUX.

VI. ARC CHAMBER COOLING SYSTEM

The general requirements on a cooling scheme for any component are:

1. The selected water flow rate and water passage configuration must ensure that the inside wall temperatures and thermal gradients through the wall are compatible with results of the stress analyses.
2. The water flow rate and pressures must be compatible with the available water supply system.
3. The flow rate must be appropriate to the demands on the pumping system by all components.
4. The cooling scheme will allow no localized boiling to occur.

If condition (1) is satisfied, tne required wall to water heat transfer coefficient may be determined. However, this will be a function of both flow rate and cooling passage geometry, with no optimum combination apparent. Limits will exist when one considers conditions (2), (3), and the requirement of fabrication practicability. Therefore, a cooling scheme that is commensurate to the existing pumping capabilities will be the strongest governing factor.

Just as in the case of the other aspects of the arc heater design, the unknown magnitude of radiation losses at elevated pressure tends to slant the design of this component towards a system capable of handling high thermal loads. Therefore, an arc chamber cooling scheme is needed which allows for the possible monitoring of temperature distribution along the chamber wall and easy introduction of additional cooling water if hot spots are detected.

The cooling scheme used is shown in Fig. 23. It consists of a continuous copper tube soldered to the outer wall of the arc chamber. A spiral groove (thread), is machined in the outer wall of the arc chamber and the copper tube placed in the groove. This arrangement gives a flexible, accessible cooling system and in addition the machining and installation effort for it is not overly complicated. This system requires the tube to be imbedded into the surface which can, by proper mating to the chamber, produce an effective cooling surface area greater than the surface of the arc chamber. Some simple expressions establish the depth the tube must be imbedded.

The required cooling surface per unit length of arc chamber is

$$A_c = \pi D_c \tag{89}$$

The surface area of the tube in contact with the chamber will be:

$$A_{Tube} = S\pi D_c N \tag{90}$$

$$S = r_t \theta \tag{91}$$

Equating the two surface areas we get the angle subtended by the tube surface to be:

$$\theta = 2 \text{ radians}$$

Some pertinent dimensions of the coil-surface interface are found from the geometric construction in Fig. 23.

$$d = r_t \left(1 - \cos \frac{\theta}{2}\right) \tag{92}$$

and

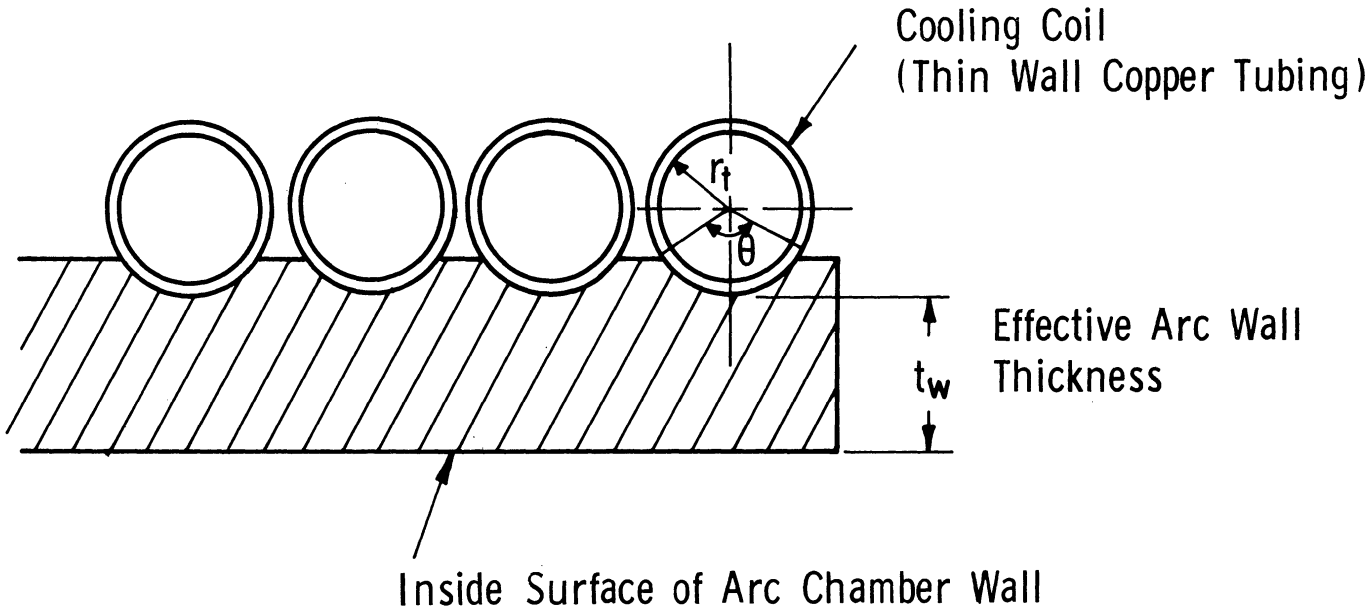

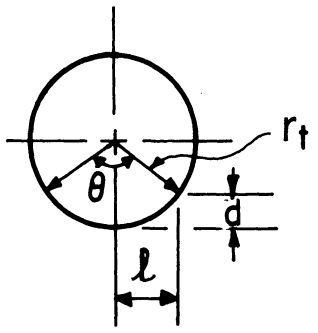

FIG. 23. ARC CHAMBER COOLING CONFIGURATION.

$$\ell = r_t \sin \frac{\theta}{2} \tag{92}$$

The range of cooling coil-tube sizes considered are from 0. 25 to 1. 0 in.

By imbedding a given cooling tube greater than d, an effective cooling surface greater than the cylindrical surface of the arc chamber can be realized. A "fin effect" can then be obtained, resulting in a cooling scheme more efficient than enclosing the arc chamber with a water jacket.

A. EFFECT OF A FINNED SURFACE

Although this effect is not as pronounced when using coolants with high heat-transfer coefficients it can be advantageous when using high conductivity materials. This is shown by equating the film-transfer resistance and the thermal-conduction resistance of a plane wall of thickness equal to one-half the fin thickness. The fin will result in high heat transfer rates if,

$$\frac{2k}{h\delta} > 1 \tag{93}$$

Typical values for copper and water would indicate:

$$\frac{2k}{h\delta} = O(\delta^{-1}) \tag{94}$$

For the geometry shown we will assume δ to be equal to 0. 32 r_t. Since the largest cooling coil-tube considered was 1 in. O. D. ,

$$\frac{2k}{h\delta} \geq 6.25 \tag{95}$$

Therefore, this cooling scheme can result in high cooling capabilities.

To better establish the effectiveness of this cooling scheme and/or an optimum height, a simple fin-surface geometry is needed. Considering the cooling-coil

geometry and assuming the fin height, S, to be no greater than the tube diameter

$$S \leq 1.54\, r_t \tag{96}$$

Taking the ratio of chamber diameter to fin heignt and assuming the cooling coil-tube to be 1 in. O. D. or smaller

$$S/D_c \leq 0.1 \tag{97}$$

Therefore, to establish the fin characteristics, the arc chamber surface is assumed to be a plane finned surface.

If we now analyze it as a fin of rectangular profile, we can establish an optimum cross section for a given Nusselt number range. Aviame and Little (35) gave a general derivation of this problem with optimum values as shown in Fig. 24. For our range of interest, the following values for fin height are indicated.

$$S = .21\, r_t \rightarrow .54\, r_t$$

Thus the imbedment depth into the chamber wall will vary from $0.75\, r_t$ to $1.07\, r_t$. Considering the fact that there will be some thermal contact resistance between the cooling coil and the arc chamber (conductivity of bonding material), one would like this contact surface to be as large as possible, within this optimum range. It was therefore concluded that the cooling coil would be imbedded one tube radius, resulting in both a low thermal contact resistance while still producing an optimum finned surface on the arc chamber.

The increase in heat rejection for this system is found by looking at a "surface effectiveness." This is the ratio of the heat rejected from a finned surface to the same heating surface with no fins. Letting this ratio be η and

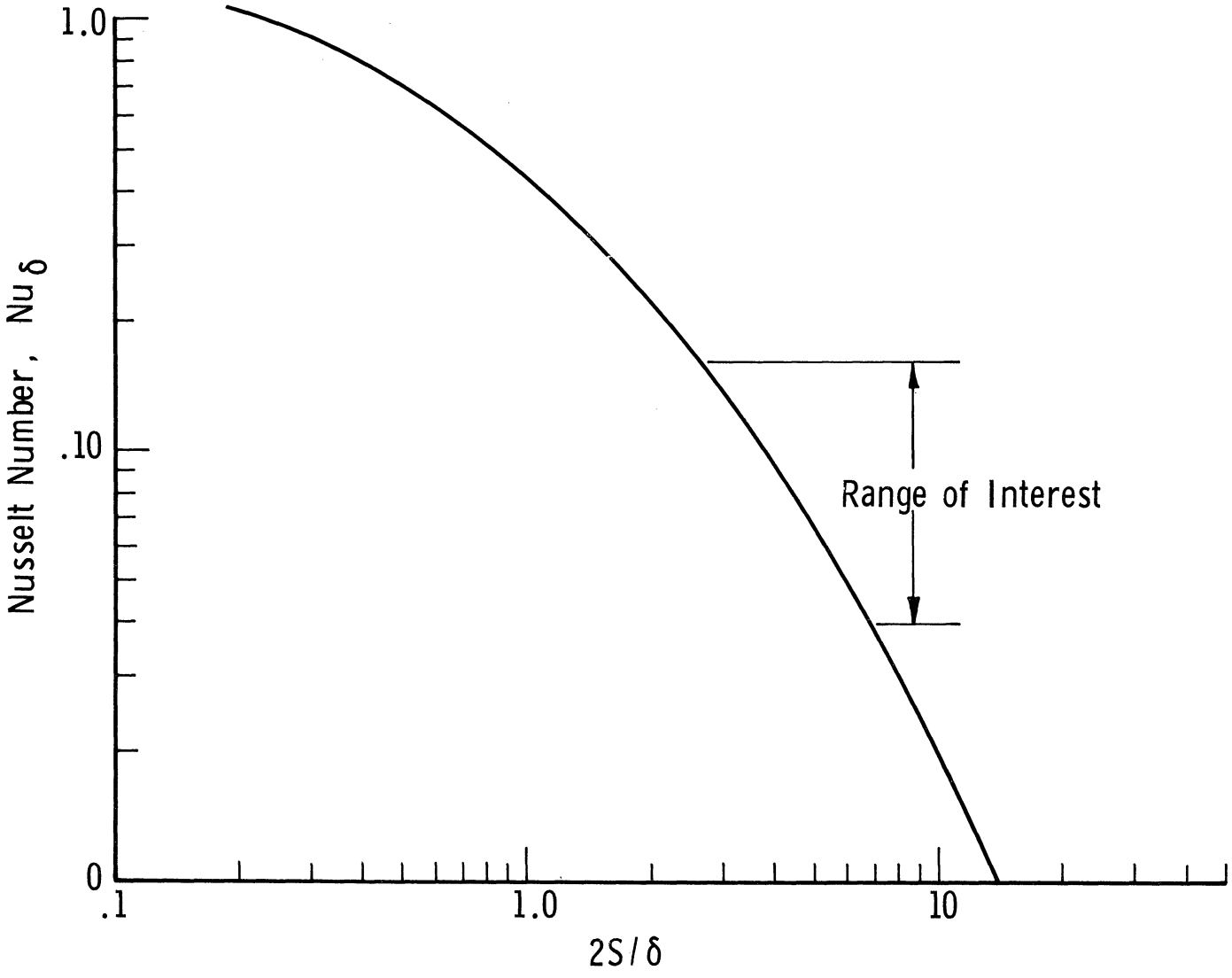

FIG. 24. OPTIMUM FIN CROSS SECTION vs. NUSSELT NUMBER

looking at a fin more representative of our specific design, i. e., fin of triangular profile,

$$q = L(2hk\delta)^{1/2} \frac{I_1 (2\sqrt{BS})}{I_o (2\sqrt{BS})} \Delta T \tag{98}$$

where, q, is the heat loss from the fin. Defining the heat loss from the surface without fin as

$$q_o = L\delta h \Delta T \tag{99}$$

then

$$\eta = q/q_o$$

$$= \left(\frac{2k}{\delta h}\right)^{1/2} \frac{I_1 (2\sqrt{BS})}{I_o (2\sqrt{BS})} \tag{100}$$

Substituting into Eq. (99) for the range of values previously used

$$2.0 \leq \eta \leq 3.0$$

The finned surface is, therefore, able to transfer 2 to 3 times that of a plane surface.

Equation (99) also shows that η varies inversely with tube size. Therefore, if the cooling system were optimized by this criterion, it would tend toward small tube sizes. This trend unfortunately increases the pumping requirements of the cooling system. Since the existing pumping system has moderate pressure capability it is expected it will strongly influence the final choice of tube size. The above analysis, however, does enter strongly, when one considers the heat transfer characteristics of the cooling coil.

B. COOLING COIL MASS FLOW CHARACTERISTICS

The flow through the cooling coil will be calculated by taking an energy balance across a typical section of the coil. The functional form and complexity of the equation will depend strongly on whether the flow can be considered laminar or turbulent. The laminar or turbulent nature of the flow will be felt not only in the equation describing the wall shear stress, but also help establish whether the curvature effects of the coil or nonisothermal character of the flow need be considered. Therefore,the Reynolds number regime for the flow through the coil must be established.

For flow through a tube the Reynolds number is expressed as

$$Re = \frac{4\dot{m}}{\pi D \mu} \tag{101}$$

The range of mass flows needed is estimated from an energy balance

$$q_c = \dot{m}\, C_p\, \Delta T \tag{102}$$

For $q_c > 50$ KW and assuming a maximum allowable temperature rise of $150^{O}F$

$$\dot{m} \geq 19 \text{ lb/min}$$

The corresponding Reynolds number range for the range of tube sizes considered is

$$Re \geq 1.4 \times 10^{4}$$

The frictional data of Nikuradse (36) on flow through smooth tubes would indicate the coil flow to be well into the turbulent regime.

Since the flow is turbulent, the effects of velocity profile distortion (curvature of coils) and dependence of fluid properties on temperature are not as pronounced (37). Therefore, the ensuing analysis will neglect them. It will be shown later that the nonisothermal value of the flow can be accounted for by evaluating the fluid properties at a "reference" temperature.

The pressure drop through the tubing is calculated from the well known relation,

$$\lambda = \frac{P_1 - P_2}{L} \frac{D}{4} \tag{103}$$

Introducing a resistance coefficient (friction factor)

$$\lambda = \frac{1}{8} f \rho \bar{u}^2 \tag{104}$$

Prandtl's equation (36) for f is used since it gives excellent agreement with the experimental data of Nikuradse over our particular Reynolds number range.

Defining the mean velocity of flow through the tube as

$$\bar{u} = \frac{4\dot{m}}{\rho \pi D^2} \tag{105}$$

and combining Eq. (103) through (105) we can plot the pressure required to pass a given mass flow through a specific tube size and length. These data are presented for a tube length of 50 ft for water at a mean temperature (T_b) of 100°F. The fluid properties used for this and the following analysis are those shown in Fig. 25.

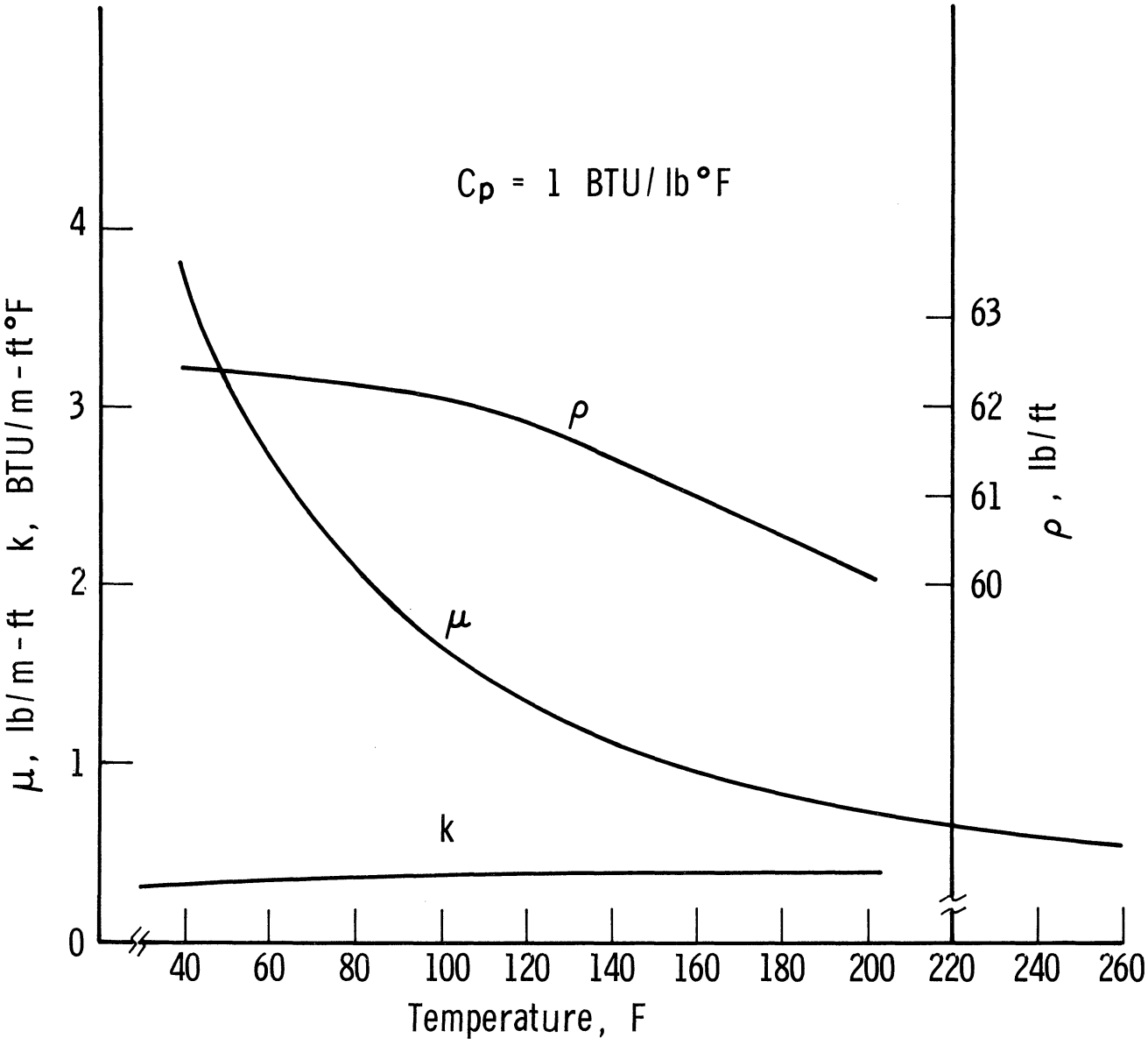

FIG. 25. VARIATION OF THE PROPERTIES OF WATER WITH TEMPERATURE.

Plots of ΔP and $\bar{u}$ versus $\dot{m}$ and tube outside diameter are given in Fig. 26 and 27. Superimposed on them are the maximum pressure capabilities of the existing laboratory pumps. The pressure data of Fig. 25 coupled with the Eq. (102) clearly indicate that the cooling coil tube must be larger than 0.3 in. if any but minimal arc chamber heat losses are assumed.

C. COOLING COIL HEAT TRANSFER CHARACTERISTICS

The following analyses are aimed at determining the range of tube diameters capable of handling the required heat loads with respect to their mass flow capability.

For the present we assume; (1) the fluid properties are constant, (2) the mean temperature at any radius does not vary with angular position or time, (3) there is no appreciable radial velocity, and (4) the tube flow is turbulent and fully developed. The latter assumption allows the equations to hold for the entire length of the cooling-coil. (The intake length for the development of the temperature field in turbulent tube flow is of the order of 10 diameters which, for our geometry, will be approximately 2% of the coil length.)

The order of the required heat transfer coefficient is established by equating the heat flow from the tube wall to the heat removed by the coolant. That is,

$$q_c = hA\,(T_w - T_b) = \dot{m}\,C_p\,(T_{out} - T_{in})$$

or (106)

$$h = \frac{\dot{m}\,C_p}{A}\,\frac{(T_{out} - T_{in})}{(T_w - T_b)}$$

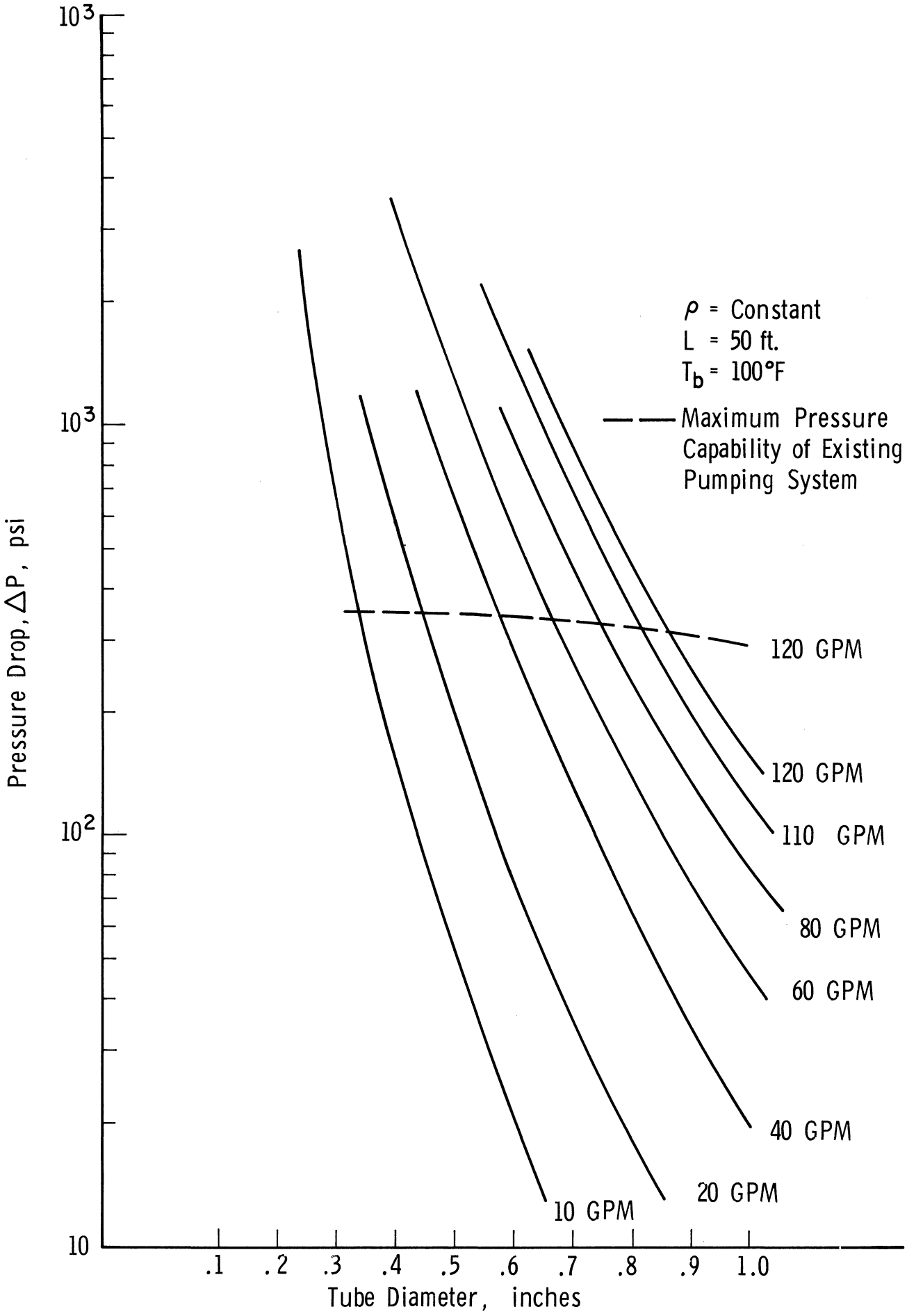

FIG. 26. EFFECT OF TUBE SIZE ON PUMPING REQUIREMENTS.

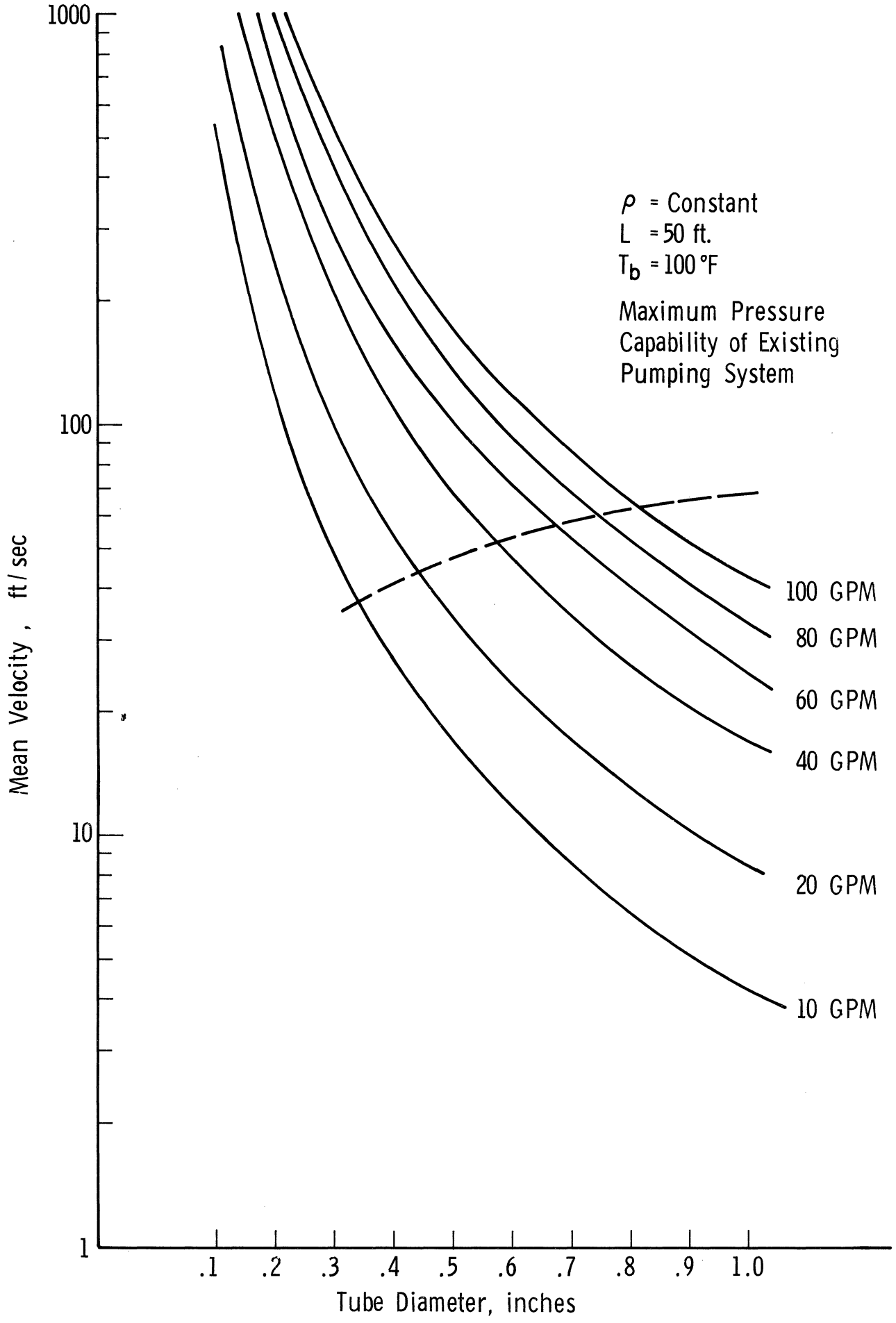

FIG. 27. VARIATION OF FLOW MEAN VELOCITY WITH TUBE SIZE.

For the purposes of this analysis, T_w is allowed to vary such that $(T_w - T_b)$ $= (T_{out} - T_{in})$. Equation (106) becomes

$$h = \frac{\dot{m} C_p}{A} \tag{107}$$

For our application this is considered to be the necessary heat transfer coefficient, i. e. the character of the tube flow must be such that it produces these values of h.

Combining this into a Nusselt number

$$Nu_{(required)} = \frac{\dot{m} C_p D_t}{Ak} \tag{108}$$

The presence of a finned surface on the arc chamber is felt through an "effective" area term in Eq. (108). To establish this area the heat transfer characteristics of a finned surface are investigated. In the previous sections it was shown that imbedding the cooling coil into the chamber resulted in a finned surface. Therefore we have an available heat transfer surface greater than the outer surface of the arc chamber. It was also shown that an optimum fin height is obtained if the tubing were imbedded about one tube radius into the arc chamber. The resultant surface area available for heat transfer, Fig. 22, is

$$A = \frac{\pi^2 D_c L}{2} \tag{109}$$

Equation (106) for the transfer of heat from the tube wall assumes the surface to be a uniform temperature T_w. The presence of the fins on the surface, however, create just the opposite effect. Due to the finite conductivity of the material

composing the fins, a temperature gradient exists along the fin. Therefore, the available surface at temperature, T_w, will be less than shown in the above equation. To accommodate the assumptions of Eq. (108) an "equivalent" fin surface area at temperature, T_w, is defined, which when added to the area between the fins results in what is considered the effective heat transfer surface area.

Equating the heat flow into the fin to the heat loss from this "equivalent" area

$$q_1 = - k A_b \frac{dT}{dn} = h A_e (T_w - T_b) \tag{110}$$

or

$$A_e = \frac{q_1}{h (T_w - T_b)} \tag{111}$$

In the previous section on the cooling requirements a surface effectiveness, η, was defined as the ratio of heat rejected from a finned surface to that of the same surface with no fins.

$$\eta = \frac{q_1}{h A_b (T_w - T_b)} \tag{112}$$

Substituting into Eq. (4)

$$A_e = \eta A_b \tag{113}$$

with

$$\eta \geq 1$$

The resulting expression for the "effective" heat transfer surface area is

$$A = A_c + \eta A_b \tag{114}$$

Equation (114) shows the effects of fins on the arc chamber wall. They essentially increase the area available for heat transfer by the amount, ηA_b. Rewriting Eq. (114) with respect to the cooling system geometry,

$$A = \pi L \left(D_c + \eta \left\{ 2 (r_t - \ell) [D_c + (R_t - d)] \right\} \right) \tag{115}$$

The actual heat transfer coefficient that characterizes the flow through the cooling coil is obtained from the equation given by Dittus and Boelter (38). That is,

$$\frac{hD}{k} = .023 \left(\frac{Du}{\nu} \right)^{0.8} \left(\frac{C_p \mu}{k} \right)^{0.4} \tag{116}$$

written in terms of Reynolds number, Prandtl number, and Nusselt number.

$$Nu = .023 (Re)^{0.8} (Pr)^{0.4} \tag{117}$$

with the Reynolds number and Prandtl number evaluated at the average fluid temperature.

Examination of Eq. (107) with respect to the coil mass flow characteristics indicates that the heat transfer coefficient necessary to remove a given heat flux from the arc chamber will increase as some power of the cooling coil tube diameter. The equation describing the actual heat transfer coefficient produced by the tube flow also shows a power law dependence. Hence, by using these equations, along with the data shown in Fig. 25, and iterating a tube diameter can be found beyond which the confined tube flow cannot transport the necessary heat flow.

To circumvent this process, curve fits were made on the data of Fig. 26 and 27. This coupled with the following equations allows for a solution in terms of tube diameter. Rewriting Eq. (99) for η in terms of Nusselt number

$$\eta = \frac{2k_{cu}\, D_t}{\delta\ Nu\ k_w}^{1/2} \frac{I_1\left[2\left(\frac{2\ Nu\ k_w\ S^2}{Dt\ k_{cu}\ \delta}\right)^{1/2}\right]}{I_o\left[2\left(\frac{2\ Nu\ k_w\ S^2}{D_t\ k_{cu}\ \delta}\right)^{1/2}\right]} \tag{118}$$

Assuming the following to represent the ratio of I_1 to I_o over our range of interest,

$$\frac{I_1(\alpha)}{I_o(\alpha)} = 0.45\ \alpha^{.558} \tag{119}$$

and substituting for k_w and k_{cu} gives

$$\eta = 9.27\ Nu^{-.22} \tag{120}$$

The "effective" heat transfer area is expressed as

$$A = 2.09 + 3.1\ Nu^{-.22} \tag{121}$$

The required Nusselt number can now be written

$$Nu = \frac{\dot{m}\ C_p\ D_t}{k_w\ (2.1 + 3.1\ Nu^{-.22})} \tag{122}$$

while the actual Nusselt number is

$$Nu = .023\ (N_{Re})^{.8}\ (N_{Pr})^{.4} \tag{123}$$

Equating Eq. (122) and (123) and substituting in values for (μ, C_p, k) the following expression in terms of the tube mass flow and diameter is obtained

$$\dot{m} D_t = .026 \left[\frac{\dot{m}}{D_t}\right]^{.8} + .08 \left[\frac{\dot{m}}{D_t}\right]^{.62} \tag{124}$$

Assuming the tube mass flow appropriate to the existing pumps can be expressed as

$$\dot{m} = 5.4 \times 10^{7} D_t^{2.61} \tag{125}$$

the following equation in terms of D_t is obtained

$$10.6 \times 10^{3} D_t^{2.61} - 8 D_t^{.288} - 1 = 0 \tag{126}$$

Solving the above for D_t gives

$$D_t = 0.6 \text{ in.}$$

Therefore the results of the previous analysis indicate an upper limit, on D_t of 0.6 in. A specific tube diameter in this range would be establisned by the total heat loss to the arc chamber cooling system. Since the cooling system is slanted toward a design capable of handling the highest possible heat loads, the largest commercially available tubing appropriate to the upper limit was chosen. The final choice was 5/8 in., thin wall copper tubing, with an inside diameter of 0.55 in.

D. COOLING SYSTEM PERFORMANCE

The following summarizes the performance of the arc chamber cooling scheme. It must be shown that the cooling scheme with the cooling-coil sized as

indicated will meet the basic requirements previously outlined. For this purpose a heat flux of 0. 5 Megawatts into the arc chamber wall is used and the system investigated to the extent that the maximum design arc chamber wall temperature is not exceeded.

In the previous analysis the fluid was assumed to be isothermal, i. e., fluid properties throughout the flow were constant and evaluated at T_b. Figure 25 indicates this to be a good approximation for all properties except the flow viscosity. This quantity in turn enters into both the equations describing the cooling coil mass flow and heat transfer characteristics.

Eckert (39) and Deissler (40) have both shown that this effect can be corrected by using the same equations, but with the fluid properties evaluated at a "reference" temperature. Following the reasoning of Ref. 38, the viscosity variation of the fluid is represented by a simple power function. Using as a base, the properties evaluated at the tube wall temperature, a "reference" temperature as a function of Prandtl number is calculated. Evaluating the flow Reynolds number and Prandtl number at this temperature corrects the tube flow pressure drop and Nusselt number for variable viscosity. The "reference" temperature, Tr, is defined as

$$Tr = R\,(T_w - T_b) + T_b \qquad (127)$$

where R is a function of Prandtl number. The values for R used were those given by Deissler (40).

The flow, Nusselt number, Prandtl number and friction factor have been evaluated at this temperature and the tube flow characteristic established

for a tube diameter of . 55 in. It is assumed that the water inlet temperature remained constant at 50°F. The pressure calculations also reflect the requirements for the velocity head and water saturation pressure, the latter required to prevent local boiling.

The characteristics of the arc chamber cooling system are summarized in Fig. 28 through 30.

Figure 28 shows the required pressure-mass flow for the arc chamber cooling system and indicates a maximum mass flow capability of 35 GPM with the existing pumping system. Figure 29 shows the effects of coolant mass flow on the arc chamber wall temperature. Superimposed on this plot are the maximum design chamber wall temperature and the maximum flow capability of the cooling system. These data show that the water flow requirements decrease rapidly with increases in chamber wall temperature. The required water pressure as a function of wall temperature, Fig. 30, show a minimum pressure point to exist at 420°F. Above this point the pressure required rises sharply due to the increased pressure needed to prevent local boiling. This latter effect is also reflected in Fig. 28. These data indicate that the arc chamber wall temperature can be maintained below the maximum design point of 600°F with the existing pumping system, the optimum occurring at a wall temperature of approximately 420°F. It is felt that the cooling scheme not only meets the basic requirements for the arc chamber, but has a fairly wide range in which these requirements can be realized.

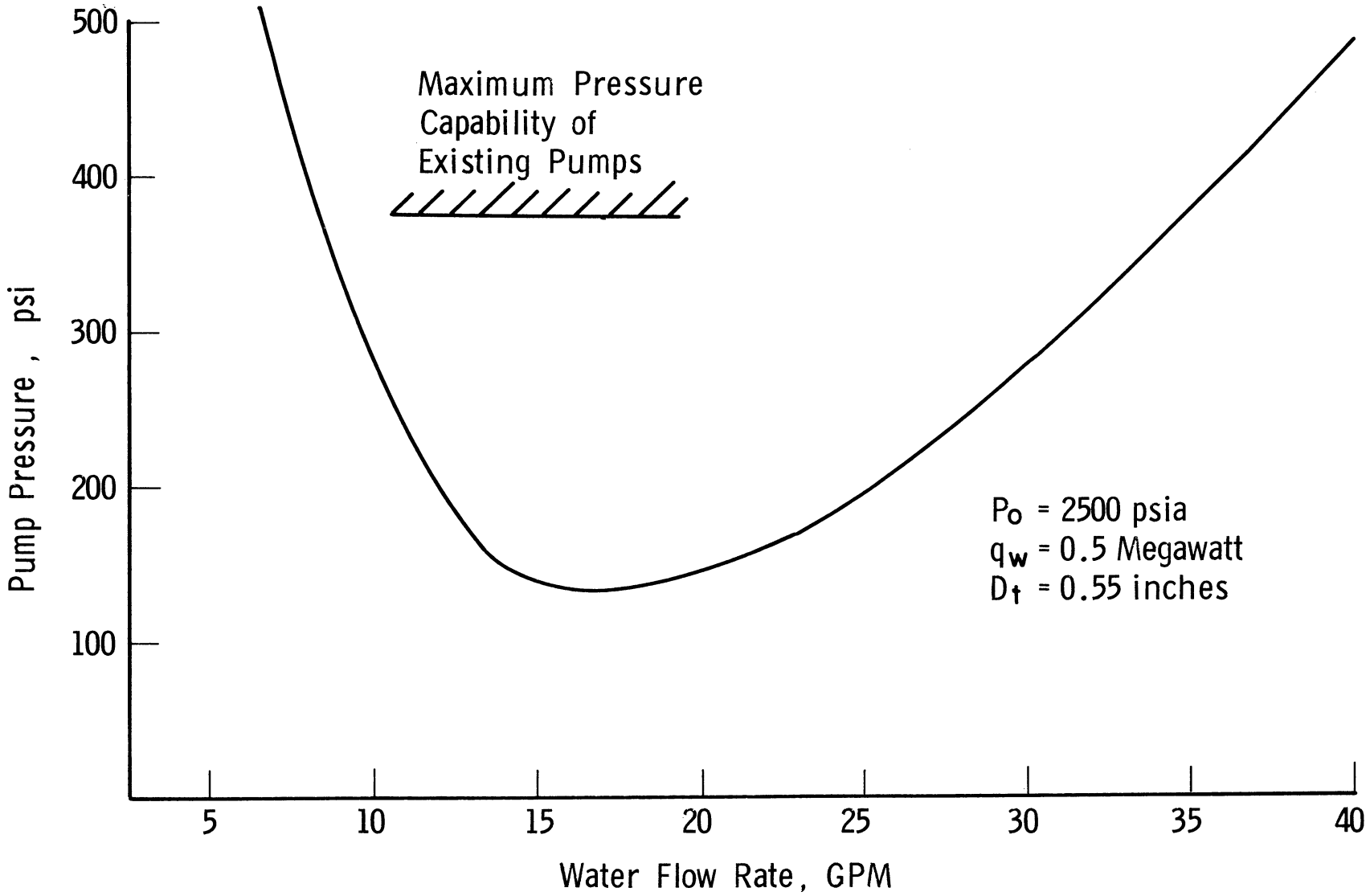

FIG. 28. PRESSURE REQUIREMENTS vs FLOW RATE FOR THE ARC CHAMBER COOLING SYSTEM.

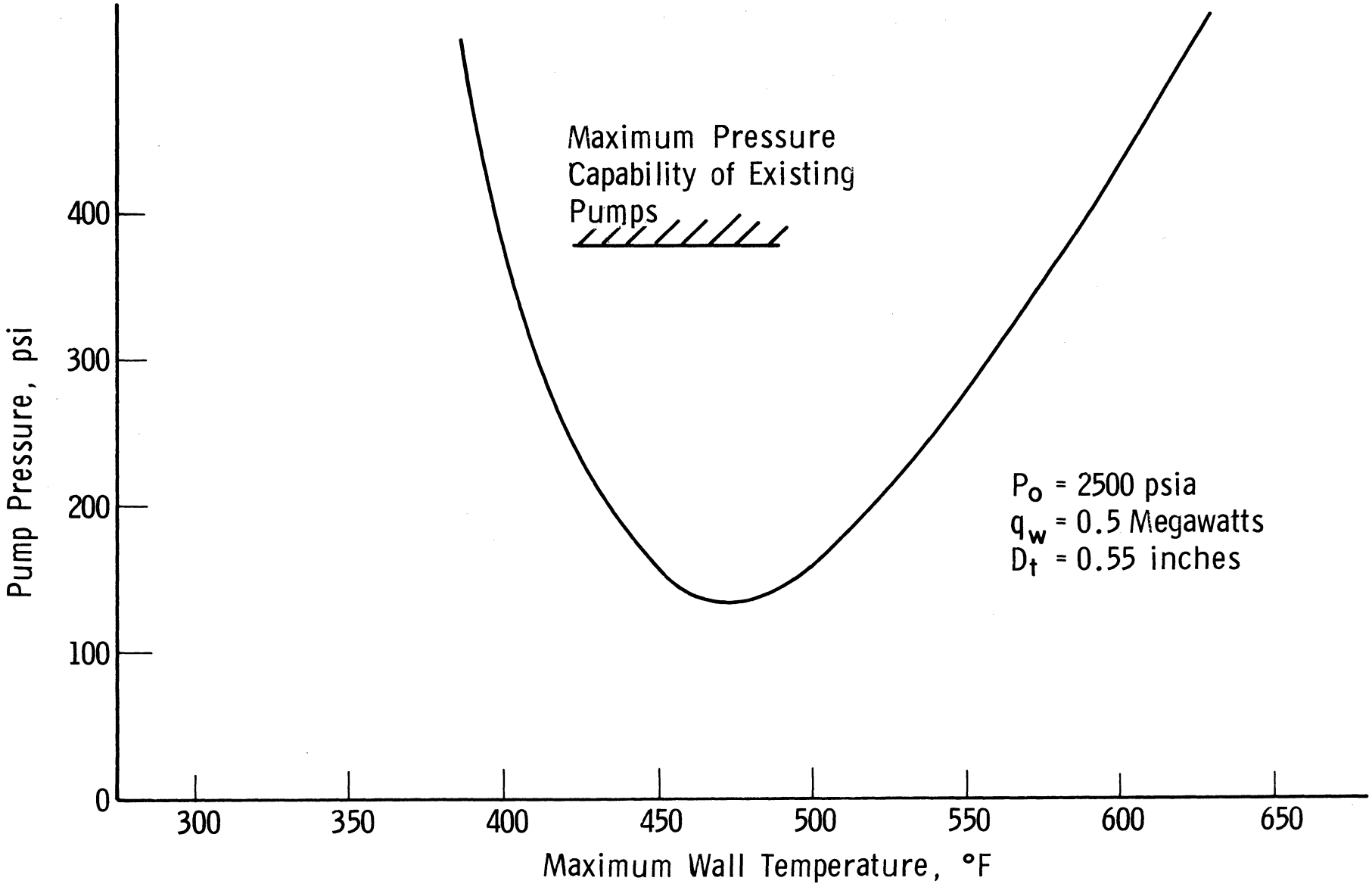

FIG. 29. EFFECT OF PUMP OPERATING PRESSURE ON ARC CHAMBER WALL TEMPERATURE.

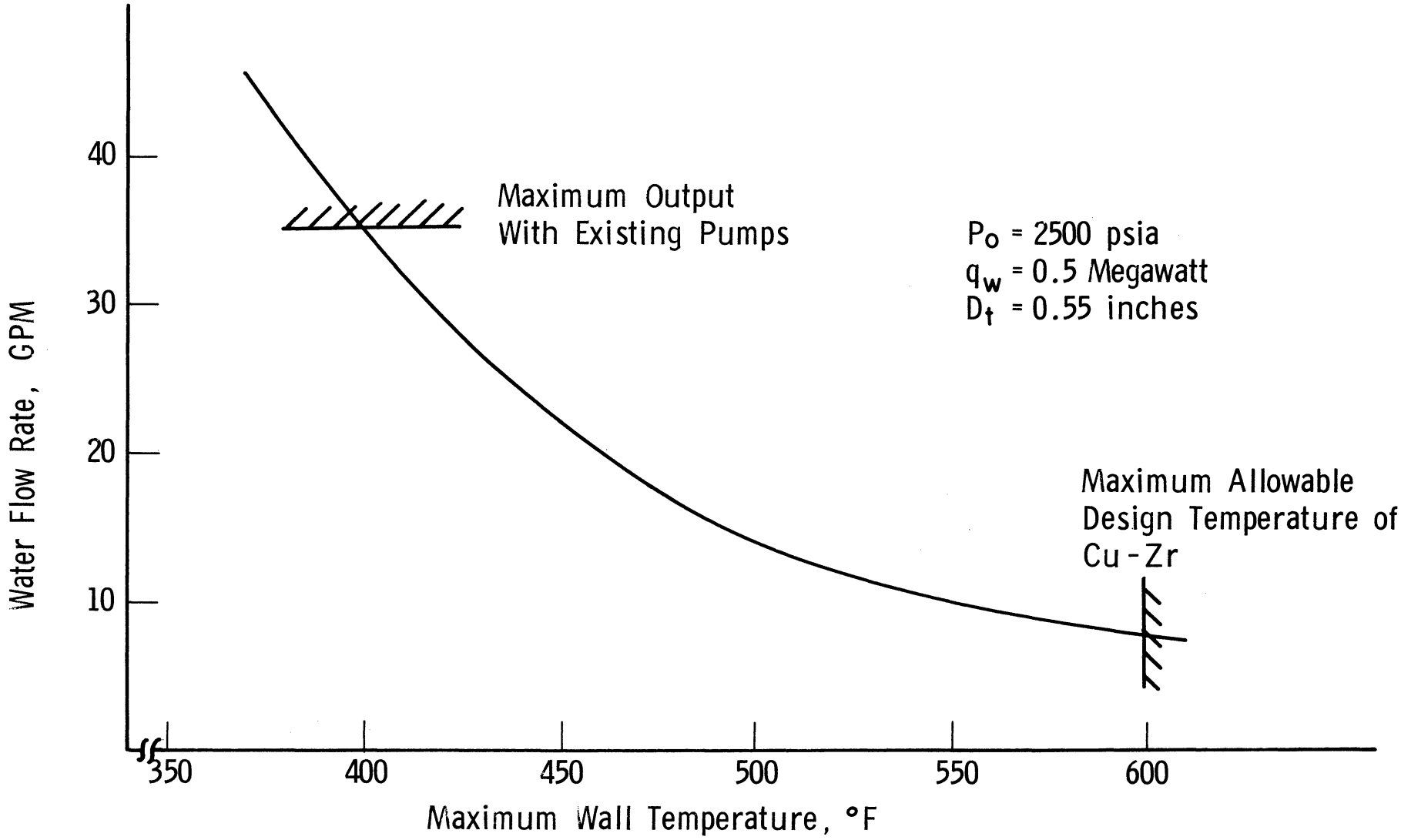

FIG. 30. EFFECT OF WATER FLOW RATE ON ARC CHAMBER WALL TEMPERATURE.

VII. SUMMARY AND CONCLUSIONS

An A. C. arc heater capable of steady state operation at 2500 psia has been designed. This represents an extension of our earlier investigations into the heating of gases by an A. C. arc column. The previous unit built was operated at pressures up to 500 psia. The studies and analysis leading to the design of the high pressure unit are summarized below.

The new arc heater represents a substantial increase in operational capability over the lower pressure unit. Accordingly, the problem of scaling an arc heater to new operational levels was investigated in detail. As a result of these studies a generalization based on the arc column-gas flow interaction is postulated which divides all arc heaters into two types. The "parallel" flow type is characterized by the gas flow being parallel to the arc column whereas in the "normal" flow type the gas flow is perpendicular to the column. A further distinction between the two is that a strong applied D. C. magnetic field is an essential feature of the latter type. In the "parallel" flow case a simple analytical model of the gas-arc column interaction is available which provides a basis for the scaling process. The lack of such a model, complicated by the strong D. C. magnetic field, for the "normal" flow arc heater makes the scaling process difficult. Scaling trends, however, were found for each type and are presented. It was concluded from this study that the "normal" flow arc heater is best suited for our application which uses a 3-phase A. C. power source. The importance of the D. C. magnetic field strength as pressure level increases cannot be over emphasized for the "normal" flow arc heater.

Using the results of the scaling studies and previous experimental data, detailed analysis concerning the material selection, expected heat transfer rates, stress levels, and the required cooling system were made. This study indicated that standard OFHC-copper would not withstand the expected pressure and thermal stresses. Two copper alloys, copper-beryllium and copper-zirconium, were found to have the necessary strength characteristics, however, the brittle nature of copper-beryllium at elevated temperatures made it unacceptable as the arc heater structural material.

At these pressure levels the effects of thermal radiation must be included in any heat transfer analyses, therefore, a model was chosen that included all three modes of heat transfer. It was found that the magnitude of the conductive and radiative heat loss to the arc heater walls is established by the parameter, N, and the gas optical thickness, τ_o. For the arc chamber, $N \ll 1$ and $\tau_o \leq 1$, so that radiation is the dominant heat loss mechanism. Just the opposite was found for the nozzle throat where convective heat losses predominate.

The stress analyses clearly indicated that the wall thickness determinations had to be based on a model which included both pressure and thermal stresses. The thermal stress was equal to or greater than the pressure stress. The analyses indicated, for both the arc chamber and nozzle throat, optimum wall thicknesses that were smaller than fabrication practicability allowed. The final wall thicknesses selected were 0. 6 in. for the arc chamber and 0. 04 in. for the nozzle throat. It is felt that the increase in wall thicknesses, from the indicated optimums, will not reduce the arc heater performance capability.

The high thermal loads imposed on these components coupled with the limited laboratory pumping equipment indicated the need for an effective cooling system. A cooling system which incorporated fins on the surfaces next to the coolant was used. Analysis indicated that this system would be two to three times more effective than the conventional water jacket. The method of producing this surface on the arc chamber is to machine a thread on its outer surface and solder a copper tube in the thread. The heat transfer capability of this arrangement in conjunction with the existing pumping equipment indicated an optimum tube size of 0.6 in. The resultant cooling system will maintain the wall temperature below the design maximum of $600^{o}F$.

From these studies, it is concluded that it will be possible to operate, steady state, a three phase arc heater at 2500 psia with power inputs greater than 1 Megawatt and mass flows up to 0.5 lb/sec. It is also concluded that, if higher pressure levels are desired (to 5000 psia) the next generation arc heaters would have to be multi-walled, i.e., an inner wall or liner of high conductivity, low strength material supported by an outer wall made of high strength, low conductivity material. This is based on the assumption that a "normal" flow arc heater would again be used and that a reduction in diameter appropriate to the increase in pressure levels would be very difficult to obtain.

As a result of the heat transfer studies, it is felt that the type of heat transfer surface used on the arc chamber and nozzle (finned copper) will, in future arc heater development, be one of the most efficient means of handling high heat loads. This type of surface can also be effectively used in multi-walled arc chamber

designs. The only limitations foreseen on its heat flux handling capability would be produced by the microscopic properties of the materials' thermal conductivity and the structural design imposed by stress producing loads. Further studies into both the structural and heat transfer character of this type of surface should be made; the resultant information applicable to all types of arc heaters. Finally, if pressure levels of the order attained in hot shot facilities are required (greater than 10,000 psia), in conjunction with a three-phase A.C. power source, the "parallel" type arc heater would have to be used. In order to adapt this power source to the "parallel" flow arc heater a substantial research program is foreseen.

REFERENCES

1. Shepard, C. E. and Winovich, W., "Electric-Arc Jets for Producing Gas Streams with Negligible Contamination," paper presented at the ASME Plasma Jet Symposium, December 1961.

2. Eschenbach, R. C. and Skinner, G. M., "Development of Stable, High Power, High Pressure Arc Air Heaters for a Hypersonic Wind Tunnel," WADD Technical Report 61-100, July 1961.

3. Raezer, S. D. et al., "Application of D. C. Plasma Arc Heating to Hypersonic Propulsion Testing," J. Spacecraft, March-April 1964.

4. "Megawatt Arc-Heated Tunnel," Republic Aviation Corp., RAC 2268, May 1964.

5. Phillips, R. L., "Fundamental Considerations in the Design of an AC Arc Heater," ARL 64-9, Aerospace Research Laboratories, Wright-Patterson AFB, Ohio, February 1964.

6. Phillips, R. L. et al., "Three-Phase AC Arc Heater," ARL 64-29, Aerospace Research Laboraotires, Wright-Patterson AFB, Ohio, February 1964.

7. Geister, D. E., "Characteristics of a High Pressure A. C. Arc Heater System," to be published as an ARL 67- report.

8. Uhlenbusch, J., "Zur Theorie und Berechnung stationarer und quasistationarer zylindrischer Lichtbogen," Dissertation, Rhein. -Westf. Technische Hochschule, Aachen, 1962.

9. Stine, H. A. and Watson, V. R., "Theoretical Enthalpy Distribution of Air in Steady Flow Along the Axis of the Direct-Current Electric Arc," NASA TN D-1313, 1962.

10. Smith, R. T. and Doyle, J. P., "A 50-Megawatt Arc Heater: Scaling Parameters and Performance Prediction," AF Flight Dynamics Laboratory, Wrignt-Patterson AFB, Ohio Technical Documentary Report FDL TDR 64-91, August 1964 (AD 607710).

11. Suits, G. G. and Poritsky, H., Physical Review, 55, 1939.

12. Theoretical and Experimental Investigation of Arc Plasma-Generation Technology, Part I, "Applied Research on Direct and Alternating Current Electric Arc Plasma Generators," ASD-TDR-62-729, September 1963.

13. Jedlicka, J. A., "Shape of a Magnetically Rotated Arc in an Annular Gap," NASA TN D-2155, October 1964.

14. Mayo, R. F. and Davis, D. D., Jr., "Magnetically Diffused Radial Electric-Arc Air Heater Employing Water-Cooled Copper Electrodes," paper presented at the ARS Electric Propulsion Conference, Berkeley, California, March 1962.

15. "Development of High Enthalpy, High Power Arc Air Heaters," RTD-TDR-63-4055, February 1964.

16. Browning, J. A. and Poole, J. W., "Arc Gas Heaters Present and Future," AGARDograph 84, September 1964.

17. Bond, C. E. et al., "The Development of a Ten-Megawatt Multi-Arc and its Operational use in Hypersonic Re-Entry Vehicle Studies," AVCO Research Laboratory Technical Memorandum RAD-TN-62-5, February 1962.

18. Schlichting, H., Boundary Layer Theory, McGraw-Hill, New York, 1960.

19. Chandrasekhar, S., Radiative Transfer, Dover, New York, 1960.

20. Seban, R. A. and Shimazaki, T. T., "Heat Transfer to a Fluid Flowing Turbulently in a Smooth Pipe with Walls at Constant Temperature," Trans. ASME, 73, 803-809 (1951).

21. Goulard, R. and M., "One-Dimensional Energy Transfer in Radiant Media," Intern. J. Heat Mass Transfer, Vol. 1, Pergamon Press, 1960.

22. Viskanta, R. and Grosh, R. J., "Heat Transfer in a Thermal Radiation Absorbing and Scattering Medium," Intern. Heat Transfer Conf. Boulder, Colorado, 1961.

23. Usiskin, C. M. and Sparrow, E. M., Intern. J. Heat Mass Transfer 1, 28, 1960.

24. Viskanta, R., "Interaction of Heat Transfer by Conduction, Convection and Radiation in a Radiating Fluid," J. Heat Transfer, C85, 1963.

25. Yoshikawa, K. K. and Chapman, D. R., "Radiative Heat Transfer and Absorption behind a Hypersonic Normal Shock Wave," NASA TN D-1424, September 1962.

26. Hansen, C. F., "Approximations for the Thermodynamic and Transport Properties of High-Temperature Air," NASA TN 4150, March 1958.

27. Theoretical and Experimental Investigation of Arc Plasma-Generation Technology, Part II, "Applied Research on Electric Arc Phenomena," ASD-TDR-62-729, September 1963.

28. Keck, J., Kivel, B., and Wentink, T., Jr., "Emissivity of High Temperature Air," AVCO Research Laboratory Research Report 8, April 1957.

29. Kivel, B. and Bailey, K., "Tables of Radiation from High Temperature Air," AVCO Research Laboratory Research Report 21, December 1957.

30. Viskanta, R., "Heat Transfer in a Radiating Fluid with Slug Flow in a Parallel-Plate Channel," Appl. Sci. Res., 1964.

31. Einstein, T. H., "Radiant Heat Transfer to Absorbing Gases Enclosed Between Parallel Flat Plates with Flow and Conduction," NASA TN D-R-154.

32. Proceedings of the Round Table Conference held in London, 25-27 October 1960, on "Low Pressure Aerodynamic Facilities," TCEA TM 12, J. J. Smoldern (ed.).

33. Horn, D. D. and Lewis, H. F., "Property Investigation of Copper Base Alloys at Ambient and Elevated Temperatures," AEDC-TDR-64-52.

34. Technical Handbook - Copper-Zirconium Alloy, American Metal Climax, Inc.

35. Avrami, M. and Little, J. B., J. Appl. Physics 13, 255, 1942.

36. Schlichting, H., Boundary Layer Theory, McGraw-Hill, New York, 1960.

37. Kreith, F., "The Influence of Curvature on Heat Transfer to Incompressible Fluids," Trans. ASME, November 1955.

38. McAdams, W. H., Heat Transmission, 3rd ed., McGraw-Hill Book Co., New York, 1954.

39. Eckert, E. R. G., "Engineering Relations for Heat Transfer and Friction in High-Velocity Laminar and Turbulent Boundary-Layer Flow over Surfaces with Constant Pressure and Temperature," Trans. ASME, 78, No. 6, August, 1956.

40. Deissler, R. G., "Analysis of Turbulent Heat Transfer, Mass Transfer, and Friction in Smooth Tubes at High Prandtl and Schmidt Numbers," NACA TN 3145, May 1954.

UNCLASSIFIED

Security Classification

DOCUMENT CONTROL DATA - R & D

(Security classification of title, body of abstract and indexing annotation must be entered when the overall report is classified)

1. ORIGINATING ACTIVITY *(Corporate author)*
The University of Michigan
Aerospace Engineering Department
Gas Dynamics Laboratories

2a. REPORT SECURITY CLASSIFICATION
Unclassified

2b. GROUP

3. REPORT TITLE
ANALYSIS AND DESIGN OF A HIGH PRESSURE A. C. ARC HEATER

4. DESCRIPTIVE NOTES *(Type of report and inclusive dates)*
Scientific. Final. Jan 1964 to July 1966

5. AUTHOR(S) *(First name, middle initial, last name)*
Donald E. Geister

6. REPORT DATE	7a. TOTAL NO. OF PAGES	7b. NO. OF REFS
December 1967	106	40

8a. CONTRACT OR GRANT NO. AF33(615)-1326

b. PROJECT NO. 7065

c. DoD/Element 61445014

d. DoD Subelement 681307

9a. ORIGINATOR'S REPORT NUMBER(S)

9b. OTHER REPORT NO(S) *(Any other numbers that may be assigned this report)*
ARL 67-0276

10. DISTRIBUTION STATEMENT

1. This document has been approved for public release and sale; its distribution is unlimited.

11. SUPPLEMENTARY NOTES
This is continuation of work reported in ARL 64-29.
TECH OTHER

12. SPONSORING MILITARY ACTIVITY
Aerospace Research Laboratories (ARF)
Office of Aerospace Research
Wright-Patterson AFB, Ohio 45433

13. ABSTRACT

This work reports on the analysis and design of an A. C. arc heater capable of steady state operation of 2500 psia. Included are discussions on the problems of designing an arc heater for a new operational regime. A generalization on the arc column -gas flow interaction is postulated whereby all arc heaters are divided into two types. Specifying each group as either a "parallel" or "normal" flow arc heater the problem of scaling each type is discussed. Scaling trends were found for each type and presented.

Using the results of the scaling studies and previous experimental data, detailed studies concerning the material selection, expected heat transfer rates, stress levels, and the required cooling systems are presented.

DD FORM 1 NOV 65 1473

UNCLASSIFIED

Security Classification

14. KEY WORDS	LINK A		LINK B		LINK C	
	ROLE	WT	ROLE	WT	ROLE	WT
Arc Heater						
Arc Chamber						
High Temperature Research						
Steady State Operation						